

Repurposing Electric Vehicle Batteries in a Mixed Array for Grid Storage

by

Benjamin Thompson

Submitted in partial fulfilment of the requirements
for the degree of Master of Applied Science

at

Dalhousie University
Halifax, Nova Scotia
April 2018

© Copyright by Benjamin Thompson, 2018

Table of Contents

List of Tables	iv
List of Figures	v
Abstract.....	viii
List of Abbreviations and Symbols Used.....	ix
Acknowledgements.....	x
Chapter 1 Introduction	1
1.1 Driving Factors: Global Warming and Renewable Energy	1
1.1 Modern Electricity Grid and Challenges	2
1.2 Energy Storage as Solution	3
1.3 Opportunity of Electric Vehicle Batteries	9
1.4 Research Objectives.....	14
Chapter 2 Literature Review.....	15
2.1 Industrial Projects	15
2.2 Academic and Research Lab Projects	19
2.3 Summary	24
Chapter 3 Mixed Battery Array Concept.....	28
3.1 Description of Electric Vehicle Batteries.....	28
3.2 Basic Layout	30
3.3 Details of Layout	39
3.4 Strengths of Mixed Battery Array Concept.....	46
3.5 Weaknesses of Concept.....	48
3.6 Experimental Research Objectives	49
Chapter 4 Batteries and Experimental Procedure.....	51
4.1 Batteries.....	51
4.2 Test Equipment.....	66

4.3	Test Protocols	77
Chapter 5	Results and Analysis	85
5.1	Constant Current Test (CC)	86
5.2	Constant Power Test (CP)	88
5.3	Frequency Regulation Test (FR)	95
Chapter 6	Discussion.....	103
6.1	Influence of Thermal Design on Operational Performance	103
6.2	Energy Density and Specific Energy	119
6.3	FR Performance Metrics using Measured Capacity	123
6.4	Ranking of Batteries for Storage Services	124
Chapter 7	Conclusions and Recommendations	131
7.1	Conclusions	132
7.2	Recommendations	134
	Bibliography	136
Appendix A	Example Parameter Script.....	142
Appendix B	Example Cycling Script	145
Appendix C	Frequency Regulation Unit Timeseries from PNNL.....	148
Appendix D	Alternative Frequency Regulation Signals	149
Appendix E	Uncertainty Analysis	151

List of Tables

Table 1- Summary of highlighted EV batteries	10
Table 2- Description of Popular EV Batteries.....	30
Table 3- Battery Specifications Overview	52
Table 4- Power Cycler Specifications	66
Table 5- DAQ specifications	67
Table 6- Summary of Thermistor Calibration	68
Table 7- Current Shunt Specifications.....	70
Table 8- BMS Specifications	72
Table 9- Cycling Parameters	78
Table 10- CC Coulombic Capacity Summary	87
Table 11- CC Peak Temperatures during Test.....	87
Table 12- CP Energy and Efficiency	89
Table 13- CP Step Duration and Temperatures	93
Table 14- FR Throughput and Equivalent Cycles.....	97
Table 15- FR Cycle Efficiency and Temperature.....	99
Table 16- Summary of Experimental Thermal Parameters per Battery	104
Table 17 Tabular Peak Temperatures by Battery and Hour Rate	116
Table 18- Literature Values for Energy Efficiency, Specific Energy, and Energy Density.....	120
Table 19- Measured Values for Energy Efficiency, Density and Specific Volume.....	120
Table 20- FR Metrics comparison of Rated Values vs. Tested Values	124
Table 21- Peak Shaving Performance Values.....	126
Table 22- Peak Shaving Performance Rankings.	127
Table 23- FR Service Numerical Performance Values	128
Table 24- Frequency Regulation Performance Ranking.....	129
Table 25- Selected Measurement Errors	151

List of Figures

Figure 1- California ISO average daily power consumption by month	4
Figure 2- Example Frequency Regulation Cycle	5
Figure 3- Grid Services Ragone Plot	6
Figure 4- Storage Technology Ragone Plot	7
Figure 5- EV and PHEV Sales and Projection	9
Figure 6- Annual US EV Sales Figures with line showing market share	11
Figure 7- Cumulative US EV Sales Figures since 2011 with line showing market share	11
Figure 8- USA Cumulative Brand Market Share of PEV	12
Figure 9- PHEV Battery Cost and Density	13
Figure 10- Lishen EV-LFP battery as an example of flat-pack layout	29
Figure 11- Conceptual Drawing of Mixed Battery Array Plant with Detail of Bays and Racks	31
Figure 12- Detail view of Rack	32
Figure 13- Detail View of Bay	33
Figure 14- Wire Diagram of Example Local Scale Plant Hierarchical Layout, DC Collector	36
Figure 15- Wire Diagram of Example Central Grid Scale Plant Hierarchical Layout, AC Collector	37
Figure 16- BMS connectors of a) Volt, b) Tesla, c) Leaf and d) custom lab configuration	41
Figure 17- Chevrolet Volt Battery	53
Figure 18- Chevrolet Volt Cooling Detail	54
Figure 19- Panasonic Tesla Instrumentation	55
Figure 20- Tesla Cooling System	57
Figure 21- AESC Nissan Leaf 2012	58
Figure 22- AESC Leaf Thermistor Locations	59
Figure 23- AESC Leaf 2015 Battery, Pack and main cables	60
Figure 24- AESC 2015 Leaf Thermocouple Locations	61
Figure 25- Lishen EV-LFP	62
Figure 26- Lishen EV pack detail	63
Figure 27- Enerdel Pack and Cell	64
Figure 28- Enerdel Cooling System	65
Figure 29- Gustav-Klein 100 kW Power cycler	66
Figure 30- Greenlight Innovations DAQ	67
Figure 31- Thermistor Calibration- Linearized Resistance vs. Temperature	68

Figure 32- Ballast Circuit Diagram.....	69
Figure 33- Example Control Flowchart with a CP Cycle	70
Figure 34- Liquid Cooling Loop.....	73
Figure 35- System Line Diagram.	75
Figure 36- Full Testing Overview.....	76
Figure 37- Leaf cell harness and main terminals	76
Figure 38- Orion BMS and CANbus channels.....	76
Figure 39- Orion Thermocouples and GLI DAQ Thermocouples.....	77
Figure 40- Cell Harness Interconnect with BMS and other voltages	77
Figure 41- Example a) Constant-Current and b) Constant-Power Test Cycles	81
Figure 42- Example FR Signals from PNNL Protocol.	83
Figure 43- Scaled Capacity and Temperature vs. Hour Rate	88
Figure 44- Discharge and Charge Energy Capacity during Constant-Power Testing.	90
Figure 45- Ah-Depletion, Current, Voltage Relationship at Constant Power	90
Figure 46- Average Step Cell Voltage vs. Hour Rate.	91
Figure 47- Constant Power Round Trip Energy Efficiency Test Results	92
Figure 48- Constant Power Step Time and Peak Discharge Temperature by Battery and Hour Rate.....	94
Figure 49- CAISO electricity hourly demand average by month.....	95
Figure 50- Amp-hour Depletion through cycle.	97
Figure 51- Demonstrating Steady-State Temperature in Leaf 2012 FR Operation.....	100
Figure 52- FR Efficiencies and Recharge Factor.	102
Figure 53- Leaf 2012 Temperature Sensor Nomenclature	105
Figure 54- Temperature Response of 2012 Leaf.....	106
Figure 55- Leaf 2015 Temperature Sensor Nomenclature	107
Figure 56- Temperature Response of 2015 Leaf.....	108
Figure 57- Moxie+ Temperature Sensor Nomenclature	109
Figure 58- Temperature Response of EnerDel Moxie+.....	110
Figure 59- Chevrolet Volt Coolant Flow	112
Figure 60- Temperature Response of Chevrolet Volt.	113
Figure 61- Tesla Temperature Sensor Nomenclature.....	114
Figure 62- Temperature Response of Panasonic Tesla.....	115

Figure 63- Peak Temperature by Battery and Hour Rate	117
Figure 64- Peak Temperature Rise above Rest Threshold Temperature.....	117
Figure 65- Peak Temperature Rise above Cooling Medium	118
Figure 66- Energy metrics contrasted with Energy Efficiency	121
Figure 67- Literature and Measured Value of Energy Density, Specific Energy, and Energy Efficiency	122
Figure 68- Measured and Greatest-Error Estimate of Charge Energy and Their Error.....	152
Figure 69- The Relative Error of a 200 A CCCV charge in a Panasonic Tesla	152
Figure 70- Measured and Maximum-Error Estimates of Energy and Their Error.....	153
Figure 71- Relative Error in 400 A CCCV Charge with a Panasonic Tesla	153
Figure 72- Growth of Error with Change in Current	154

Abstract

In the face of the global transition away from fossil fuels, the electricity grid faces many challenges. The growth of renewable energy requires investment in new methods of matching supply and demand with intermittent resources. Energy storage has become a leading technology to meet this challenge. At the same time, electric vehicles are taking to the world's roads, with 2 million plug-in vehicles in cumulative sales this year. Once their automotive life is completed, the batteries may still be useful for other purposes.

Used electric vehicle batteries may be re-purposed for grid electricity storage. Batteries from different manufacturers and use history may be aggregated to optimally draw on the locally available supply of used batteries. A mixed battery array concept is created for a new implementation, along with a list of priority research topics. Five EV batteries are tested according to PNNL suggested protocols, to determine their relative performance. It is found that EV batteries can provide grid services including peak shaving and frequency regulation. In deep-discharge constant-power cycling, energy capacities were within 10% of nominal rated values, with DC energy efficiency between 95-98%, at a 4 hour discharge rate. When increased to a 0.5 hour rate, energy capacity reduced to 50-70% of nominal, and energy efficiency reduced to 85-95%. When providing frequency regulation services, all batteries reached an apparent limit near a power bid factor equivalent to a 0.5 hour rate. Cooling performance was best with parallel liquid cooling, then parallel forced-air cooling, then series liquid cooling, then passive cooling. Liquid cooling vs. air cooling was not a strong indicator of cooling ability, rather series vs. parallel configuration was the dominant factor. The conclusion drawn from testing is that second-life batteries are technically viable for re-purposing. A performance ranking was created to assist in selecting batteries to provide grid services.

List of Abbreviations and Symbols Used

AESC	Automotive Energy Supply Corporation
BMS	Battery Management System
CC	Constant Current
CES	Community Energy Storage
CV	Constant Voltage
CP	Constant Power
FR	Frequency Regulation
LFP	Lithium-Iron-Phosphate
LMO	Lithium-Manganese Oxide
MBA	Mixed Battery Array
NCA	Nickel Cobalt Aluminum Oxide
NMC	Nickel-Manganese-Cobalt
OEM	Original Equipment Manufacturers
PHEV	Plug-in Hybrid Electric Vehicle
PNNL	Pacific Northwest National Labs
SOC	State of Charge, Coulombic
VPC	Voltage Per Cell

V	Voltage
i	Current
P	Power
T	Temperature
SOC	State of Charge
R	Resistance
β	Thermistor exponential coefficient
r_{∞}	Thermistor offset coefficient
T	Thermistor temperature

Acknowledgements

I would like to thank my partner Zach for his endless patience and support throughout this time, and my supervisor Lukas Swan for his invaluable abilities as guide and mentor.

I would also like to thank my supervisory committee, Dr. Dominic Groulx and Dr. Tim Little for their work in overseeing this project.

This work was made possible with funding from NSERC and the Network of Energy Storage Technology, NEST, and Nova Scotia Graduate Scholarships. Research equipment was provided by CFI and NSRIT.

And finally, I would like to thank all my other friends and family, who were always there to lend a helping hand or a friendly ear.

Chapter 1 Introduction

Used electric vehicle batteries present an opportunity for repurposing as an inexpensive supply energy storage to the electric grid, to for use in managing the effects of non-dispatchable renewable resources. Before their implementation, their ability to provide relevant services such as peak shaving and frequency regulation must be verified. This research creates a new concept on how these batteries may be implemented in a “Mixed Battery Array” and quantifies their performance while providing such services.

This introduction discusses the background and motivations pertaining to the research. The principal motivation for the research is the successful transition to a 100% renewable electricity grid to mitigate global warming. This requires large-scale implementation of energy storage to compensate for the variable nature of renewable energy sources. Used electric vehicle batteries can be repurposed for energy storage, but several important questions need to be answered:

- How do the range of EV batteries perform relative to each other?
- Are they able to operate in a grid storage application, as they were designed for automotive service?
- How would batteries from many brands and backgrounds be aggregated?
- What operational constraints are present when the batteries are used in grid service?

Answering these four questions is the goal of this project.

1.1 Driving Factors: Global Warming and Renewable Energy

The recent signing of the Paris Accords establishes a global consensus on an average global warming target of no more than 2°C above 20th century average global temperatures [1]. The signatory nations have agreed to take actions to limit their greenhouse gas emissions to levels required to remain within the 2°C limit. For context, in 2015, global land temperatures reached 1.3 °C above the 20th century baseline [2]. At most recent account, no industrialized nation is on track to meet their pledged emissions targets. These targets have been re-evaluated considering the most recent climactic models, and are now understood to be at least twice as high as is required to realistically meet the 2°C target, which itself is an uncertain limit for considering the stability of the global climate [3]. Christiana Figueres et al. have argued [4] that there are 13-25 years remaining for the world to eliminate fossil fuel emissions to maintain the target set by the

Paris Accord. Electricity and heat production contributes to approximately 42% of global greenhouse emissions, the largest sector by emissions [5]. Accordingly, most nations are transitioning to alternative energy resources, such as wind, solar, and hydro.

Renewable electricity generation has grown to account for 1,811 GW of capacity in 2015, or 28% of global capacity of electricity generation¹. Renewable electricity produced approximately 5660 TWh in 2015, or 23.5% of global generation. For comparison, by total energy, they accounted for 18.3% of all energy production in 2014 [6].

Considering the urgent timeline for elimination of greenhouse emissions, and the role of electricity generation in emissions, a rapid rise in renewable electricity generation is a necessity.

1.1 Modern Electricity Grid and Challenges

1.1.1 Non-dispatchable, stochastic renewable energy

The primary modern forms of renewable energy generating resources are on- and off-shore wind, solar photovoltaic, and hydropower, with the latter being the largest contributor at 17% of total generation [6].

One disadvantage of wind and solar power generation is that they are **non-dispatchable**; they do not always supply when needed. Another disadvantage is that they are **stochastic**, making it difficult to quantify or predict how much energy will be generated by a specific site.

This is because each depends on the environment, with solar power depending on the time of year and day, latitude, and daily cloud cover, and wind power depending on the weather, season, and time of day. These factors result in variation in generated or available power on daily, seasonal, and yearly timescales.

Supplemental technology is required to insure a stable supply of electricity, within the uncertainty of prediction and the variability of renewable generation.

1.1.2 Matching asynchronous supply and demand

The primary requirement of the grid is the supply of as much power as demanded at any given time, plus transmission and distribution losses. With high penetrations of renewable generation, available supply of solar and wind can exceed demand, requiring that they be curtailed.

¹ Including hydro generation

Conversely, during slack periods, or at night, demand will exceed renewable supply, requiring the dispatch of coal, natural gas, or other dispatchable sources. The chief difficulty of the modern grid will be the combination of many sources in such a way as to meet reliability demands 99.99% of the time, etc. [7]. This challenge presents itself in a few broad ways:

- Predicting the resource available on-site, such that the grid operator has a realistic estimate of the power to be generated at future times.
- Building a diverse supply of resources to maximize the independence of the energy streams.
- Positioning stored energy levels, including hydro reservoirs, fuel supplies, and states of charge to maximize their utility.
- Other methods of matching supply and demand, such as demand management and time-of-use fees combined with smart appliances capable of turning themselves off.

While the above list highlights the many paths towards grid reliability, Jacobson [8], Pickard [9], Jewell [10], and Budischak [11] all implement energy storage technology as a means of balancing the non-dispatchable sources. Budischak proves energy storage to be an integral part of the cheapest grid composition by simulation. This justifies focus on energy storage technology.

1.2 Energy Storage as Solution

Energy storage is a solution to the dynamic challenges of a modern grid. Many different technologies are available, from flywheels to pumped hydroelectric storage, compressed air energy storage, and batteries, with each technology having strengths and weaknesses. The tasks that storage is expected to handle will be discussed, followed by the size of the problem- just how much does the world need?

1.2.1 Provision of services

Energy storage technology is unified by a common purpose- the need to move energy through time. All types of energy storage perform this fundamental operation. Within this description there are different specific services that can be provided. The services relevant to this research are described below. For more information, see [12].

Renewables Integration

Solar and wind power are subject to three scales of variation: macro, meso, and microscale.

- Macro: Year-to-year and season-to-season, average and peak wind and solar outputs can rise and fall. Wind tends to peak in the winter, and solar in the summer [13]. Integrating renewable energy on this scale requires enormous quantities of storage capacity which are not presently economical, and is best handled by combining resources to maintain a good match between rising and falling generation [14].
- Meso: Day-to-day variation also exists, and can be seen in day-ahead and hour-ahead prediction and electricity markets [15]. This type of renewables integration requires days to hours of storage and can be used as a bridge to withstand cloudy weeks or sustained slow winds.
- Micro: Second-to-second variation exists from clouds passing over solar panels, or gusts of wind and other eddy behavior with wind turbines. This kind of renewable integration can also be called firming, allowing the grid operator to act as though the generator is ideally following the predicted behavior, rather than constantly increasing and decreasing. This service requires a high-power ramp rate capability [16].

Peak Shaving

Over the day, electricity demand rises and falls. As people wake up in the morning, lights come on and coffee is brewed. Air cooling and heating is turned on at the office. This leads to a *morning peak*. When people return home, stoves, televisions, and kettles are all turned on. This is called the *evening peak*. The relative power levels of these peaks vary from place to place, and summer to winter, leading to a usage profile as below in Figure 1. The highest electrical demand in the year is usually met by natural gas peaking plants. In a zero-emissions grid, this service may be performed by energy storage.

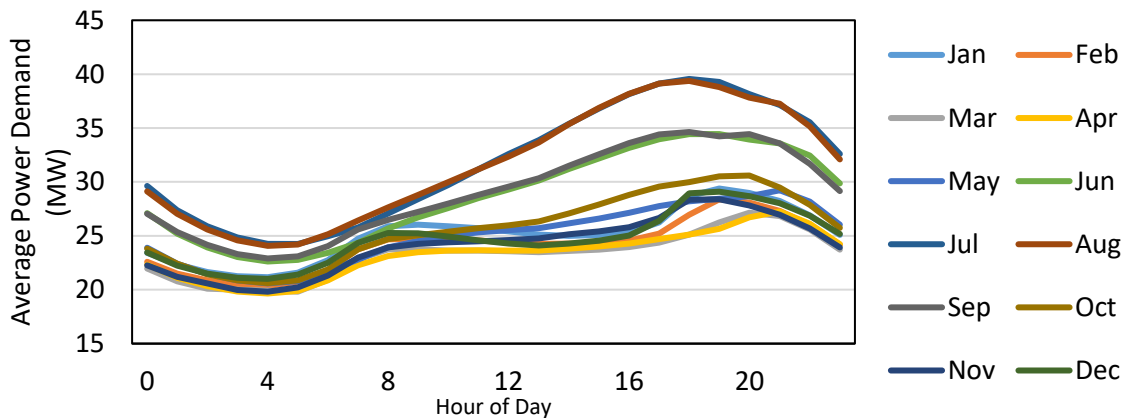


Figure 1- California ISO average daily power consumption by month [17]

The salient characteristic of this profile is a single high-intensity energy storage discharge period of variable width, and variable power, followed later by a charge period during times of low demand, usually overnight.

Peak shaving has the same duty cycle as demand charge reduction, which is forecasted to be [18,19] the first mass-market profitable service, and some companies are already selling products to provide this service [20]. It is included in this research because of this high value yield.

Frequency Regulation

When heavy machinery is turned on or off, it affects the load and consequently the frequency of the grid. Maintaining the frequency of the grid at a precise value is a key responsibility of the grid operator, and so generators are traditionally commanded to increase or reduce power supplied to the grid to compensate for fluctuations. Energy storage devices can also fulfil this service. An example of the duty cycle can be found in Figure 2.

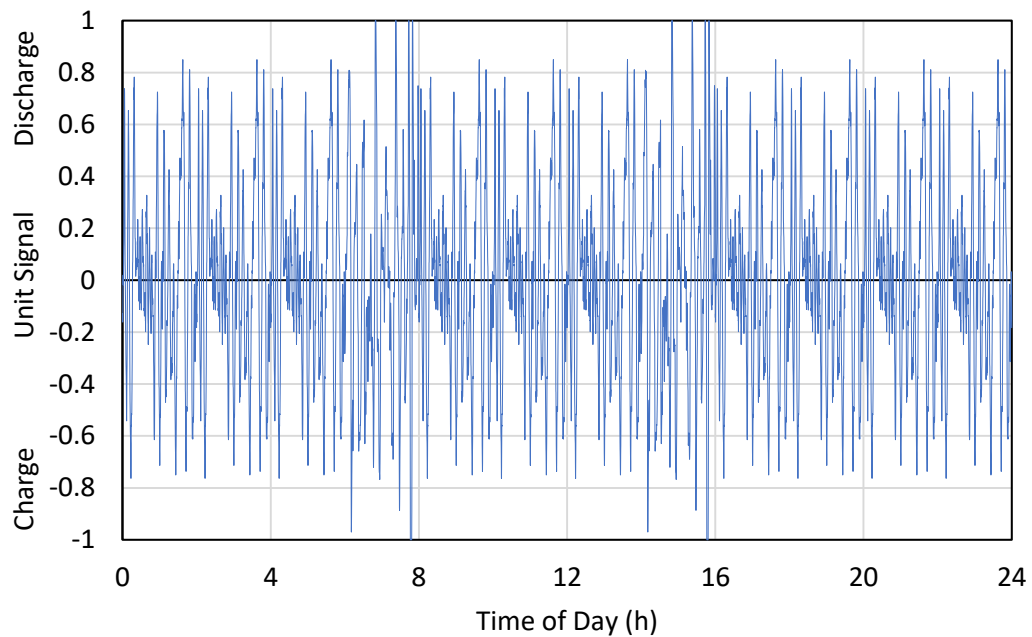


Figure 2- Example Frequency Regulation Cycle

The frequency regulation (FR) duty cycle typically has an average power value of zero, with high instantaneous power calls in both directions. This lends itself to a technology with a low energy capacity, but a high power capability.

Frequency regulation is commented on by NREL [19], PNNL [16] and Sandia National Labs [21] as one of the presently profitable stand-alone services for energy storage to provide, and as such it is included in this research.

Commonalities of Services

Despite the differences in the wide variety of services that can be provided by storage, they can be described in some common ways. Figure 3 shows how services fall on a power-energy axis.

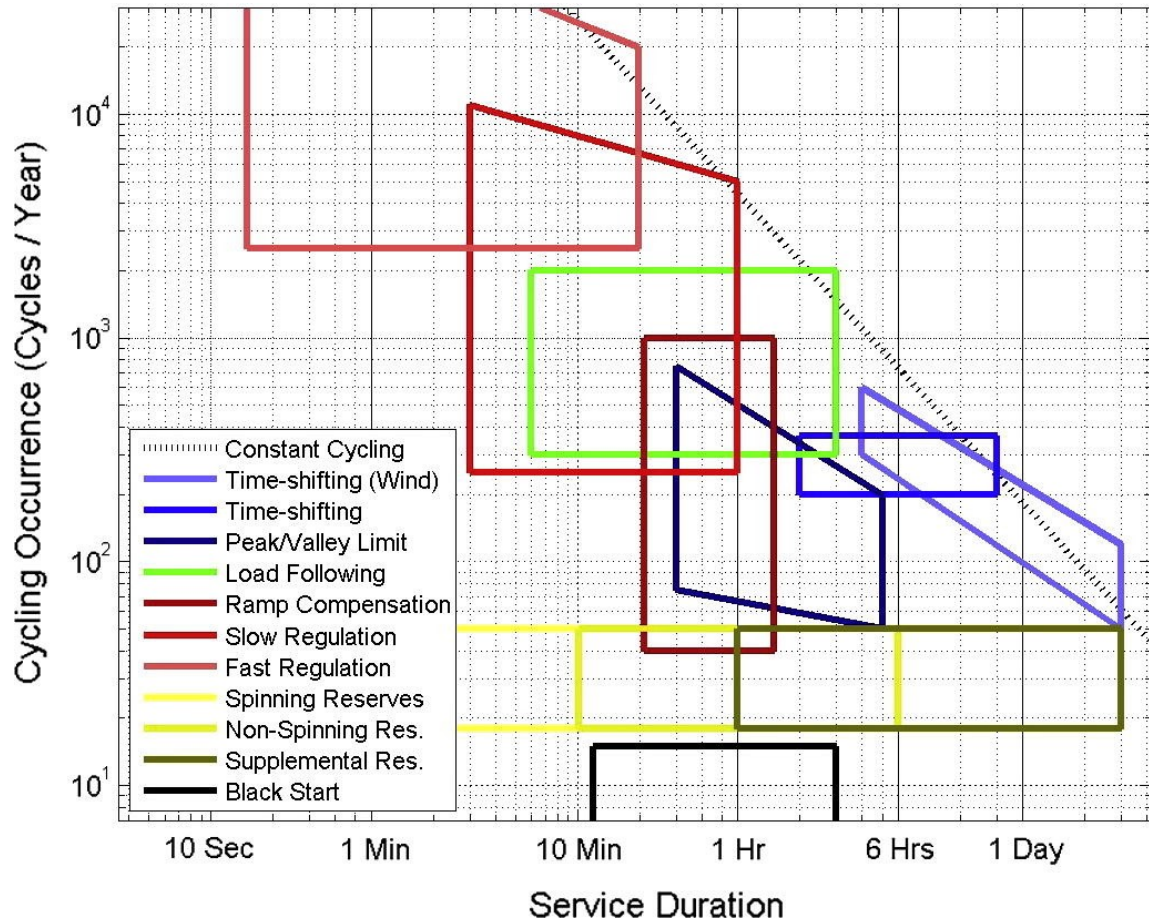


Figure 3- Grid Services Ragone Plot. Source:[22]

The most desirable capability would be both high energy and high duration, and this is also the most difficult to achieve. Most services fall along a spectrum of energy to power ratios, with frequency regulation being furthest towards high-power, low-energy, and peak shaving being the most high-energy, low-power kind of service. Other, hybrid cycles such as renewables integration fall in between these categories.

Storage technologies can also be described with a power-energy ratio, as seen in Figure 4.

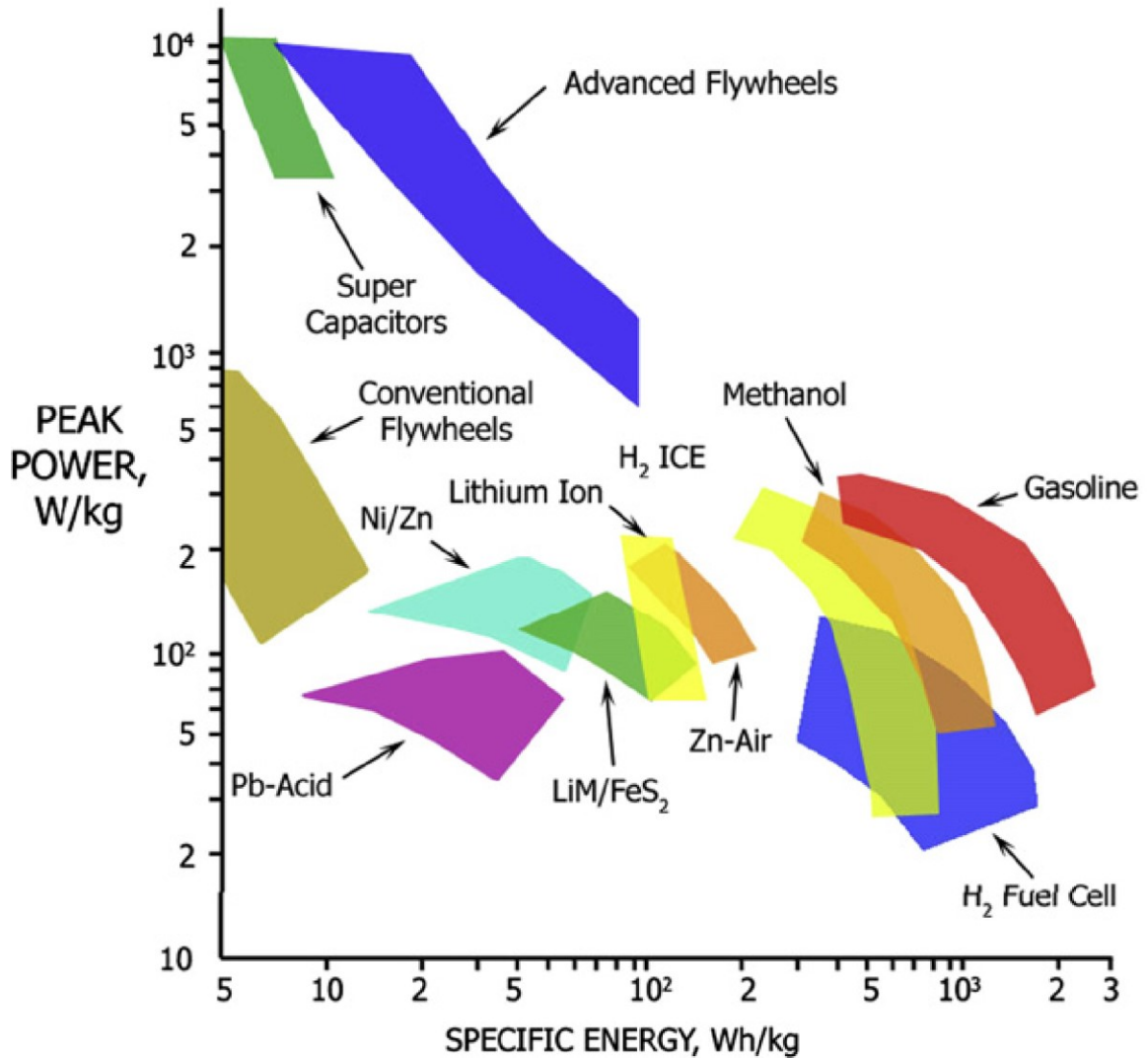


Figure 4- Storage Technology Ragone Plot. Source:[23]

Batteries have two important characteristics in this context: one purchases battery power and energy simultaneously², as these properties depend on the chemistry and geometry of the cell and pack, and their capacity changes depending on the power rate one cycles the battery at.

This means that batteries are purpose-built to fulfil some service and are best used for that purpose in most cases. For example, a Tesla battery pack is optimized for peak power capacity and energy density for a high-performance EV, where other batteries focus on cost and efficiency. Nonetheless, a battery may be usable for other services than they were originally

² As opposed to ex. fuel cells and flow batteries, where energy and power capacity are purchased separately

designed for. Determining the ability of batteries to push their operational envelopes and provide varying services is one of the key research questions of this project.

1.2.2 Scope of challenge

In the case of Pickard [9] and Budischak [11], 2-3 days of energy storage at average power are recommended. Pickard provides an educated estimate, and Budischack performs simulations optimizing for least-cost combinations of renewable energy and storage for meeting the year's demand. Normalizing Budischak's estimates for absolute storage capacity by the average yearly power, approximately 3 days of average generation are required to be stored at a given time to satisfy demand and accommodate wind lulls. The total installed storage capacity of the world as of 2015 was **1616 GWh**. The world's annual energy consumption was 164,700 TWh in 2016 [24]. Averaged over the whole year, this would correspond to 18,800 GW of consumption. To store 3 days of energy at this average rate would require 1,353,699 GWh. Thus, the world is 0.1% of the way towards this objective, assuming energy demand does not increase.

If only electrical energy is of interest, 23816 TWh of electricity were produced in 2016 [25]. This would translate to an average production of 2718 GW, which would require 195,696 GWh of storage to store 3 days' worth. The world is **0.8%** of the way towards this reduced scope.

The cheapest technology to build grid-scale energy storage is pumped hydro storage, on an order of US\$10/kWh [26]. The bulk of presently installed capacity comes from this technology; however, installation rates have fallen to the point few if any new pumped hydro capacity has been added in the last 7 years. Most sources attribute this to having already used all the best sites for installation, pumped hydro having specific geographic requirements and a lack of interest in mega-infrastructure projects.

By contrast, investment in lithium-ion batteries has risen sharply, with hundreds of new projects being pursued at the same time pumped-hydro investment has fallen. This is due to improvements in cost, energy density and efficiency, which are priorities for the burgeoning electric vehicle market. Where hydropower is dependent upon local geography, lithium-ion batteries can be installed in any location quickly and effectively. Combined with lowered cost, high efficiency, and high volumetric energy capacity, utilities are investing heavily in battery storage, with record size installations every year³. Despite these improvements, the cost per

³ 40 MWh in 2016, 125 MWh in 2017, proposed 400 MWh in 2018.

kilowatt-hour is still expensive compared to pumped hydro for bulk storage, so finding a means of bringing cost down is a high priority. For example, re-purposed electric vehicle batteries may be an untapped source of cheap storage.

1.3 Opportunity of Electric Vehicle Batteries

Electric vehicles have large, well-engineered batteries that may be re-usable after their automotive service life, and millions of electric vehicles have been sold, representing a large potential pool of available storage.

1.3.1 Growing market

Electric vehicle sales have grown sharply in the past 5 years. In 2016, approximately 1.2 million battery electric vehicles and just over 2 million plug-in hybrid and electric vehicles were registered globally, per Figure 5.

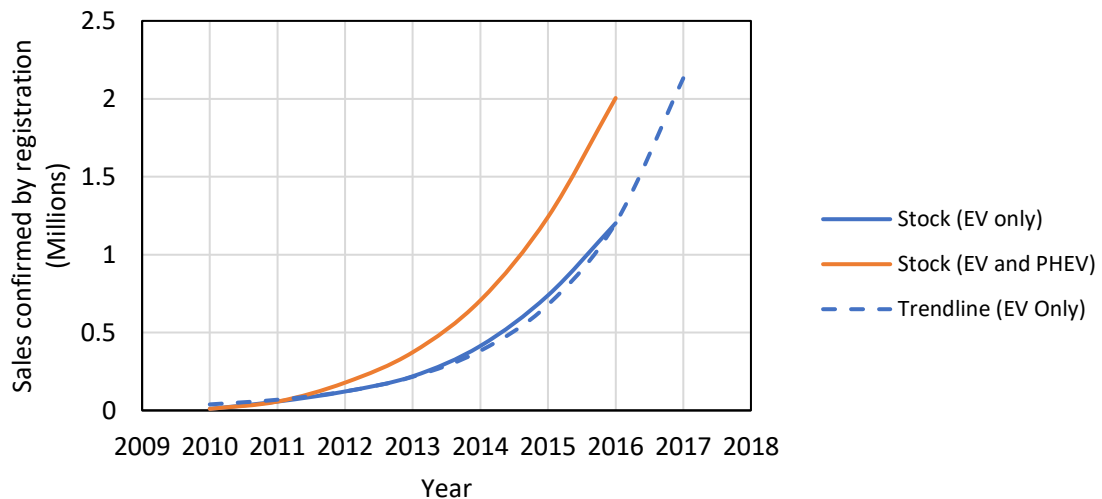


Figure 5- EV and PHEV Sales and Projection

If the trend continues, by the end of 2017, approximately 2.1 million purely electric vehicles will be confirmed on the roads. Per some sources, the rate of sales is accelerating even more [27].

Notable countries responsible for this trend include Norway, which has achieved 22% market share of EVs, and China, which is purchasing 40% of EVs worldwide. [28]

1.3.2 A brief portrait of the batteries

Electric vehicle batteries vary widely in designs, from prismatic to cylindrical format, and air or liquid thermal management and vertical vs. horizontal cell and module layouts. Battery voltage

is typically around 400 V maximum due to common equipment convergence points, especially with fast-charging infrastructure. Current peak values tend not to exceed 400 A (With the notable exception of the Tesla at 1500 A). Battery pack dimensions are necessarily limited to the car's size, usually fitting in the flat space under the seats and between the wheels in the floor of the vehicle. Table 1 below shows some characteristics of EV batteries.

Table 1- Summary of highlighted EV batteries

Manufacturer	Vehicle	Format - Chemistry	Pack ⁴ configuration	Nominal Voltage (V)	Rated Energy (kWh)	Physical Dimensions (cm)	Thermal Mng't
Panasonic	Tesla Model S	Cylindrical	74P6S16S	366	85	296x196x10	Liquid
AESC	Nissan Leaf	Prismatic	2P96S	365	24	157x119x26	Passive
LG Chem	Chevrolet Volt	Prismatic	3P96S	360	16	178x100x40	Liquid
			NMC-LMO				

Figures 6 and 7 show annual and cumulative EV sales in the United States as an example market. Figure 8 shows the present market share of the PHEV/PEV⁵ market in the US. The top three models account for 63% of all EVs sold, in roughly equal measure.

⁴ xPyS refers to the electrical layout of the battery, x referring to the cells in parallel, y to the cells in series.

⁵ Plug-in hybrid electric vehicle/plug-in electric vehicle.

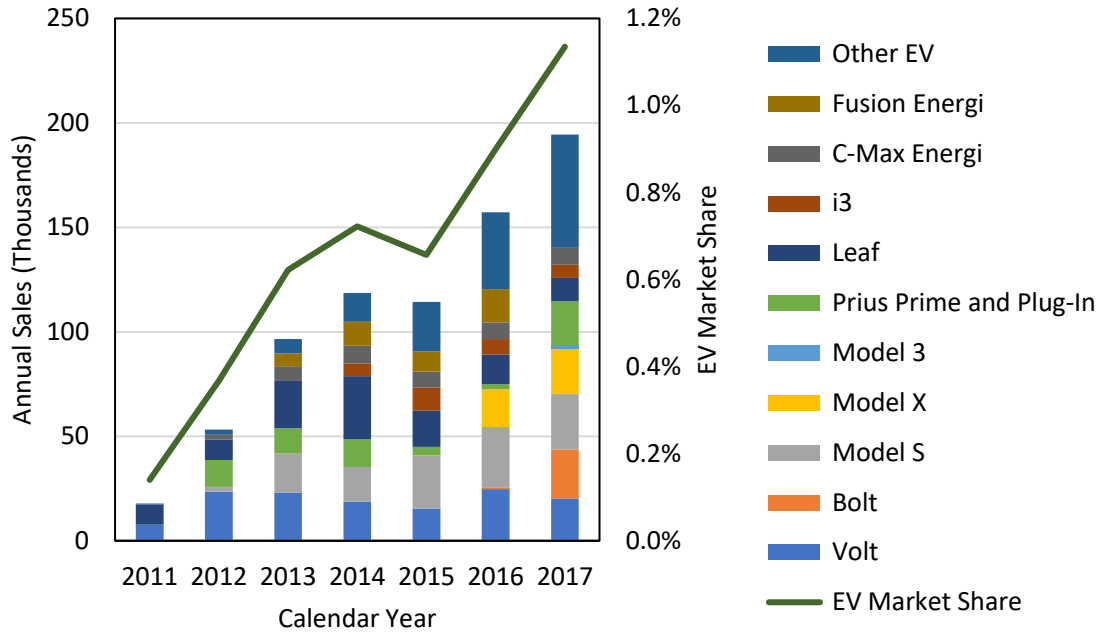


Figure 6- Annual US EV Sales Figures with line showing market share [29]

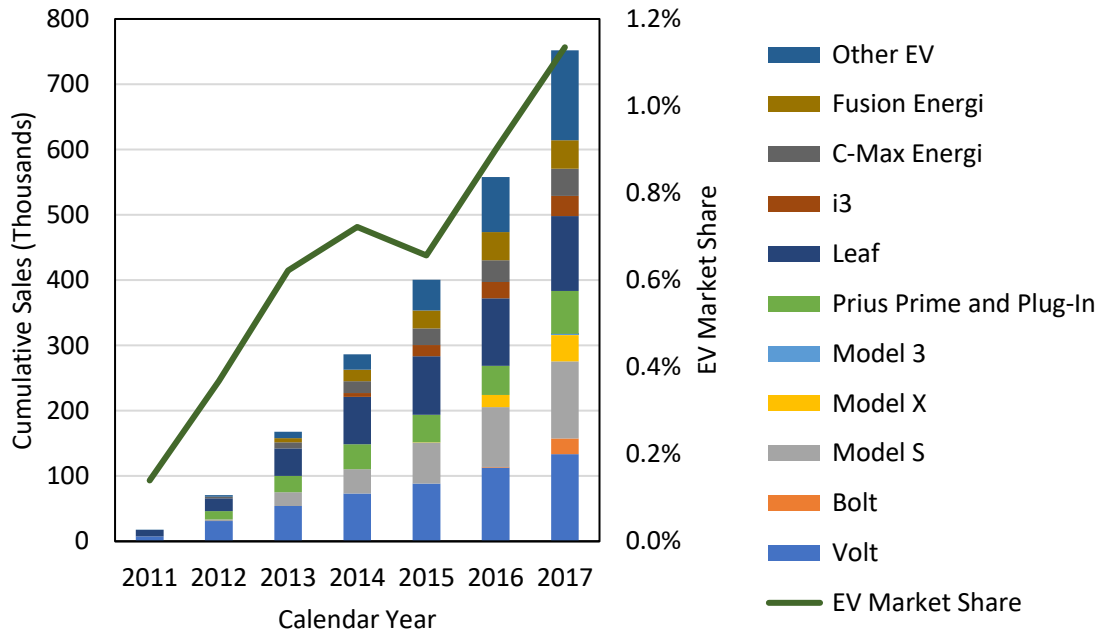


Figure 7- Cumulative US EV Sales Figures since 2011 with line showing market share [29]

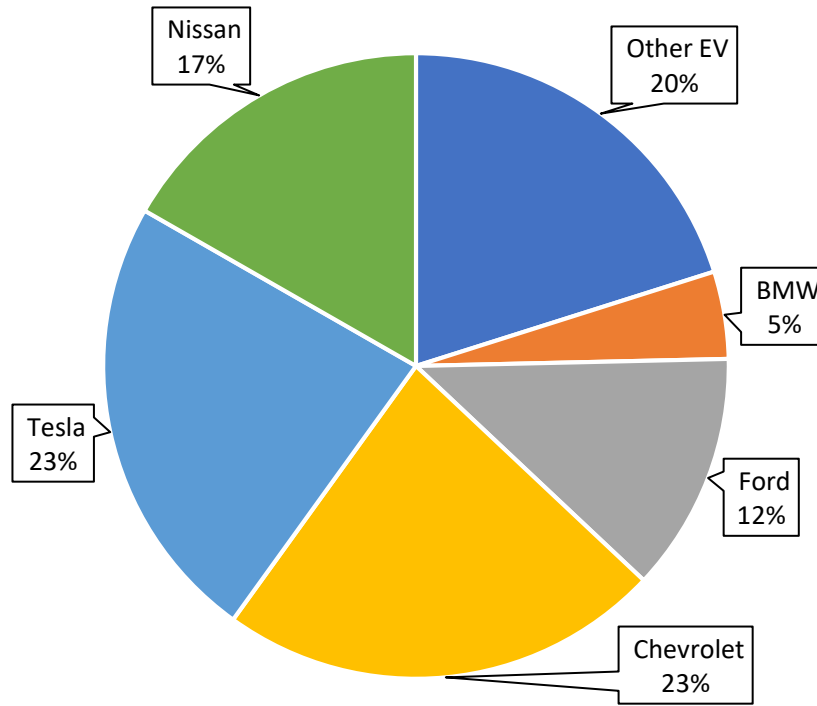


Figure 8- USA Cumulative Brand Market Share of PEV [29]

1.3.3 Cost and Lifetime

As batteries are used, their discharge energy storage capacity degrades due to wear. The rate of this degradation is complex, and depends on several factors, including at least [30]:

1. The range of voltage and capacity used.
2. The rate of charge and discharge.
3. The frequency of cycling.
4. The temperature of the battery.
5. The state of charge of the battery.
6. The age of the battery.

Because of this, the remaining useful life and performance of a battery can be hard to determine: how much usage a buyer will get from it depends on its usage patterns.

At present, little information is available on what capacity will remain at the end of the automotive lifetime. Several estimates place the health of the battery from 60%-80% of its

original value at the end of automotive life, assuming an automotive lifetime ranging from 8-15 years.

Because the electric vehicle battery is used, it no longer carries an attached price tag from the manufacturer. Thus, the **following economic factors constrain the price of the battery**:

- The buyer of the battery is unwilling to pay a price near that of a new battery in terms of US\$/kWh. If the price of new batteries falls fast enough, it may not be worth purchasing used. See Figure 9 for the trend in EV battery prices.

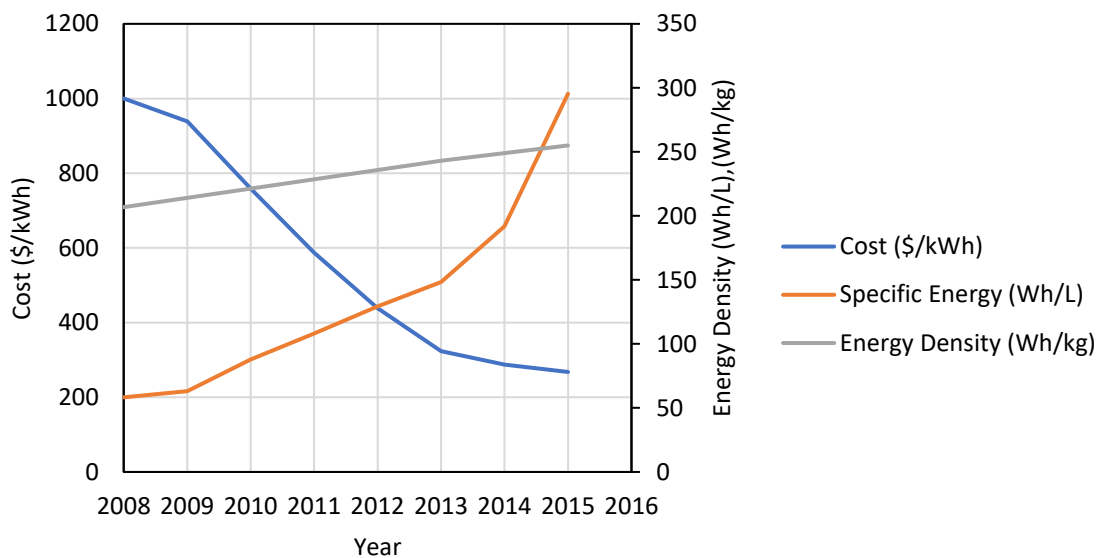


Figure 9- PHEV Battery Cost and Density. Source:[31,32,33]

- Costs of repurposing are incurred for second-use batteries that would not be for new batteries. If the price of new batteries falls lower than this cost, it would make more sense to purchase new batteries.
- The shipping distance from the vehicle to the repurposing location incurs a cost. Thus, batteries will be more likely to be drawn from local sources.

NREL has suggested a potential stable price of US\$38-US\$132/kWh of usable capacity [19] as the likely price of buying electric vehicle batteries in a used market. This compares with the present price of new lithium-ion batteries of US\$275-US\$200/kWh [28], and the target cost of US\$125/kWh by the US DOE vehicle technologies office [34].

NREL estimates from past and predicted sales of electric vehicles an available useful capacity from 32.3 GWh to 1 TWh [35]. Compared to the present volume of storage, 1.6 TWh, adding this capacity would nearly double our global storage capacity at generous estimates.

1.4 Research Objectives

The framing objective of this research is the need to manage a growing fraction of renewable energy using energy storage. Because energy storage itself is quite expensive, and the magnitude required so large, pursuing means to reducing this cost for bulk storage is a priority and it is the research objective to do so with low-cost used EV batteries repurposed for grid energy storage.

1.4.1 The Mixed Battery Array Concept

The repurposing of electric vehicle batteries is a promising avenue for adding inexpensive storage to the electricity grid. Existing pilot projects have weaknesses that a flexible third-party usage concept would overcome. Because the sales of electric vehicles are distributed, local energy storage system developers must work with nearby supplies, which will include batteries of many brands, ages, and environments. The services provided by the storage will most likely include a form of peak shaving and frequency regulation. The scale required is large, so collecting hundreds or thousands of batteries is required, rather than single batteries at a time. To manage this collection, they should be collected in a single industrial center, governed with an advanced controller. This concept is developed in Chapter 3 and contrasted with the state of the art given in Chapter 2. The examination of this concept leads to the next research objective;

1.4.2 Experimental Investigation

The experimental portion of this research will characterize and compare the four most popular plug-in electric vehicle batteries by performing a series of standardized tests on each of them, including coulombic and energy capacity characterization, and frequency regulation. Analysis will focus on the relative performance of each battery, including its available energy capacity, energy efficiency, thermal management, and peak FR provision. This is conducted in Chapter 4 and Chapter 5, with discussion given in Chapter 6. The grounding for this objective is established with Chapter 2 and Chapter 3, and is formalized in section 3.6.

Chapter 2 Literature Review

Organizations involved in the development of repurposed EV battery usage are from three different domains: Industrial OEMs, third-party companies, and academic governmental researchers. The proposed repurposing concepts have evolved with time, ranging from single residential packs to reconfigured storage centers of hundreds of uniform batteries. The first section will discuss the most prominent implementations of re-purposed EV battery storage, and the strengths and weaknesses of each approach. Then, the academic literature and investigations will be reviewed, with a focus on what experimental data is available. Finally, the gaps in the contemporary research will be discussed, and how that leads to this research thesis.

The industrial groups are investigated first to provide a context for what is being practically implemented now, and what the **implicit** priorities are in the field of repurposing EV batteries. The academic research will discuss what might readily be expected for third-party groups in terms of economic viability and quantitative performance.

2.1 Industrial Projects

This section discussing industrial projects is divided into the automotive Original Equipment Manufacturers (OEMs) of vehicles and third-party corporations who are not automotive companies, but work with automotive products. The first-party users are all noted to make use of in-vehicle performance tracking of the battery, and are assumed to have more information on the “correct” usage parameters of the battery, so the projects they undertake may provide ideas of how to organize and operate, and the scale of the projects indicates the confidence that OEMs have in their analysis and understanding of their equipment. Third-party operators are more limited in access to data, so their projects indicate the ability of the field to accept, repurpose, and operate EV batteries.

2.1.1 First-Party/OEM

Nissan

Nissan, in cooperation with Green Charge Networks [36, 37] and Eaton [37], began in 2016 pilot project-scale testing re-using Nissan Leaf EV batteries for second-life energy storage, as of 2016. Green Charge Networks advertises residential and enterprise versions of their products for US markets, and Eaton is advertising residential version for the UK. Each of the two residential versions use one battery from a Nissan Leaf (Approximately 30 kWh, from the 2016 model year).

The enterprise version has separated a pack into modules and racked them in cabinets. Approximately ten leaf batteries may have been used in its construction, accumulating 300 kWh.

Nissan has also partnered with Renault and The Mobility House in Germany to test a 100 MW grid scale battery project using second-life batteries, announced June 2017 [38]. A previous project by Nissan in Japan, working with the Sumitomo group, created a 600 kW/400 kWh battery energy storage system made from 16 second-life Leaf batteries at a solar power plant, announced February 2014 [39], to demonstrate PV smoothing services. Given the much larger Renault project, it can be inferred that the results were positive.

General Motors

General Motors in 2017 commissioned a local energy storage facility for their Milford Proving Ground in the United States to integrate their on-site solar and wind turbines in June 2017. Created with 5 Chevrolet Volt batteries, it is estimated to provide approximately 80 kWh of storage capacity [40]. It is intended to supply energy to their datacenter on-site, likely serving as UPS backup, as well as possibly optimizing the usage of renewables onsite.

General Motors is also partnering with Duke Energy and ABB to pilot a **Community Energy Storage** device [41], meant to be placed near the end of distribution networks and supply power to a small neighborhood as a roadside device. This follows the same construction as their Milford Proving Grounds device but is intended to provide different services: back-up power, peak management, renewables integration and a few reliability-based grid services. In 2013, they demonstrated a 25 kW/50 kWh prototype.

BMW

BMW has constructed a 2 MW/2.8 MWh energy storage facility in Hamburg, Germany, announced October 2016 [42]. It is made of over 100 battery packs from BMW i vehicles. Constructed in cooperation with Bosch, the facility is designed to provide a short-term power buffer for EV charging stations, as well as optimizing the power output of a nearby solar plant. The plant is designed as a fully complete turnkey solution, with no expected swapping of batteries for its lifetime. This is significant as the concept proposed in this thesis in Chapter 3 is of a similar size but uses a very different design philosophy.

Toyota

Toyota has installed an 85 kWh energy storage facility at Lamar Buffalo Ranch in Yellowstone National Park in May 2015, using repurposed Camry HEV batteries⁶ [43]. The facility is totally off-grid, enabling the ranch to power itself entirely with a 40 kW PV array.

This project is different from others mentioned on its scale for having slots for each battery made to fit the original battery in its case, intending to replace each battery pack as it ages. This simplifies the installation process, but more importantly, it keeps the Ni-MH cells from expanding and contracting as they cycle by keeping the original case. The creators did make an alteration to the wiring of the original pack by making the cells link in parallel instead of in series, requiring the case to be opened and a busbar replaced.

Daimler

Daimler AG is partnering with ACCUMOTIVE, The Mobility House, and GETEC to provide a 13 MWh storage facility on the German energy market, composed of 1000 second-life batteries from Smart Fortwo cars [44]. The facility is in Lunen, Westphalia, Germany. They intend to participate directly with the market as an independent operator, instead of operating behind the meter of another business. They will market their output capacity on the weekly market, recharging automatically from renewable energy as it becomes available. This project is thus notable for being an order of magnitude larger than the next-largest competitor, but also for participating directly in the energy market instead of providing some form of secondary service. This installation is similar to the mixed battery array concept of this thesis presented in Chapter 3.

Tesla

Tesla Motors announced their interest in second-life usage of batteries for grid energy storage, but later reversed their position [45]. The given reason was their doubts about the remaining capacity after its automotive life, and the difficulty of quality control checking of every cell in a refurbished pack.

⁶ It is worth noting that the *Camry* is not a plug-in hybrid like the *Volt*, but instead recharges from the gasoline motor. These vehicles have batteries which are quite small, and not suited to deep discharge cycles.

2.1.2 Third-Party Corporations and Businesses using Repurposed EV Batteries

Relectrify

Relectrify is creating battery packs for domestic markets made from second-life EV batteries [46]. Their value-added contribution to the operation is in more advanced controllers that can selectively draw from individual cells. As the pack ages, individual cells may lose capacity at different rates. Traditional wiring methods would dictate that once the weakest cell has been discharged, the pack must cease discharging. Their method allows the lowest cells to be temporarily removed from the circuit, and discharge continues at a lower voltage, until the whole pack is evenly discharged. Their product appears to be approximately the same capacity as a Nissan Leaf unit and is made from reconfigured battery packs. The brand of battery they are using is not specified. The company has not developed a product for market as of writing, but from the promotional material it is designed to be used on small scales, either residentially or for light commercial usage.

Spiers New Technologies

Spiers New Technology resells second-life battery packs for general purposes [47]. The packs are made from reconfigured EV batteries, and the primary value-added service that they provide is the ability to take used batteries and quickly assess, characterize, and remanufacture them into new configurations. The cycling algorithm they use has machine learning behavior that allows them to identify the performance capabilities of the pack in less time than otherwise would be required.

FreeWire Tech

FreeWire Tech is using batteries repurposed from Spiers New Technologies to manufacture a rolling storage appliance for two purposes: Mobile EV charging, and on-site power storage intended to replace conventional portable generators [48]. The system has 48 kWh of storage, and the portable EV charger is designed to “top off” 10 electric vehicles in a day, and the two modules have similar sizes, and thus likely similar capacities. The brand of batteries in use are not specified.

eCamion

eCamion is an energy storage provider which produced Community Energy Storage (CES) units from repurposed EV batteries. The CES were pad-mounted 250 kWh/500 kW units, approximately the size of a large roadside transformer. They were designed to be located at the

end of distribution trunks to provide local energy services such as energy efficiency, tie of use, demand management, renewables integration and electric vehicle charging [49].

2.2 Academic and Research Lab Projects

Academic research is divided here into: Techno-Economic, and Experimental. This is partially to reflect the split in the publications, and partly to emphasize the experimental nature of this project.

There are many high-quality techno-economic assessment papers, and many draw different intermediate conclusions with different assumptions, but all suggest there is room for a profitable re-purpose of used electric vehicle batteries, albeit in rather constrained circumstances. Because of the many papers, and because the focus of this project is not on economics or lifetime analysis, only leading papers will be reviewed.

Experiments in repurposed battery performance are less common, and when results are published, they frequently do not include enough information to replicate the results, or even the brand of battery.

2.2.1 Techno-Economic Analysis

Oak Ridge National Laboratory, USA

This economic analysis supports NREL's later findings regarding the re-use of electric vehicle batteries [50]. It concludes the profitable areas for EVs are in regulation, T&D upgrade deferral, and power quality. They operated with an assumed aftermarket lifetime of 5-10 years. They target the selling price of used batteries between US\$75-US\$220/kWh. Their third recommendation was to **Validate assumptions, benefits, and feasibility through comprehensive testing of secondary use batteries on the grid, per** *"While mathematical modeling will be quite helpful in the decision-making process, the impact of experimental data summarizing the performance and residual battery life in a given grid application will be invaluable"*

National Renewable Energy Laboratory, USA

John Neubauer et al. perform an in-depth analysis of the various costs and profits available to second-life batteries in their economic overview [19]. As a primary finding, they conclude second-life batteries can be profitable in commercial and industrial applications with a 7-10 year payback. The potential conditions are quite limited, with most examined scenarios not turning a

profit. According to the sensitivity analysis, repurposed battery prices will have to fall within the range of US\$38-US\$132/kWh.

The most significant services are frequency regulation, voltage support and backup/black start. The most available services of peak shaving and demand charge reduction cannot pay back the investment due to insufficient energy arbitrage price differential.

The analysis assumed a 20 year total lifetime of the battery before calendar effects force it out of service, with 15 years in the automotive service. Most auto manufacturers are suggesting a longer lifetime, with more capacity fade, on the order of 20+ years of life, ending with 30-40% capacity fade, and this would significantly change the payback calculations.

Another paper [51] makes use of the BLAST-V simulation tool to predict battery lifetimes using a combination of simplified physics models and large empirical datasets. Using the results of the simulation, Neubauer makes several important predictions:

- Repurposed batteries can last more than 10 years in the new application, depending on the service (e.g., peak shaving, or daily cycling), but are expected to last from 4-10 years.
- The majority of batteries should only be expected to become available at the end of a 15-year automotive service life.
- Driver patterns and climate have the largest effect on battery degradation.
- After 25 years of life, performance losses will range from **65-75%** capacity remaining.
- **Keeping batteries cool** is the most significant controllable factor in extending lifetime.

Neubauer's final work focuses on identifying the most difficult problems in the mass usage of repurposed EV batteries, and how to make best use of them. The most promising application identified in this publication [35] is the replacement of natural gas peaking plants with bulk energy storage. This is attributed to the high price of energy during peak hours, and the relatively benign duty cycle (<1h discharge). Interested parties should focus their efforts on developing megawatt-scale installations that minimize integration, balance-of-system, and installation costs. The systems should monitor the health of the batteries to enable timely replacement.

The market share of the most profitable services (frequency regulation, etc) is expected to be half the size of the available supply of batteries, therefore investment should be made in opening the largest markets for service (Demand charge reduction, energy arbitrage).

It is worth noting that the sensitivity analysis showed that most scenarios were not profitable with storage functioning as peaker plants. Thus, the economic case will need to be developed further, considering carbon taxes or other policy effects.

California Energy Commission, USA

Williams and Lipman find that second-life usage of electric vehicle batteries could reduce the cost of leasing an EV by 1-22%, depending on various assumptions [52], by adding value to the car at the end of life, which would allow a leaser to reduce their rates. The application used was residential energy storage providing distributed grid storage services. All major services were examined and priced. Of the list, regulation was determined to be the most profitable, and stacking of services was extended to include energy timeshifting, T&D deferral, demand charge management, etc. Brett highlights the significance of variability in pricing of services, and the uncertainties of analysis, with a focus on the following factors: The real ability to capture multiple services, the value of performing power conditioning services like area regulation, and more accurate capacity decay models.

Sandia National Laboratories

Sandia National Laboratories has one of the earliest mentioned sources of a model and cost estimate for receiving, breakdown and repackaging of electric vehicle batteries at a centralized distribution center, akin to *Spiers New Technologies [21]*. At the time, the dominant chemistry was Ni-MH, and Li-Ion was only one promising chemistry. This report is mentioned for historical interest, and its apparent influence in the direction of investigation of research to follow, suggesting centralized repurposing plants where batteries are stripped down to cells, assembly-line style, and rebuilt into wholly new assemblies. The proposed concept in Chapter 3 differs greatly from this suggested technique.

Others

Waterloo University, Canada

Ahmadi et al. conclude by modeling the decay behavior and usage scenarios of electric vehicle batteries [53] that batteries will enter service at 80% of original capacity, validating the general

assumptions of the second-life market, and lose a further 15% over 10 years of second-life usage.

Aston University, U.K.

Strickland [54] receives 2 Honda Insight batteries and measures their capacities on arrival, finding them to be at approximately 80% of original capacity, holding with the general targets of end-of-vehicle capacity. They further use a simulation of capacity decay as a function of service performed to conclude that the useful second life is from 3-15 years, depending on historical usage.

2.2.2 Experimental Projects

University of California, USA

The University of California-Davis, established a microgrid to simulate a local winery implementing solar and storage from 20 Nissan Leaf packs. The packs were disassembled and recompiled into rack-mounted storage. No experimental data is available from the project. The estimated performance would store 50% of daily summer overproduction of electricity.

Tong et al. at the University of California-Davis confirmed the basic ability of a battery pack composed of used cells to fulfil basic grid services [55]. Tong used 2x172 Thundersky battery packs separated and reconfigured into an 8.35 kWh battery pack. The cells had suffered a wide range of capacity decay from 60-90% of rated capacity. The battery bank was used to optimize the operation of a roof-mounted solar panel located on-site. Tong concluded that the repurposed batteries could reasonably be implemented in certain environments to profitably increase the effective capacity factor of the solar panel. Caution should be taken with this work in modern applications, in that their batteries were not from any of the major modern electric vehicles, and that the individual cells were of widely varying leftover capacity, limiting the relevance of their research with modern batteries and modern standards of quality control.

Electrovaya- Manitoba HVDC, Canada

The Manitoba HVDC research center published preliminary performance results on repurposed batteries [56]. Electrovaya provided five Li-Ion batteries from EVs which were independently converted to a high DC voltage common bus and linked to a grid-tied 600 VAC converter. This was combined with a small diesel generator and power cycler allowing for simulations of an

arbitrary grid. This was used to perform simulations for island microgrids, with the intention of reducing diesel consumption.

The energy efficiency of the batteries and inverter was between 60-90%, and usable capacity was approximately 80% of OEM stated specifications. The absolute capacity is unknown, as is the model of battery.

Sandia National Laboratories, USA

Sandia National Labs performed a demonstration using five repurposed electric vehicle batteries, intended to supply 2-5 homes [57]. The estimated capacity of the test was approximately 80 kWh, from repurposed *Chevrolet Volt* batteries. Three experiments were performed, each showing the fulfilment of a service: Load flattening for T&D deferral, solar integration, and islanding. When operating to reduce peak power consumption, the peak was reduced by approximately 50%. The system served as a UPS backup, providing power to the home in the event of a simulated outage. The batteries firmed the predicted forecast of a roof-mounted solar panel in the same building.

The study did not quantify the performance of the batteries against a known metric, and only one type of battery was used. This study therefore serves to justify the supposition that EV batteries may be re-purposed for new functions.

IK4-Ikerlan, Spain

Martinez-Laserna et al. performed cell-level testing of EV batteries in two applications, with periodic cycles to check the health of the cell [58]. Martinez-Laserna does not specify the brand of battery that the cells were drawn from. The services simulated were residential PV demand-response and grid-scale PV smoothing. One month of both services were performed, following simulated usage profiles, with the residential service being scaled up by a factor of 4 to accelerate aging. The month-long cycles were repeated until cells became unsafe or unusable. Periodic capacity and impedance testing was performed, generating a cycle-life dependent second-life capacity decay curve, from experimentation, which is a rare set of data. Martinez-Laserna concluded that: 1.) Cells with large internal DC resistance were unlikely to survive usage, 2.) The cells showed an “aging knee”, a concept popular in literature, but not usually shown due to the length of testing required, 3.) Batteries entering their second-life usage with capacities at or below 70-80% are unfeasible from a technoeconomic perspective.

Martinez-Laserna uses new cells that have been forcibly aged, rather than cells that have come from EV service. The source of their cells may have been compromised, or that the cells were driven beyond manufacturer specifications, because many of their cells (3 out of 8) suffered catastrophic failures rather than gradual decay, once entering the period of testing designated as “Second-life”. Further, the conclusion of an aging knee is not well-grounded because 1.) no standard criterion of a knee was established in advance, leading individual cell capacities to be judged as having a knee on subjective grounds, 2.) no trendlines were overlaid on the capacity decay curves to demonstrate a sharp change reflective of a knee rather than an exponential decay, and 3.) not all cells tested of their set of 8 demonstrate a sudden change in rate of decline at any point in their testing.

Martinez-Laserna also does not show any absolute measurements of capacity, nor of coulombic or energy efficiency. The success at following the power signal is not qualified, nor is the throughput.

2.3 Summary

2.3.1 Limitations in literature

Industrial

The original equipment manufacturers maintain sensible limits on the published operational parameters for electric vehicle batteries (e.g., voltage and current limits, coolant temperatures, fusing, charge/discharge asymmetry, etc). While this is understandable, it means that third-party operators need to make informed choices based on engineering judgement, rather than making use of the original manufacturer specifications. All manufacturers so far have been separating their batteries into granular components, and reassembling them into a new pack configuration. This includes third-party manufacturers. Using the original pack configuration would save time and money.

Most OEMs and third-party developers are also focusing on small-scale applications, Daimler and Nissan being the notable exceptions. This means there is opportunity for investigation into using many hundreds of EV packs in synchrony at the grid level.

Academic and National Laboratories

There exist several high-quality, in-depth techno-economic analyses, and dozens more small papers which address small subsets, but they share a key weakness: Sensitivity to economic

simulation parameters. In short, the outcome of the economic payback depends on several numbers which are highly variable, uncertain or indeterminate, and likely to change soon, and very dependent on local factors: the fees available for performing services, the price of new and second-life batteries, the capacity remaining upon transition to second-life service, and the lifetime throughput of a battery. Small deviations in these numbers can dramatically alter the profitability of the proposed concept. The addition of a carbon tax would also dramatically change the economic viability of using second-life batteries.

This is especially problematic because most of the economic papers conclude that batteries may be technically viable or promising, but the margins are very slim, and most simulated scenarios do not turn out a profit. For this thesis, it serves as a reminder that driving down cost wherever possible is critical for success.

The experimental papers and presentations released so far have been very brief. Where information is available, it does not follow a replicable standard, and in no case have different brands of batteries been compared side-by-side.

2.3.2 Limitations in existing pilot projects

The existing pilot projects and companies are re-using electric vehicle batteries. Most of them are targeting domestic markets or small-scale commercial/infrastructure storage, with 1-10 batteries per installation.

The current uses are unsatisfactory for the following reasons:

- Domestic markets do not usually have access to demand charge reduction, a key revenue stream for energy storage.
- Applications that don't have dedicated technicians or comprehensive fire protection systems are at greater risk of fire hazard, which is already a hazard with lithium-ion batteries, moreso if they are used, and coming from unknown backgrounds and usage conditions.
- Electric vehicles in circulation will be heterogeneously dispersed, and collecting packs of only one type is made harder by their geographic dispersion, rather than collecting all pack types available locally (Shipping can account for up to half of refurbishing costs, per [50]).

- Used batteries are at greater risk of sudden failure due to contact faults or other small, critical errors. A system which cannot quickly and easily replace batteries as they fail is not well-positioned for providing reliable service.
- Using only one type of battery will prevent the system from taking advantage of the relative strengths of different sizes, configurations, and chemistries of the variety of EV battery packs. In addition, even the same brand of battery pack will evolve over time, changing its capacity, communications code, and layout.
- All industrial projects under discussion, OEMs and third party, are separating their battery packs and reconfiguring them into new packs. This represents a large investment of money and time into shop work, when most economic analyses do not suggest there is wiggle room for these expenditures.

2.3.3 Selection of research direction

The Concept

The concept proposed in this thesis is in response to the existing projects not optimally using repurposed batteries. Ideally, a design should capitalize on the strengths of used batteries being a cheap source of storage while sidestepping or avoiding their weaknesses of unreliability and uncertainty. Most existing projects attempt to manage it by exerting greater quality control, rather than allowing the variances to be averaged out *en mass*. And a larger storage plant is needed simply due to the scope of transitioning the electricity grid. Daimler and Nissan are the only OEMs testing a 10+ MWh-scale system. The Daimler project is making use of only their own batteries, which are from a car which has not sold nearly as well as its competitors and is constrained as such. Therefore, a new concept should be conceived.

The Experiments

The technoeconomic work performed by NREL and others clearly indicates that the possible success of second-life systems depends on several factors. The price and lifetime of the batteries is the most significant but is also out of the sphere of influence of third-party operators. The experimental work which is available is not comprehensive, not comparative, and not standardized and easily replicable. For third-party operators, critical information is missing, that being a description of how the most popular electric vehicle packs perform, especially in comparison to each other, and how to automatically generate a performance profile of any given battery. Thus, this research thesis focuses on doing comparative performance testing of

the most popular batteries while following a standard method which is fully detailed and replicable.

Chapter 3 Mixed Battery Array Concept

The concept proposed in this section is to collect and aggregate hundreds to thousands of used electric vehicle batteries in a dedicated warehouse and use them in large numbers to offer a range of electricity grid services like peak shaving and frequency regulation. Unlike existing projects, it allows for and encourages the use of batteries from different brands and can handle batteries of different states of health. The usage of batteries at this scale mitigates some of the inherent risks of used and repurposed batteries: the possibility of thermal events, the mixed lot of batteries available to a local operator, the high level of skill required to assess and adapt used batteries and buffering the possibility of individual failures and variation with many units. This could range from cell failures in individual cells to design faults affecting an entire model of battery. In such a case, the extraction and replacement of a faulty battery module is a simple and quick procedure.

A new control strategy is required to identify characteristics of each used EV battery, select the most appropriate batteries for each electricity service, and predict and compensate for degrading performance of batteries as they are further used.

Manufacturers of electric vehicles have advantages when re-using their own batteries: they have a wealth of data from the operation of the vehicle to correctly identify the health of the battery, they know the original specifications in detail, and they know the protocols for communicating with the original battery management system (BMS). For third-party operators, the converse of each of these points holds. Because the OEM has sufficient information and expertise, and their scope is restricted to only in-house batteries, this research is directed towards third party integrators/aggregators who wish to operate a mixed battery array and must do so from a position of uncertainty.

3.1 Description of Electric Vehicle Batteries

In this research, modern electric vehicle batteries can be assumed to have some common features. Most batteries have a common bulk geometry, similar to that shown in Figure 10.

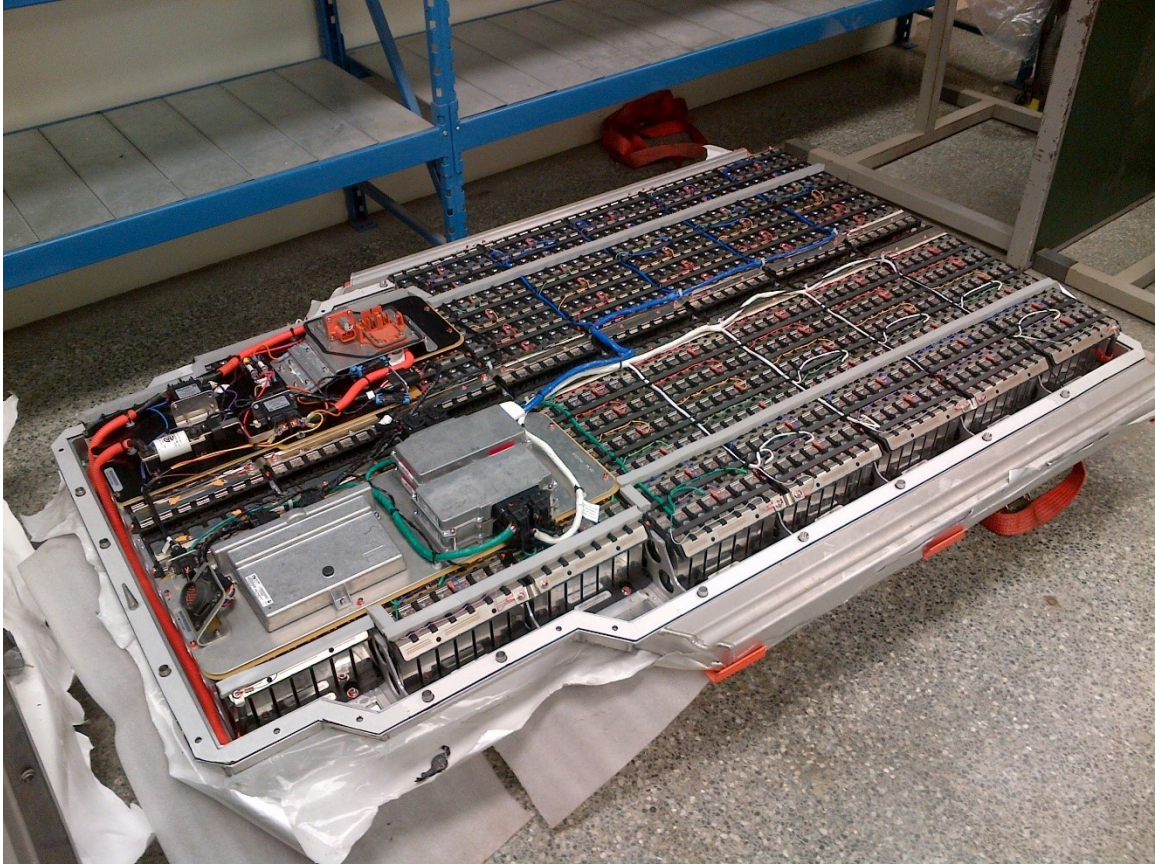


Figure 10- Lishen EV-LFP battery as an example of flat-pack layout. 1.14 m by 1.92 m by 24 cm.

This is called the a “Flat-pack” or “Floor Pack” design. This design is made to fit in between the wheel wells and under the seats of a modern sedan car. There are exceptions, such as the Chevrolet Volt, which has a T-shape, but fits within the same envelope. Notably, its successor car, the Chevrolet Bolt, does use the flat-pack shape. All packs have a battery-management system from the manufacturer, which taps every cell group for voltage measurement. All have thermistors for temperature measurement, as a safety requirement. Each has a packing case which protects and, in some cases, carries coolant lines. Table 2 summarizes the most common, hence the most available, EV packs on the market.

Table 2- Description of Popular EV Batteries

Nissan Leaf	A battery for a mid-size passenger car. Multipurpose, passive cooling, no clear strengths or weaknesses.
Chevrolet Volt	Plug-in-Hybrid compact car designed for short, high intensity use in city driving. Smaller battery capacity than a full EV, but well adapted for thermal management. Complex internal layout with many contact faces, liquid seals. Liquid-cooled.
Panasonic Tesla	Large high-performance sedan designed for high quality and long-range driving. EV battery designed for fastest charging, high peak power output. Uses 74 cells in parallel, far more than other brands, corresponding to high peak current. Liquid cooled.

3.2 Basic Layout

3.2.1 Racks and Stacks, Bays and Trays

The mixed battery array is intended for grid-scale storage provision. To achieve this, hundreds to thousands of batteries must be mounted within a limited footprint. Rack mounting akin to server racks are suggested for this, adapted to the size and requirements of electric vehicle batteries. Figures 11, 12, and 13 sketch the general appearance and layout of the mixed battery array. Figure 11 shows an example floor plan, including receiving bay and rack mounting. The two cooling methods are displayed side-by-side. Figure 12 shows a side view of an example rack, with the various bays highlighting a single feature at a time. Figure 13 shows a detailed view of a single bay, showing the battery, BMS and main power connections.

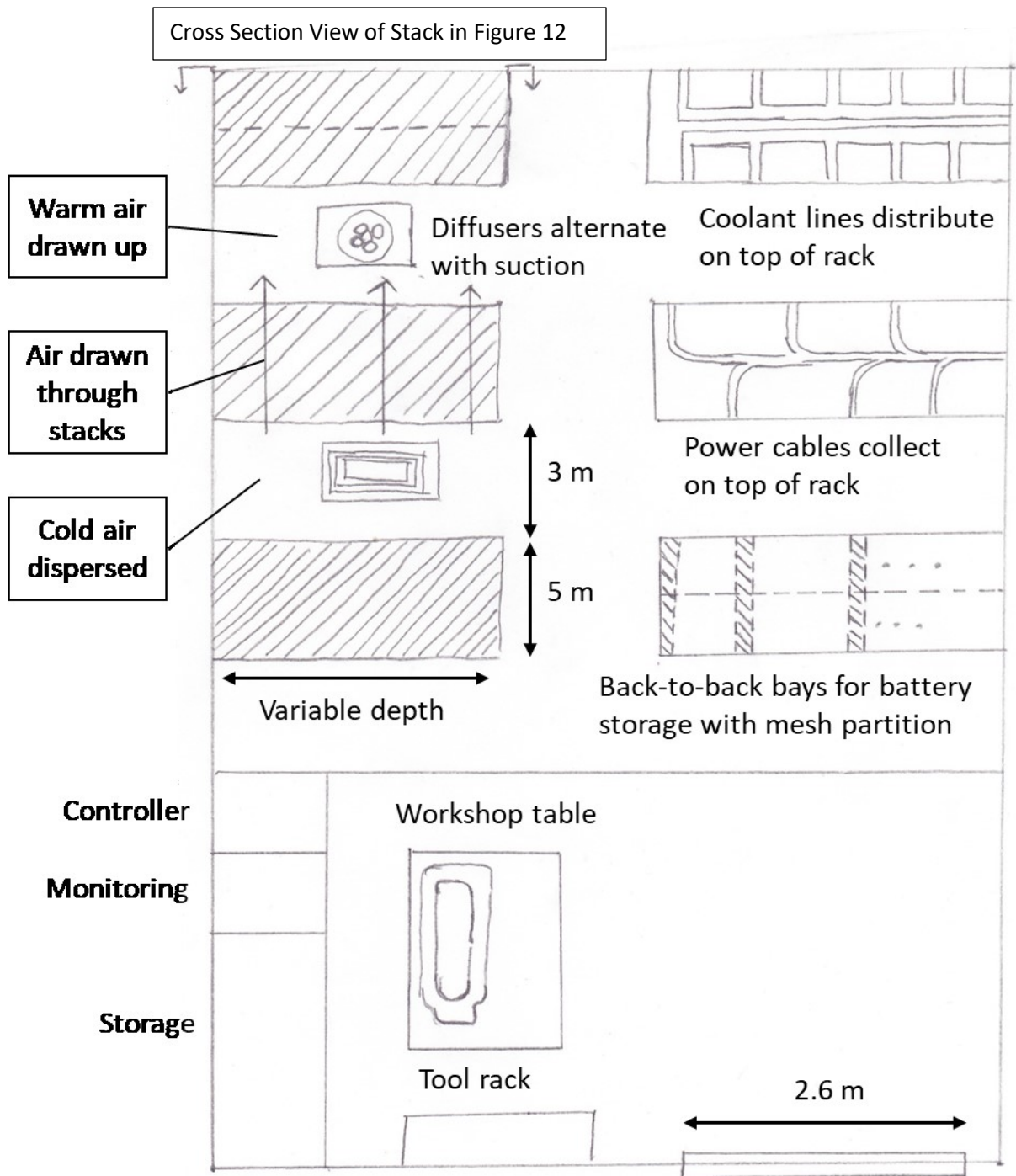


Figure 11- Conceptual Drawing of Mixed Battery Array Plant with Detail of Bays and Racks

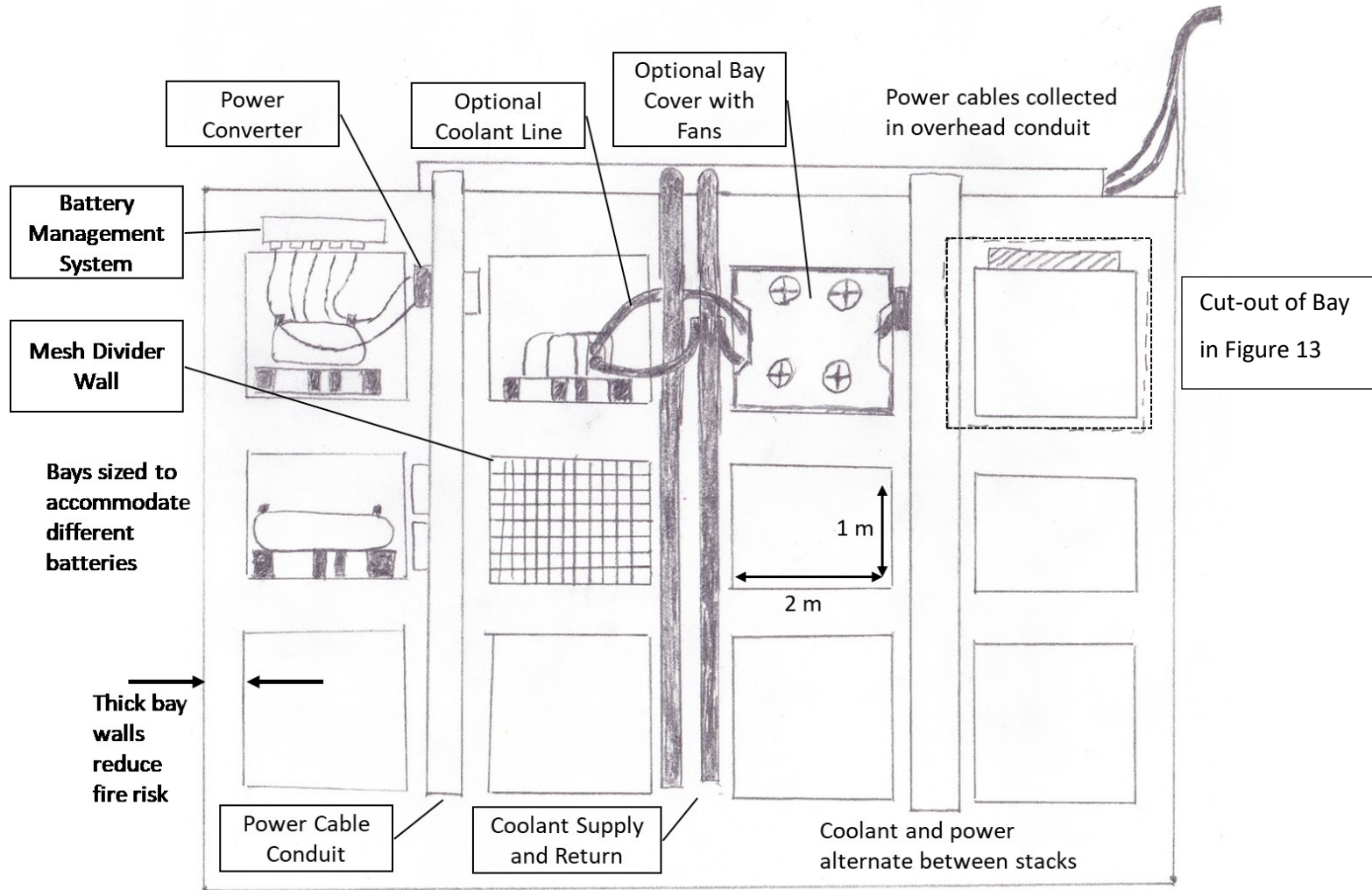


Figure 12- Detail view of Rack

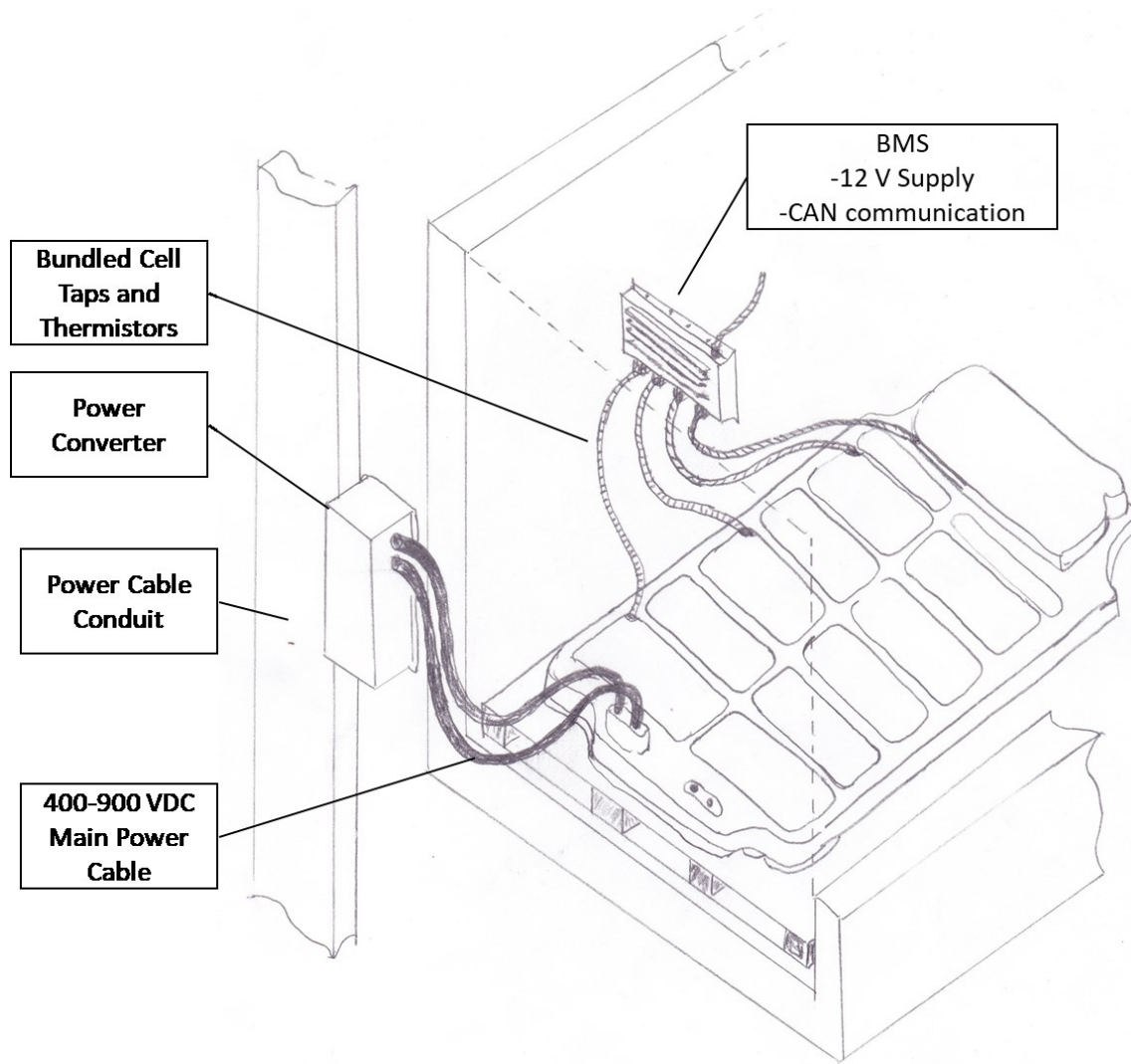


Figure 13- Detail View of Bay

Each battery can be assumed to fit within a certain bay size⁷, and has common requirements of DC power connection, BMS communication, and thermal conditioning coolant taps. When the battery reaches end-of-life, it will need to be replaced rapidly. Therefore, each bay will hold a tray with sufficient space to hold a battery of the maximum nominal envelope, which can be forklifted in without adaptations or fasteners.

Each bay will have standard connectors for electrical and cooling connection, feeding in from the front, where the battery contacts will be located. Each bay will also have fire and electrical isolation from the others, such that in the event of a fire the warehouse will not be compromised.

3.2.2 Environment

Automotive applications are one of the most difficult environments in which storage operates. It has wide ranging temperature (-30 to +45 °C), is subject to vibration and mechanical abuse, can be used at peak power (hard acceleration), and can sit idle for months (e.g. driver on vacation). NREL [51] states that charging temperature is a crucial factor in the health of the battery, causing lifetime variability of up to 15%. By contrast, the MBA plant would have climate control, maintaining a tight temperature band on the optimal temperature, typically 20 °C

To maintain optimal temperatures, the batteries would be kept in a climate-controlled warehouse. One large cooling plant can feed cold air into the ventilation system and chill the thermal conditioning loop. For air-cooled batteries, fans would drive air through the stacks, keeping the casings cool. For liquid-cooled batteries a system of coolant lines circulates a chilled fluid to keep the batteries at an optimal temperature, with valves allowing flow into each battery as needed from the loop.

Vibrations will not be an issue in the plant, apart from earthquake safety, which is outside the scope of this research.

3.2.3 Power Architecture

To exchange power between the battery packs (DC) and the electricity grid (AC), a converter system must be used. The battery packs nominally range in voltage from 150 to 900 V DC. For example, hybrid vehicles such as the Honda Insight or the new model Prius operates at a the low

⁷ Ex: 1m by 2 m by 0.5 m, large enough to fit all under-floor model batteries.

end of this range, nominal electric vehicles for consumer markets such as the Leaf or Bolt operate between 350-400 V, and commercial or performance vehicle such as the Porsche Mission E operate at the top of the range.

The facility will likely connect to a collector/distributor or have an internal line which serves the same purpose, which ranges from 4 to 36 kV AC, which is stepped up to 60-500 kV at a substation. Because each pack may have a different DC voltage, a wide DC range converter is required to transition from the pack to the common bus voltage. Further, because of the wide range of power capacities in the packs, modular converters of approximately 50 kW per unit that can be connected in parallel are used, rather than keeping a stock of differently sized converters. In this way, low power and high power packs can be joined to a common bus.

The common bus can be AC or DC power in different architectures. A final transformer is required to raise the voltage to transmission level.

Distributed DC/AC conversion to a common AC collector system is suggested as a model hierarchy because it has isolation and can draw on the technological maturity of the solar and wind converter markets, and because AC bus components are more readily available. Example power architectures for DC and AC collectors are shown in Figures 14 and 15.

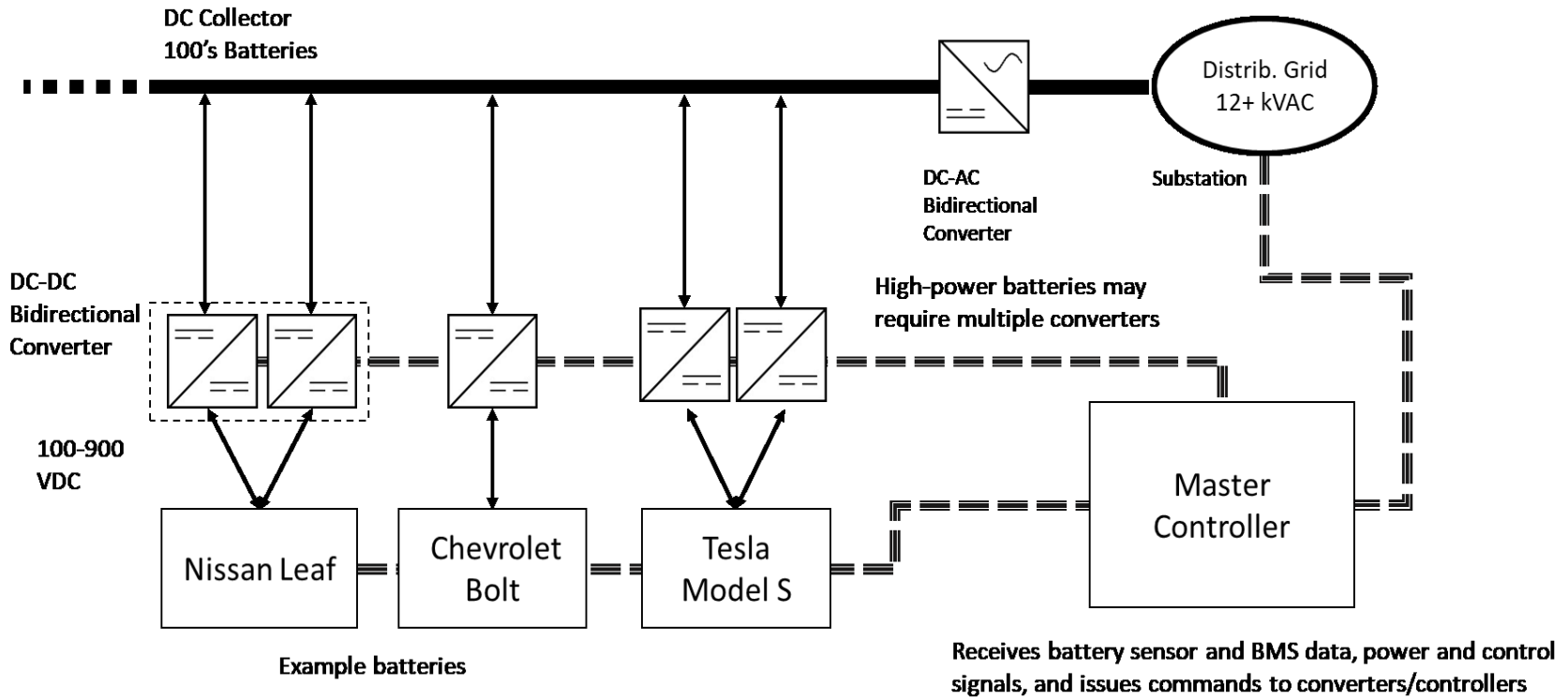


Figure 14- Wire Diagram of Example Local Scale Plant Hierarchical Layout, DC Collector

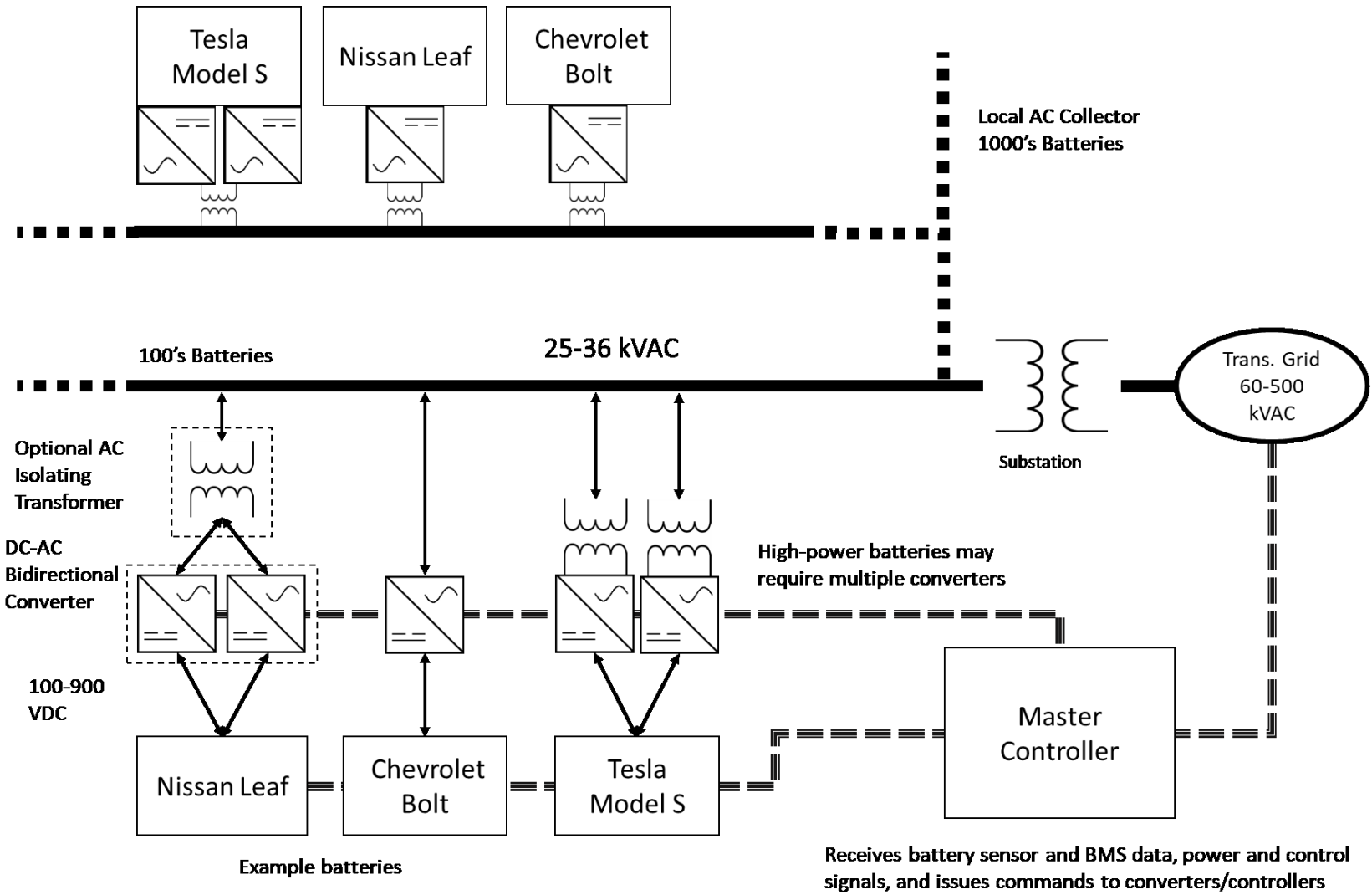


Figure 15- Wire Diagram of Example Central Grid Scale Plant Hierarchical Layout, AC Collector

3.2.4 Qualified Technician

Receiving a battery will be done in a shop section of the warehouse. A basic inspection will be performed to identify the battery's general condition. A wide array of possible issues may be present in a used battery pack, and it is unlikely that clear and comprehensive documentation and history of the battery pack will be available. The pack may have bad cells, faulty sensors, corroded contacts, blown fuses, or collision damage, among other possible problems. Therefore, having a technician dedicated to the warehouse whose responsibilities receiving and assessing of batteries, basic repair⁸, and battery installation should improve the operational efficiency of the array.

The basic procedure before installation is:

1. Identify the pack by original manufacturer and model, and reference nominal values of voltage (V), capacity (Ah), mass (kg), cell count and configuration (xPyS).
2. Apply a bar code or tag to accompany and uniquely identify the battery.
3. Perform a visual inspection, check for physical damage, leakage, for odors of leaking electrolyte, burned plastic, etc.
4. Test each cell group for open-circuit voltage and internal resistance. Analysis of data will help identify non-uniform cells and these can potentially be removed or electrically isolated by means of jumpers.
5. Remove existing BMS (See 3.3.1) and replace with a single standard BMS using conversion connectors.

The pack can then be installed by forklift in a bay, connected to a converter(s), coolant lines and the master controller. Subsequently, the master controller characterizes the battery with baseline performance tests, and places it in operation. See section 4.3 for details of how to characterize a new battery in the controls system.

⁸ E.g., jumping bad cells so as to remove them from the electric circuit.

3.3 Details of Layout

3.3.1 Battery Management System

Every lithium-ion battery requires a Battery Management System (BMS), responsible for monitoring and evaluating cell group voltages for safety, balancing the voltages of individual cells so they are evenly charged, and commanding a safety shutdown in unexpected situations.

When adapting the pack for use with a master controller, there are two battery management alternatives:

The first alternative is to use the native BMS of each pack and version, and track changes to it assiduously. This provides the best protection and operation of the battery as the BMS was designed specifically for the battery pack. However, the original BMS system is usually proprietary, and may prohibit certain battery operations which are possible in grid storage service but are not common in EV service. Each manufacturer and possibly each new generation of each battery has its own system of messages in OBD2⁹ or CANBUS¹⁰ format. It is critical to know these messages precisely, as they carry all the relevant pack safety information.

Unfortunately, the messages are proprietary, and may change without notice. Therefore, a dictionary of the messages must be supplied by the OEM. Further, the messages may not even carry all the required information for the control system of the plant. While the technician could keep the message database updated, the overall system is likely to change abruptly and create a safety risk. In addition, if faulty cells are bypassed, the BMS would immediately enter an error state due to a missing cell reading. At low capacity, the BMS may attempt to prevent the pack from operating at this reduced capacity due to built-in limitations set by the OEM, which may be above the working capacity for grid operation values. Therefore, this alternative is not optimal.

The second alternative is to remove and replace the original BMS with a flexible custom model that is uniformly used for all battery packs in the plant. Upon receipt of the pack, the connections between the pack and the original BMS would be severed, and a new custom BMS adapted. In doing so, the new BMS could operate on the same communication language as the facilities distributed converters, and report back to a central controller. Adapting the existing wiring harness may be done by:

⁹ OBD2, for On-Board Diagnostics, is the internal communications protocol of most vehicular BMS's.

¹⁰ CANbus, for Controller Area Network is a common communications protocol for vehicles and BMS's.

1. Creating a custom-fabricated connector-adaptor to convert between a specific brand of battery and the standard BMS connector.
2. By clipping each sense wire individually into a premade piercing contact.
3. By snapping a penetrating contactor onto the wire.

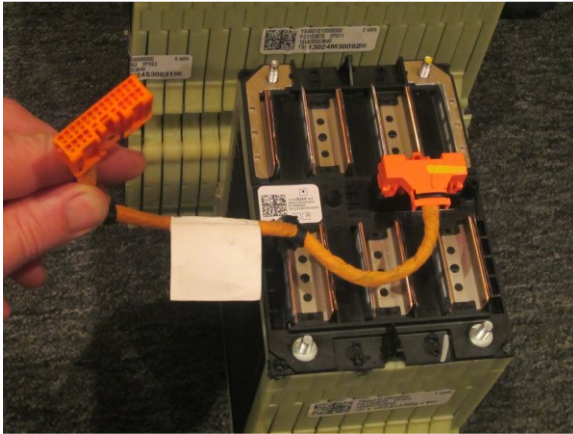
For 2 and 3, the usage of labor would not be profitable per the scale of NREL's analysis [51].

For some models, this is the only option, as there is no plastic connector, such as the Tesla, where that cell tap wires are soldered directly to the onboard BMS. The additional cost of labor and custom BMS must be accounted for when estimating the profitability of a pack. The BMS can be re-used for successive packs, saving on cost when batteries are replaced. Using a secondary BMS will incidentally require wiring for power to be supplied to the BMS itself, in the event that it cannot be powered from the battery directly. The consistency, reliability, and uniformity of implementing a common BMS likely outweighs the cost savings of re-using the OEM BMS.

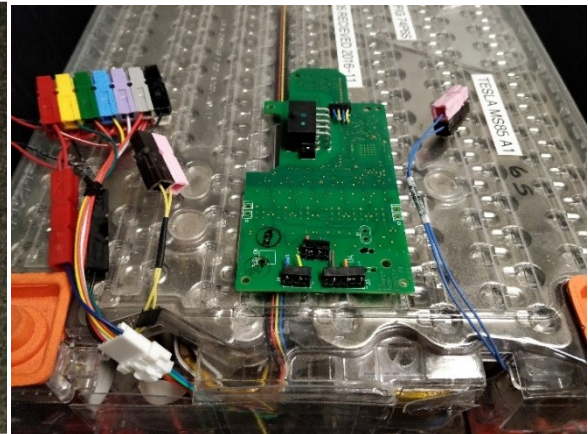
Pinout Adaptors

If a standard replacement BMS is used, an adaptor may be developed specific to the battery model, to convert between the pinout of the battery and the pinout of the BMS. Each battery model has a different pinout (See Figure 16), and hence a stock of many brands would need to be maintained.

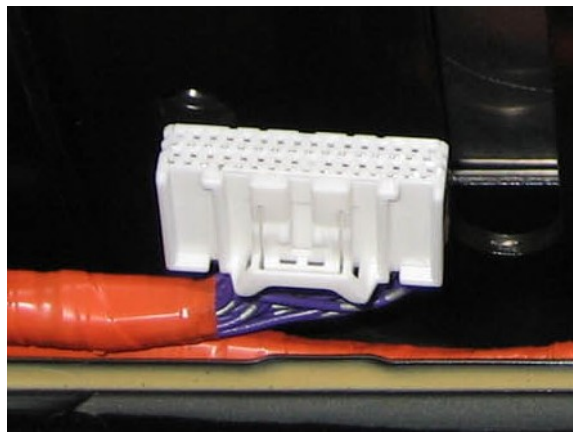
a)



b)



c)



d)

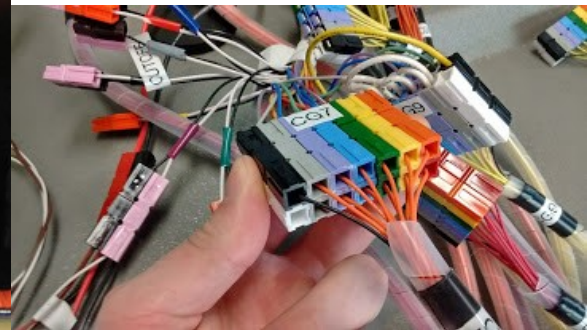


Figure 16- BMS connectors of a) Volt, b) Tesla, c) Leaf and d) custom lab configuration. Tesla BMS board shown with severed connections, and OEM wires with new connectors, as it does not have an insertable connector.

No matter which alternative is used, a communications network must exist to report back and forth between the plant, master controller, BMS, and converters. A CANBUS area network may be feasible or an alternative communications protocol may be used.

3.3.2 Temperature Measurement

The temperature of the battery is a critical measurement for safety. All packs have a method of measuring this with built-in sensors however the precise sensor model may not be known. Further, since most of the sensors are inside the pack, visual inspection may be difficult or impossible. Despite this, using these sensors is a good option when possible, because the sensors are ideally placed and high quality. To make use of existing thermistors, a voltage must be supplied by the same electrical connection network, and a measurement must be taken.

The temperature sensors that come pre-made with the pack may be supplemented or replaced with external sensors, such as a thermocouple.

3.3.3 Thermal Requirements

The plant must have a dedicated cooling system, at minimum for the whole warehouse, to counteract the heat dissipated during battery cycling. The cooling system will also be responsible for removing heat from the dedicated liquid cooling lines to specific batteries. Specifics on cooling the battery depend on what method of cooling is used: passive, air or liquid.

Passively cooled

Passively cooled packs do not have a built-in forced air cooling system, nor a finned heat exchanger. As such, when the battery is in the bay, all its cooling will be via heat transfer between the case and the ambient air. Forcing the air across the case will improve the heat transfer rate. This can be done by either: 1. Having a fireproof bay open on two ends, with fans to force air through the whole cavity, holding either one or two batteries, or 2. Having a single open end, and a duct which sucks air from the back of the cavity and blows out the front. In either case, no air passage should exist between adjacent bays, so as not to compromise the fireproofing. Depending on the usage scenario for the pack, fans may not be required if the pack has adequate time to cool between service calls with no active air circulation, only the natural convection of the bay interchanging with the plant's air conditioning.

Air-cooled

The same fan system which cools the passive batteries can be made use of for air-cooled packs. Depending on the specific model, the pack may have fans which circulate ambient air through the pack, which would work in tandem with the whole-cavity air exchange on their own, or fins to improve the area for heat transfer. If fins are in use, it may be cost-effective to create an adaptor for the duct to channel air directly through the fins to improve their rate of heat transfer.

Liquid-cooled

Liquid cooling is more complex than air cooling. The following factors must be handled:

- The liquid loop must be maintained at the correct temperature, approximately 20-30 °C supply.
- The liquid loop must circulate at sufficient flow rate.

- The liquid loop must be filtered to prevent debris from clogging coolant pipes.
- The coolant must be distributed between packs in the MBA. This is accomplished by managing the inlet pressure to each pack with the master controller.
- The coolant must be selected to have low corrosion or deposition with the batteries.

Specifying such a system is outside the scope of this research, but it is worth noting the difficulty of cooling such a large and diverse array.

Each battery model has a different coolant manifold, including port sizes. For example, the Tesla has a 1/4" port, where the Volt has a 5/8" port. Connecting each battery to the coolant lines could be done with custom adaptors per model, or with a universal adaptor that clamps on the port flange.

Cooling Loads

The thermal conditioning system load can be estimated by examining the cycling throughput and energy efficiency of the tested batteries. The discharge capacity of a typical Tesla battery pack (rated 85 kWh) operating at a 0.5 h rate is approximately 46 kWh. A complete cycle conducted at these rates, including time for thermal recovery, would take approximately 2 hours, and achieve a round-trip energy efficiency of 82%. This equates to an average heat dissipation rate of would require 5 kW. Contrasting this with a gentler cycle and more efficient battery, a 4 h discharge rate using a Chevrolet Volt pack would be achieve rated capacity of 16.6 kWh. Using a total cycle time of 8 hours and round trip energy efficiency of 97%, gives an average heat dissipation rate of 64 W.. With one thousand batteries, this could range from 2.5 MW to 50 kW of cooling- a factor of 50 between them.

Local Liquid Cooling Heat Exchangers

As an alternative to having a hybrid air-liquid cooling plant with coolant lines running to every battery bay, the cooling plant may only provide air conditioning. For batteries that require liquid cooling, an air-liquid heat exchanger could be installed in the bay, with a fan forcing the cool ambient air across the cooling manifold.

Only Liquid Cooling

As a third possibility, no air conditioning may be used, instead cooling every battery with liquid cooling. For air-cooled or passive batteries, a fan with a heat exchanger could be installed across the bay, linked to the coolant circulation lines. By forcing the cool air through the bay, air

conditioning behavior can be emulated. Because all recent (Past 2 years) major models of PEV have had liquid cooling, it seems likely that the market will move towards a default usage of liquid cooling. If this is the case, the coolant lines will suffice for the new majority of batteries, and the operator can spare the expense of air-conditioning, including ducts, fans and heat exchangers. This option would also potentially increase fire safety, by making the front fan panels fireproof, and hence lowering the probability of a dangerous thermal event spreading or endangering staff by containing the potential fire in an enclosed space.

3.3.4 Control Strategy

Characterizing the Battery

When first installed in a bay, the battery should be run through a standard deep discharge test with periodic current pulses to establish its current performance characteristics, such as:

- Power capability.
- Internal resistance profiles- at rest, and as a function of capacity.
- Coulometric capacity.
- Energy capacity at a nominal hour rate.
- Roundtrip energy efficiency.
- Thermal response.

As the batteries are used in normal operation, these parameters will be tracked with periodic test cycles devoted to verifying the current battery capacities. Three deep discharge CP cycles at a low hour rate will measure the present energy capacity and including pulses of high power at intervals will measure the internal resistance of the battery, which is a good proxy for its health in terms of electrode degradation. Conducting these tests monthly on each battery allows the operator to have an accurate model of the performance capabilities of each battery. Following the trends of these measures over time allows the operator to make informed decisions about the remaining lifetime of the battery, and how best to maximize expected profits from the expected remaining throughput. Sudden rises in internal resistance or a large change in the voltage-capacity curve would also indicate impending failure and allow the operator to remove unsafe batteries before any critical events.

Controlling the Mixed Battery Array

When the battery enters normal operation, a new control strategy will be used, called a **Hierarchical Control Strategy**, based on selectively using subsets of the available batteries to fulfil service calls and intelligently sharing the load among that subset of batteries.

The control strategy must decide between different combinations of batteries to fulfil electricity grid service calls; for example, to satisfy a demand for 100 kW, should 1 pack be called at 100 kW, 10 packs for 10 kW each, or 100 packs for 1 kW each? Should different packs be called on if the expected duration is 10 seconds, 10 minutes, or 10 hours? What range of battery capacity will be used? Should the lifetime throughput be used up as quickly as possible to make way for the next pack? Will there be better benefits to maintaining the battery through gentle usage? How much energy should be left for potential future calls?

These questions can be divided into two broad categories, one where many questions are general to energy storage systems (ESS) of many different technologies, and another which specifically relates to building a combined battery profile second to second in real time operation, from a mixed pool of resources. This second group of questions are outside the scope of the present research, which focuses on the relative performance of EV batteries, and their ability to provide services. Nonetheless, these questions are significant, and must be addressed in future research on the topic.

Factors in common to many ESS include:

1. Accurately costing and predicting forecasted demand, to position the energy reserve of the system for optimal returns.
2. Determining a consistent basis for comparing actions (Creating a cost function).
3. How to effectively stack services such as energy arbitrage and frequency regulation, accounting for extra revenue but balanced against the possible penalties for violating agreements to perform services.

Specific issues to be addressed with the Mixed Battery Array control strategy include:

1. The life of the pack is not well-determined, which interferes with allocating the usage of the pack according to expected performance.
2. Tracking and comparing a multitude of different performance factors for hundreds of packs.

3. Assembling a sub-array of batteries of varying size and condition, when the usage profile could change at any time due to service stacking.
4. Comparing the value of degradation due to cycling to degradation due to calendar life.
5. Distributing the needed service calls among batteries in an optimal manner.
6. Deciding between packs with different strengths, such as peak power, sustained power, maximum energy capacity or energy efficiency.

Creating this hierarchical control strategy will be a focus of future research

3.4 Strengths of Mixed Battery Array Concept

3.4.1 Safety

Using separate bays for each pack mitigates propagation of a thermal event (i.e. fire), which is the single largest hazards of using Li-Ion batteries. If this were to happen in a home, or in a small roadside box, the fire could propagate. Isolating the EV packs from each other, while also having properly designed fire suppression and ventilation systems with trained technicians on hand, is proactive, diligent management.

Isolated systems at the residential or commercial level are less likely to have properly updated and carefully managed control systems. Homeowners are not battery experts, and while isolated systems could be remotely monitored, a lack of trained expertise represents a risk. By collecting the used EV packs and operating them with their original pack and configuration, and trained personnel, the dangers of thermal events and active high voltage connections are minimized.

Finally, centralization allows a single large capital investment (i.e., an automatic foam extinguishing system) to be much more manageable, as the cost is only applied once, but the added security of such a system applies to every battery pack housed in the warehouse.

3.4.2 Flexibility

By having a warehouse capable of housing and making use of multiple pack types, the supply can more easily be filled by the local used EV market. As transportation costs may comprise half of repurposing costs [59], any means of reducing this expense is of great benefit.

The local supply of batteries will vary with respect to model, age, wear, mechanical and electrochemical condition. The mixed battery array concept can accommodate this range of batteries due to its unique electrical, physical and control systems. This is in contrast to

conventional industrial perspective, which strives for homogeneity in used packs before repurposing.

The location of the plant affects the kind of services it may best perform. If placed close to distributed generation, it may serve to integrate intermittent generation sources, and regulate the power of wind turbines and solar arrays. It can also deal with ramping of renewables, such as power fluctuations from clouds or gusts of wind.

If the warehouse is located near end-users, it can reduce peak values of power consumption and defer transmission/distribution upgrades. It can also serve as a microgrid uninterruptible power supply for storm conditions, where more distant power lines may go down, but local neighborhoods can stay active.

If the plant is centrally located on the trunk of the network, it can perform area regulation, black-start services, and ramp rate compensation.

The warehouse may be housed sensibly in any of these locations.

3.4.3 Expertise

A key feature of the concept is staffing with trained battery technicians in the warehouse. The knowledgeable technician can quickly examine and assess packs, implement repairs, swap batteries, and prepare new batteries for service.

Control strategies can also be adapted by a professional to serve local needs more closely, rather than following a generic control pattern. By optimizing the control strategy, the value of the plant can be maximized at no additional capital cost.

3.4.4 Scale

When dealing with grid storage, an important factor to consider is the grid operator's willingness to deal with independent actors. Generally, contracting and transmission/distribution limitations make it difficult to allow numerous small independent contractors onto the system. By collecting the packs into a single location with one grid interconnection point, these barriers are minimized. A grid operator is more likely to contract with a single plant with a hundred packs, on one grid connection which can make bids and fulfil requests very easily, than a hundred distributed, storage nodes.

Additionally, such a single large plant can perform multiple services more effectively than distributed packs. Services like frequency regulation may be stacked with services like timeshifting, and transmission upgrade deferrals require a minimum amount of storage before deferral is really a viable option, as too little storage would not be enough to guarantee service to the customer base.

Finally, having hundreds of batteries available at a time mitigates the risk profile of used vehicle batteries. The higher risks of battery failure and the uncertain lifetime capacities are averaged over more units, unlike small installations of 1-10 packs, where the failure of one unit could prevent it from meeting its services at all. In a large plant, the failure of single batteries does not represent a significant loss of capability.

3.5 Weaknesses of Concept

3.5.1 Lifetime Uncertainty

The total lifetime capacity of EV batteries is still uncertain. Until the first sets reach the end of their 15-year design lifetimes in steady service, verified data on lifetime capacity will not be available. Further, because calendar aging is separate from cycling aging, there is no way to get this information in advance from hard data instead of projections¹¹. And each new model of battery could have a different lifetime decay function. Overall, this means that repurposed usage will always have to deal with uncertainty regarding the real value remaining in the batteries. This is significant because battery capacity is one of the important sensitive variables when calculating the profitability of the installation [51].

3.5.2 Technical Risk

By using a product beyond its design lifetime, the probability of suffering a failure increases. As a battery ages, its chemistry changes in ways that may cause its pouch or casing to swell. Most modern designs include expansion to compensate for this, but it is a certainty that the internal mechanical stresses will increase, raising the risk of malfunction. Along with aging comes wear, which may cause contacts to fail or short, or a pouch to leak, which can cause thermal events. Capacity loss in individual cells may cause restrictions on the capacity of the whole pack.

¹¹ Projections have a range of predicted values depending on model and assumptions but range from 60%-80% capacity remaining at end of use.

The most significant technical risk is the lack of manufacturer specifications and access to historical data. Without information on critical facts such as safe current limits, safe operating temperatures, voltage limits, capacity decay rates, third-party operators are disadvantaged. Depending on the brand, they may not be able to access the historical information on the battery collected by the car. This will force operators to run their batteries more conservatively or conduct more validation than a fully informed operator.

If the internal BMS is being used, the CANBUS communications codes may be different with newly arrived batteries of the same brand, interrupting workflow. More insidiously, the change may not be noted before installation, causing the battery to be operated unsafely while the signals are being interpreted in a way that makes it appear to be safe. If the BMS is not being used, the pinout configuration may also change, possibly causing shorts or equipment damage if the adaptor is not also updated. The biggest factor in these risks is the inability to know about the change in advance without OEM information, which may be unavailable.

3.5.3 Financial

Domestic home energy storage is presently purchased for backup and load shifting. Commercial energy storage markets have seen some success selling demand charge management and backup services, but the profitability of these may depend on local tariffs or carbon taxes. By contrast, the industrial scale must have clearly defined contracts and financial returns. It would be nearly impossible to build a mixed battery array without some form of financing to purchase the warehouse, cooling systems, and batteries. If the payback is not abundantly clear, financing will be difficult to obtain outside of pilot projects and test beds. Given the uncertain economic viability of the used EV market, and the many assumptions that underlay the present finance models, accessing financing may be an obstacle.

3.6 Experimental Research Objectives

The development of the MBA concept serves as a seed for future developers to build upon, accelerating the usage of repurposed EV batteries for grid storage.

To support the MBA concept, it is critical to have quantitative experimental data that provides performance information according to consistent metrics.:

1. There is an absence of rigorous performance data for the most popular EV batteries on the market. This absence makes it more difficult for third-party operators to predict the profitability of a storage array as described in this chapter.
2. Upon receiving the batteries at the storage facility, their performance characteristics are undetermined. Identifying these and assigning a service to the battery based on the results of a characterizing test will be part of the receiving process. Example characterizing tests and service assignments should be demonstrated.

To overcome these obstacles, two experimental objectives are determined:

1. A selection of the most popular EV batteries should be tested, and their performance reported.
2. An example test routine for identifying the performance characteristics of EV batteries should be developed and demonstrated, and a strength-service ranking should be used to assign energy storage services to each battery based on the results of the tests, replicating the intake process at a storage facility.

Chapter 4 Batteries and Experimental Procedure

The experimental procedure is separated into three parts: The batteries, the test equipment, and the duty cycles used for performance evaluation. Each battery has a section describing their format, configuration, and other characteristics. The testing equipment section will describe each piece of equipment and its usage and accuracy. The final section describes each duty cycle- constant current and constant power cycling, and frequency regulation simulation- its relevance, usage, and the necessary information to replicate it.

4.1 Batteries

This section will detail each test sample battery, and how it was instrumented.

The batteries are:

- A section of a Chevrolet Volt pack comprised of 3 cells in parallel, grouped 12 in series, which is a liquid-cooled, prismatic battery from a plug-in serial-hybrid vehicle.
- 3 modules from a 2015 Nissan Leaf battery, grouped in their original 3 modules of 4 cells each. It is a passively cooled fully electric vehicle battery.
- 32 modules from a 2012 Nissan Leaf, presenting a larger example of the Leaf battery.
- One module is from a Tesla Model S, a high-power battery designed for a performance luxury vehicle, with liquid cooling. Unlike the other batteries discussed, it made with cylindrical cells like those found in laptop batteries, wired in a highly parallel configuration (74P vs. 2P-3P).
- Three EnerDel Moxie+ MP320-409 batteries, wired in series and hereafter referred to as the Moxie+ battery, a module for heavy-duty applications such as trucking or shipping with aluminum fin air cooling.
- A Lishen EV-LFP battery pack in original case with 104 cells in series, reaching nearly 400 V, the highest voltage and energy capacity of all batteries under testing. Like the Leaf, it is passively air cooled, and optimized for high energy capacity.

Each battery is instrumented for per-cell-group voltage measurement, total pack voltage and current, and temperatures.

4.1.1 Overall Specifications

The specifications of each battery are given in Table 3.

Table 3- Battery Specifications Overview

Battery Specifications						
Manufacturer	LG Chem	AESC	AESC	Panasonic	Lishen	EnerDel
Vehicle	Chevrolet Volt	Nissan Leaf	Nissan Leaf	Tesla Model S	EV-LFP	Moxie+
Model Year	2015	2012	2015	2014	2012	2017
Nominal Capacity (Ah)	45	60	60	222	115.5	31.5
Nominal Energy (kWh)	6.0	15.0	1.4	4.84	37.3	3.9
Maximum Voltage (vpc)	4.20	4.20	4.20	4.20	3.55	4.1
Minimum Voltage (vpc)	2.50	2.50	2.50	2.50	2.50	2.50
Cells in Parallel	3	2	2	74	7	2
Cells in Series	36	64	6	6	104	36
Mass (kg)	53.4	121.6	11.4	25.4	450	48.0
Volume (cm ³)	32603	75648	7092	15925	585120	27300
Dimensions (cm)	75x22x27	54x46x30	10x30x22	66x28x8	114x192x24	53x26x20
Negative Active Material	Graphite	Graphite	Graphite	Graphite	Graphite	Hard Carbon
Positive Active Material	NMC-LMO	LMO	LMO	NCA	LFP	NMC

Other specifications for these batteries can be found in section 1.3.2, and the following sections.

Battery Subsets

In this research, most batteries tested are not full packs from the vehicle. Modules from packs which have been divided up are easier to find in the open market, and easier to ship.

The power cycler used has a power limitation of 200 A and 50 kW per channel. A full Tesla pack has an energy capacity of 85 kWh. It would require both channels to match the power requirement of 1 h cycling in either current or power, and 0.5 h rates are impossible with this equipment.

Extrapolating the results of this research requires only scaling up the energy capacities according to the number of cells in series. The temperature values are harder to extrapolate, which is why the focus is on their relative thermal performance.

4.1.2 LG Chem Chevrolet Volt

The Chevrolet Volt battery was taken from a 2015 Chevrolet Volt (Generation 1). It was originally a 7 kWh section of 4 modules (12, 6, 12, 12 cell groups in series in each), one of which was removed because it suffered a malfunction. The three remaining modules are each 3 cells in parallel, 12 in series (3P12S) for a total pack of (3P36S). It is liquid-cooled, with cooling fins interleaved with the cells, alternating with foam compression pads, such that each cell has one face adjacent to a fin. The cells measure 480mm x 195 mm x 5.2 mm. The battery is detailed in Figure 17.

Physical Description

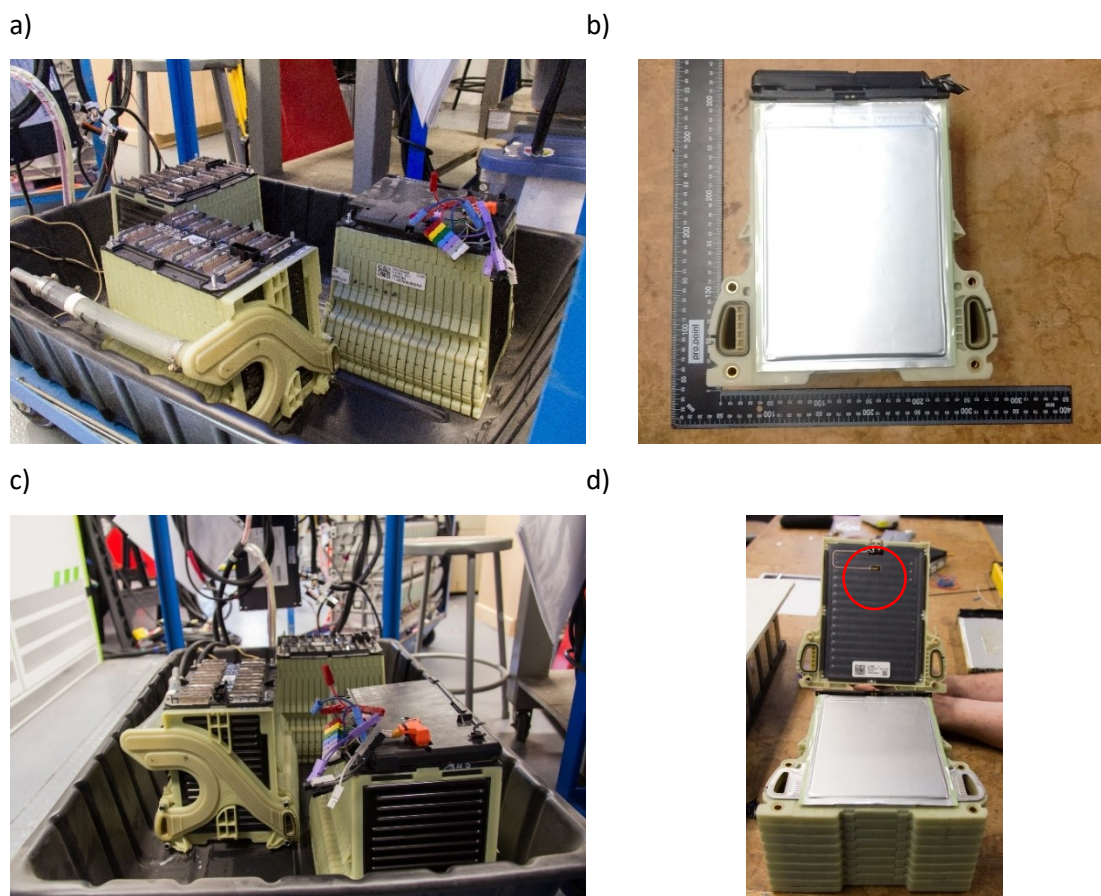


Figure 17- Chevrolet Volt Battery. a) The three modules used in testing, b) a single cell with scale, c) a side view of cooling manifold, d) location of thermistor on cell.

Parameters

The upper and lower voltage limits for the pack were selected based on chemistry. It is known that the chemistry is Li-NMC-LMN, which has upper and lower cell voltage limits of 4.2 and 2.5

vpc. The capacity of the pack is 45 Ah [60]. The energy capacity was calculated using nominal voltage of 3.6 vpc for a total of $3.6 \text{ vpc} * 45 \text{ Ah} * 36 \text{ cell groups in series} = 5.8 \text{ kWh}$, rounded to 6 kWh for nominal capacity.

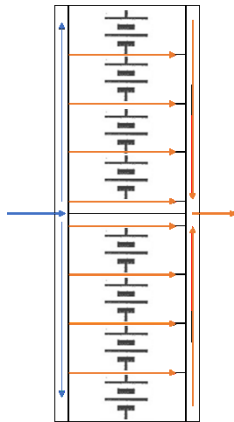
Instrumentation

The cells were tapped using the existing wiring. The top of the module has a port for the OEM BMS to connect, and a small cable to run between them. The OEM BMS was removed, the cable was severed, and the ends were identified and crimped with a standard pattern of connectors. This included the thermistor terminals. Two OEM thermistors were in each module, at the ends of the module where the outer face of the cell is farthest away from liquid cooling. The thermistor location is near the highest temperature location, on the average path of current across the cell neat the upper-middle-center of the cell, as seen in Figure 17d at the center of the red circle. T-type Thermocouples were also added to the coolant tubes to measure the temperature of the coolant stream at the inlet and outlet. The coolant pipes used are made from $\frac{3}{4}$ in PVC so there is a measurement lag between the in-stream temperature and external temperature.

Cooling

The Chevrolet Volt is liquid-cooled, with the coolant traveling away from the manifold longitudinally down the large channels seen in Figure 18b. The coolant then flows through small channels across the cells, before being collected by the manifold again.

a)



b)

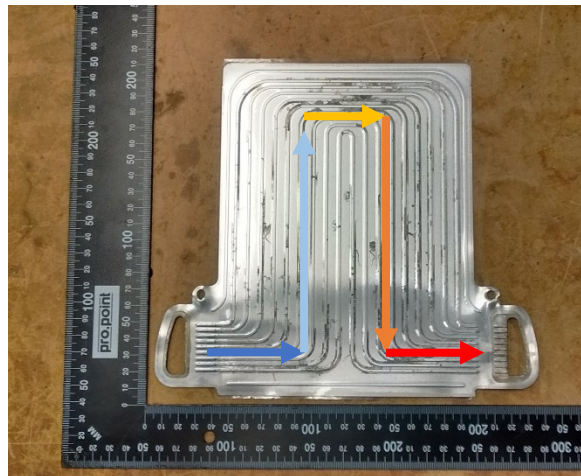


Figure 18- Chevrolet Volt Cooling Detail. a) Coolant flow, view from top. b) Coolant plate between cells.

4.1.3 Panasonic Tesla Model S

The Panasonic Tesla module came from a 2015 Model S 85. The battery is formed of 440 cylindrical cells 18 mm \varnothing by 65 mm long in a 74P6S configuration. It is liquid-cooled, with a single pipe weaving up and down the length of the pack in between the cells while making a tangential contact with one side of each cell. The cylindrical cells are formed of a “jelly-roll” of electrode, active material, separator, and electrolyte. This decreases the mean electron path and increases the contact area for current flow. This, combined with its highly parallel configuration allows for the highest peak power output of any automotive battery on the market. The battery is shown in Figure 19.

Physical Description

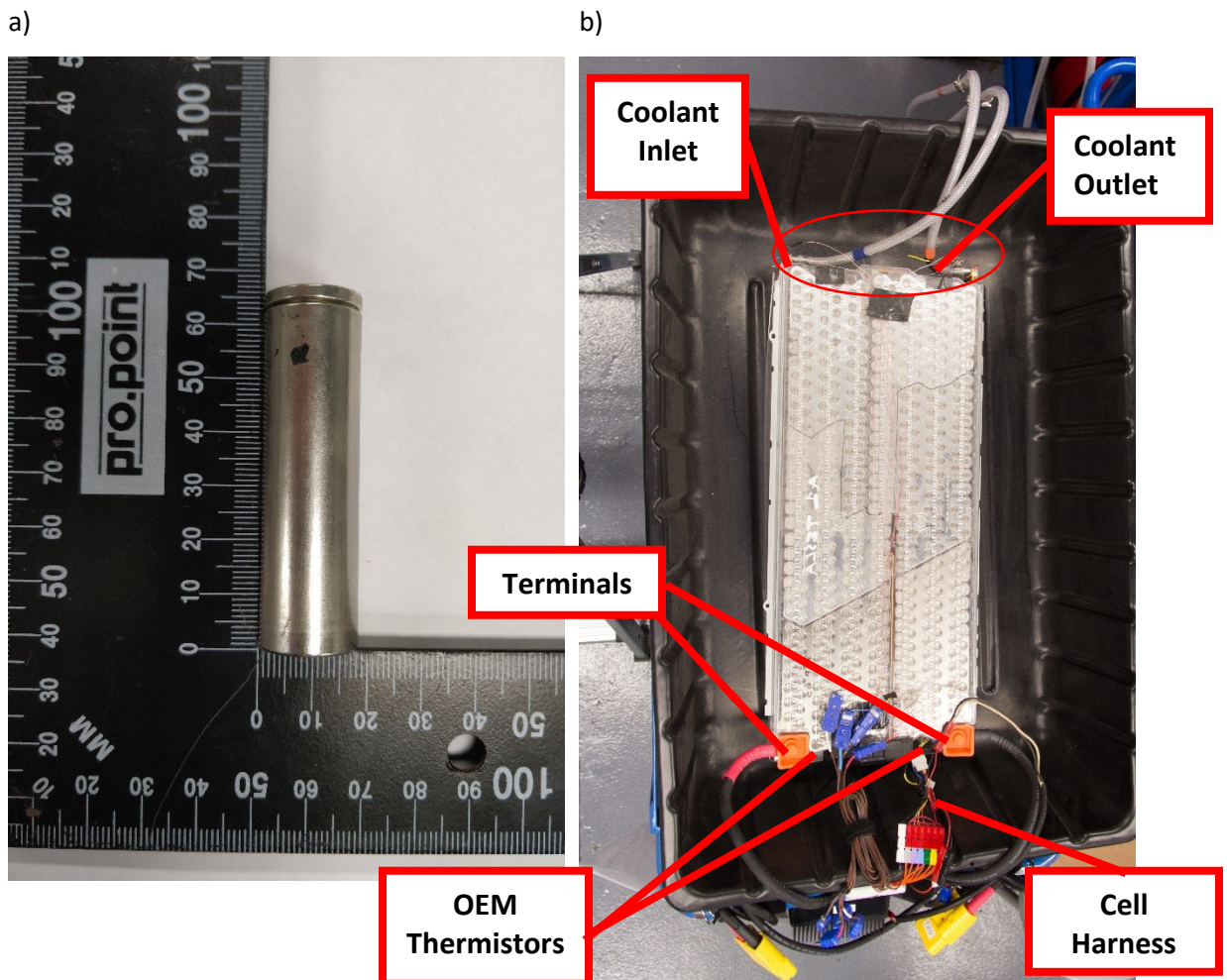


Figure 19- Panasonic Tesla Instrumentation. a) A single 18650 cell. b) Pack, with connections, including cooling. Thermocouples are mounted inside red circle.

The main current carriers are the aluminum busbars, with small fusible links welded from the caps of the cell to the plate. If an abnormal current flows through them, the wire fails, disconnecting that cell from the group of 74.

Parameters

The upper and lower voltage limits for the pack were selected based on chemistry. It is known that the chemistry is Li-NCA, which has upper and lower cell voltage limits of 4.2 and 2.5 vpc. The capacity of the module was assumed to be 222 Ah because it has been reported that the module was formed of Panasonic 18650 cells, and the rated capacity of those cells is approximately 3 Ah, by NCR18650 manufacturer specifications [61].

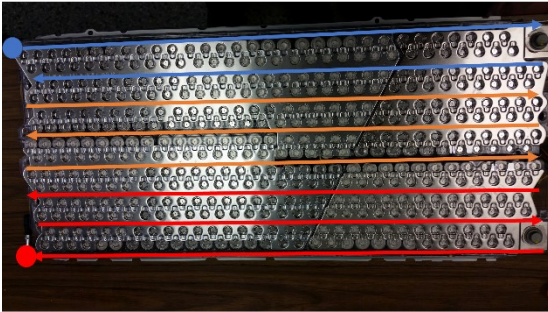
Instrumentation

Tesla has wires to cell taps on each of the metal plates. The wires are gathered at the front and soldered to a BMS, which was cut off and replaced with the custom lab connector. Three T-type thermocouples were adhered to the cells nearby the cooling ports in ascending order of expected temperature, and thermocouples were attached to each cooling port to read the temperature of the stream. The coolant thermocouples face the aluminum directly, so the temperature should not suffer from a phase delay in reading temperature, given the high thermal conductivity of aluminum.

Cooling

The liquid-cooling system of the Tesla is formed by a long rectangular pipe which has been flattened and threaded through the module. Each cell has tangential side contact with the pipe. The cells are clustered such that each cell faces the cooling pipe on one side, and a partner cell on the other. These features can be seen in Figure 20.

a)



b)



c)



d)

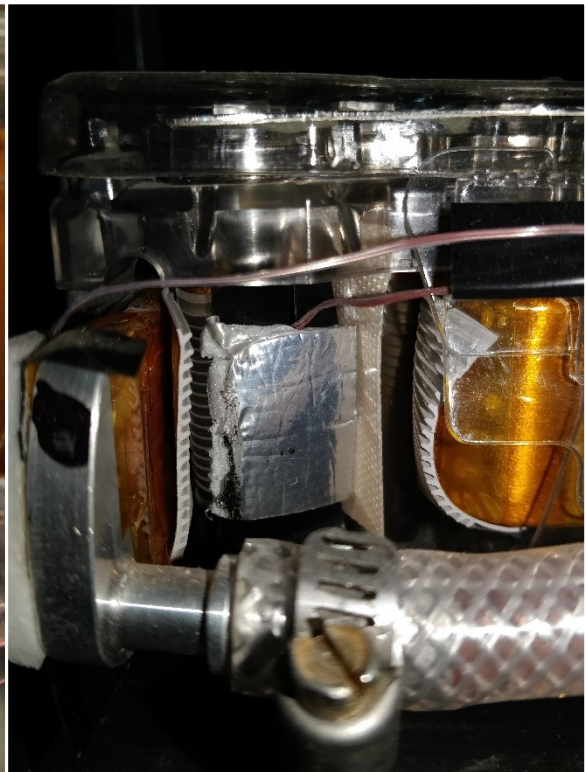


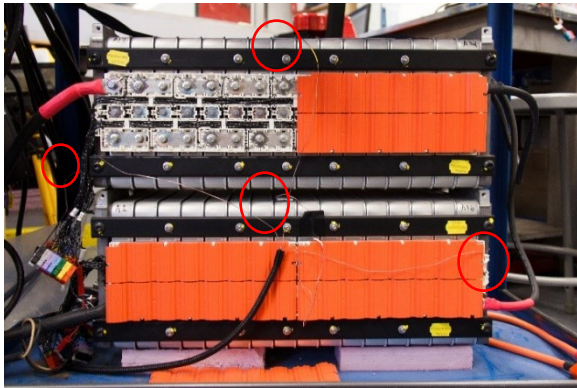
Figure 20- Tesla Cooling System. a) Coolant Flow. b) Detail view of corners of coolant pipe. c) OEM Thermistor on cell beside main terminal. d) Lab mounted thermocouple on cell beside coolant manifold.

4.1.4 AESC Nissan Leaf 2012

The Nissan Leaf uses cells manufactured by the Automotive Energy Supply Corporation wired 2P2S. In this thesis a portion of a pack is used, with 32 modules, or 64 cells in series. It is passively cooled, either in its original form, nor in this reduced version. The cells are large, flat pouch cells, measuring 200 mm x 225 mm x 6.2 mm. The battery is shown in Figure 21.

Physical Description

a)



b)

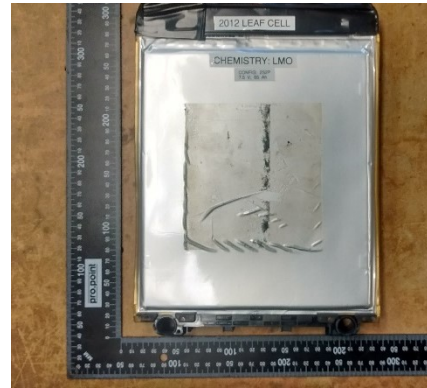


Figure 21- AESC Nissan Leaf 2012. a) Side View, including wiring harness. Thermocouples are in red circles. b) Cutaway view of cell in module

The 2012 Nissan Leaf pack is composed of 32 modules separated in two physical groups. Each This creates a pack configuration of 2P64S. The two large modules are joined by a cable with a mid-pack disconnect.

Parameters

The upper and lower voltage limits for the pack were selected based on the AESC specifications sheet [62]. Manufacturer specifications give the capacity at 30 Ah per cell. A whole pack is rated at 24 kWh, with 48 modules. Therefore, this pack, with 32 modules, is rated at 16 kWh.

Instrumentation

The OEM cell harness provided cell taps. The ends of the wires were identified, separated, severed, and crimped with connectors in a standard configuration. The built-in thermistors were similarly cut and crimped with connectors. The thermistors are located on the rear of the battery, two on the lower and one on the upper set of modules, per Figure 22.

Cooling

The AESC Leaf is passively cooled. The warmest locations were typically on the very top and in the middle of the packs, in the air gap.

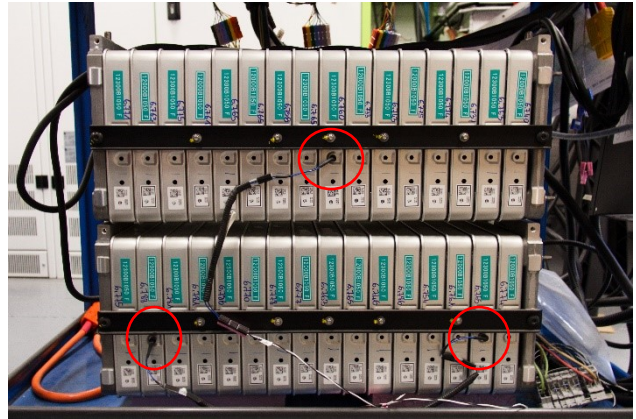


Figure 22- AESC Leaf Thermistor Locations on back of pack, circled in red

4.1.5 AESC Nissan Leaf 2015

Like the Leaf 2012 pack, the 2015 Leaf pack is composed of 2P2S modules, but only three modules are in use here. The modules have a slightly changed casing, reducing the material usage, and leaving a few gaps for better airflow. The battery is shown in Figure 23.

Physical Description

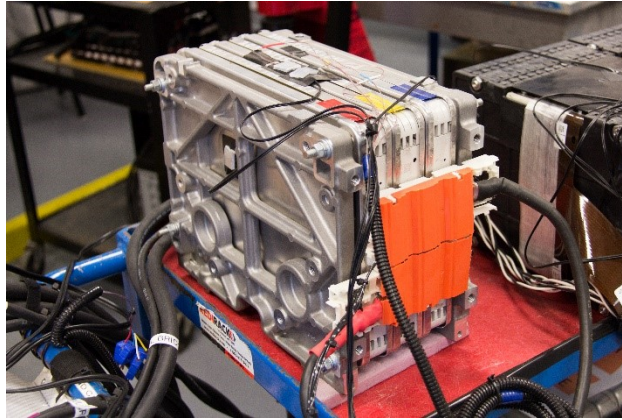


Figure 23- AESC Leaf 2015 Battery, Pack and main cables

The AESC 2015 pack is formed of three modules from a 2015 vehicle. The pack total configuration is 2P6S.

Parameters

The parameters of the 2015 pack were selected the same way as the 2012 version: The voltage and capacity were chosen based on manufacturer specification (identical to 2012 Leaf), and the energy is the proportional fraction of the original pack (24 kWh).

Instrumentation

The original cell harness was present, so the wires were cut, identified, and crimped. The 6 taps were combined into a standard configuration, as normal. No thermistors are present in the pack, so all temperature measurement is done by thermocouple. The black leads visible in Figure 23 are for the BMS backup measurement, and the primary measurements are internal, sandwiched between the modules, on top, and on the side. The locations of the thermocouples are given in Figure 24.

Thermocouple	Location
T1	Top of module
T2	Inner face of module 1
T3	Inner face of module 2, opposite T2
T4	Outside face of T1

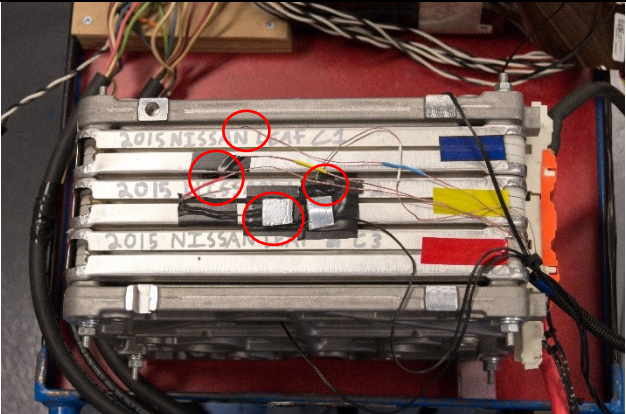


Figure 24- AESC 2015 Leaf Thermocouple Locations

Cooling

The AESC Leaf is passively cooled. The 2015 pack in the lab benefits from only having three modules under test, increasing its surface-area-to-volume ratio, lowering the average temperatures compared to the 2012 Leaf.

4.1.6 Lishen EV-LFP

The Lishen EV-LFP battery pack is a full pack version, complete with supports and shell. Inside the hard-shell protective case, the pack is divided into blocks of modules, each with 7 prismatic cells in parallel, and varying series configuration, between 5 and 7 cells. Thermistors are distributed throughout the pack, some of which are in use, as noted in Figure 26. The battery as a whole, and an example module for scale, are shown in Figure 25.

Physical Description

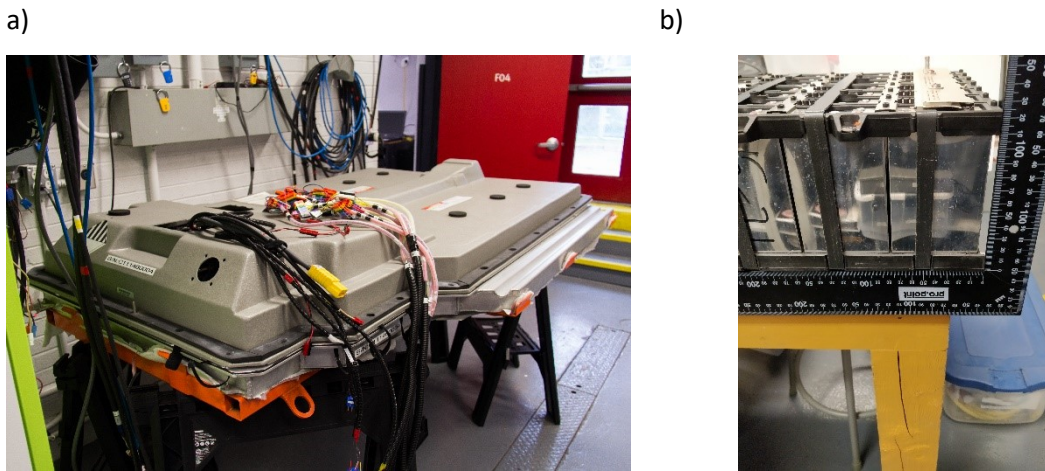


Figure 25- Lishen EV-LFP. a) Whole Pack. b) Side view of module, detail of cell.

The 2012 Lishen EV-LFP pack is an example of an entire vehicle battery pack. It is composed of 16 modules in series for a total pack configuration of 7P104S. The string runs down the length of the pack, with a midpack disconnect at the end before returning to the front.

Parameters

The voltage of the LFP cells used in the Lishen EV-LFP have upper and lower limits of 3.55 and 2.5 vpc. The capacity given by manufacturer specifications is 115.5 Ah. At a stated nominal voltage of 322.8 V, this gives 37.3 kWh.

Instrumentation

The existing wiring harness was used to tap the cells of the Lishen EV-LFP pack. The wires were cut, identified, and crimped one at a time. The connectors were formed into a standard configuration for the BMS. The pack also has thermistors in every section which were also connected, though not all were used. The implemented sensors are identified in Figure 26.

Cooling

The Lishen EV-LFP pack is passively cooled. Because of the hard case, and the absence of fans, the pack cools slowly, compared to other battery packs.

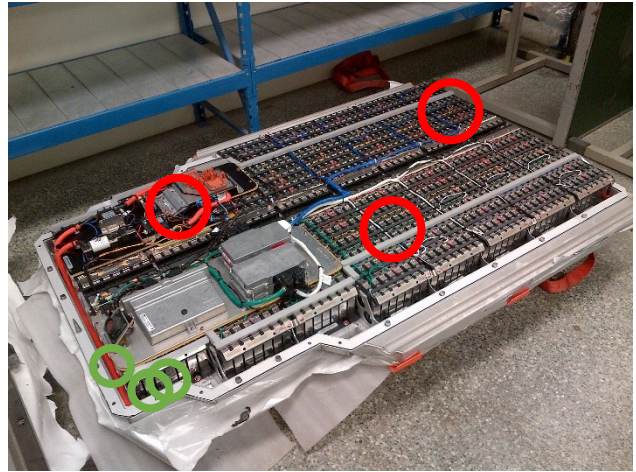


Figure 26- Lishen EV pack detail. Thermistors in use are circled in red. Thermocouples are circled in green.

4.1.7 EnerDel Moxie+

The battery described in this section is the Enerdel Moxie+ MP320 Module, seen in Figure 27. The Moxie+ is intended for heavy-duty hybrid vehicle service. The pack is composed of 3 modules, each with 2 cells in parallel, 12 in series. Thus, the pack configuration is 2P36S. The modules each have a flexible ribbon cable carrying cell taps and thermistor terminals from the block.

Physical Description

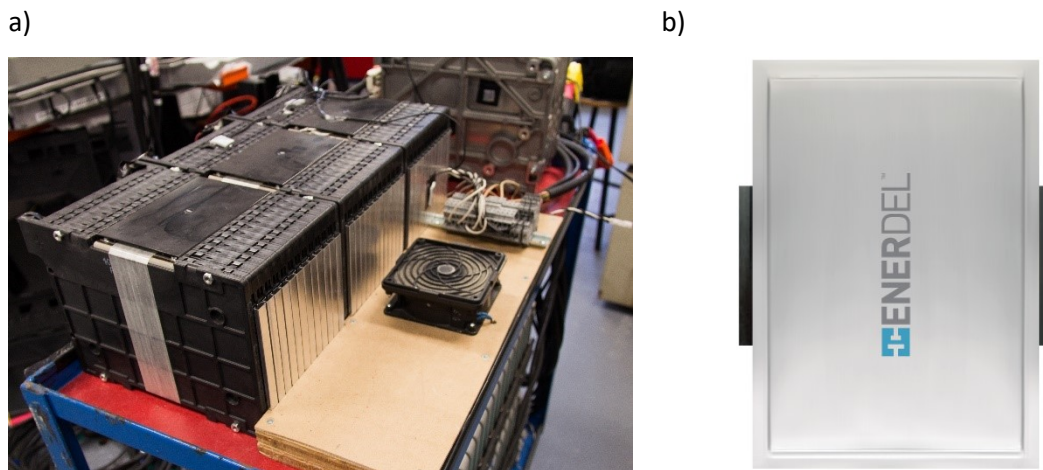


Figure 27- Enerdel Pack and Cell. a) Modules under test. b) EnerDel Moxie+ cell. Image credit: Enerdel Moxie+ Technical Specifications.

The cells are interleaved with cooling fins on a 1:2 basis, which extend out the end of the battery to an air channel. By manufacturer design, the fins make a flat panel, which can be mounted to a cooled plate.

Parameters

The voltages and capacities are all drawn directly from a manufacturer specification sheet [63]. The upper and lower voltages are 4.1 and 2.5 vpc. The manufacturer restricts current near fully charged and discharged states, but the half-hour rate does not fall in this restricted range, so the full voltage range is available for all tests. Its coulombic capacity is 31.5 Ah, and its energy capacity is 3.9 kWh.

Instrumentation

The Moxie+ has internal cell taps that are collected in a ribbon cable, terminated in a female serial bus. A male connector is used to convert the female terminator to exposed pins, and wires soldered to the appropriate pins. The wires were crimped and collected in a standard

configuration. The Moxie+ has several internal thermistors mounted at the cell edges. Two of these were used per module. The thermistor locations are in the middle of the module, and on the side.

Cooling

The Moxie+ is forced-air-cooled, and has a cooling fin system, which improves the heat transfer from forced-air cooling. A fan system to blow air through these fins was constructed and is shown in Figure 28.

Figure 28 part #	Part
1	Intake Fan
2	Plenum
3	Outlet

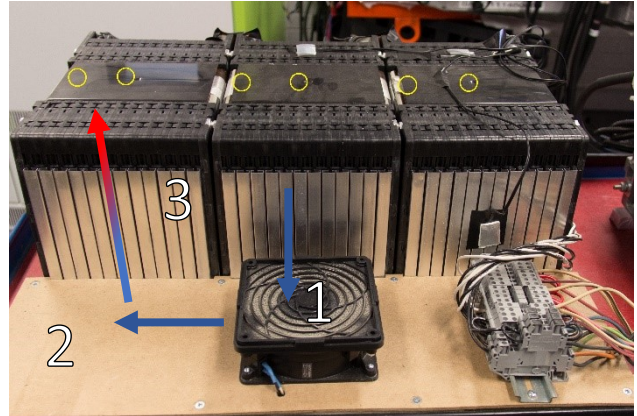


Figure 28- Enerdel Cooling System. Air is sucked through the fan and blown up through the aluminum fins. Yellow circles indicate thermistor locations.

The plenum has dimensions 18.4 cm deep by 56 cm wide by 10 mm internal height. The aluminum fins are 5 by 11.7 by 145 mm, with 12 fins per module.

4.2 Test Equipment

This section will discuss the details of each piece of testing apparatus, including resolution, accuracy, and timestep. The power cycler, linked data acquisition system, and control software form the core of the testing suite. These three provide power to the system, monitor the tests, and execute the scripts which contain the test protocols. Next is the battery management system, or BMS, which tracks each cell group's voltage, and top-balances them using a resistor which activates if a cell group's voltage exceeds the nominal charge vpc. Finally, the thermal conditioning loop which heats and cools the liquid-cooled batteries will be discussed.

4.2.1 Power Cycler

A Gustav-Klein power cycler operated by Greenlight Innovation's Emerald software is the primary testing apparatus. The power cycler is programmed to follow a testing script composed of battery test parameters and a control profile. It can operate in current, voltage, or power control modes, where it forces the relevant parameter to the specified value, within hardware limits of current, voltage, and power, per the specifications in Table 4. The power cycler can be seen in Figure 29.

Table 4- Power Cycler Specifications

Operational Range	
Current (A)	-400 to +400
Voltage (V)	0 to +800
Power (kW)	-100 to +100
Resolution	
Current (mA)	10
Voltage (mV)	100
Time (ms)	100
Accuracy	
Current (mA)	±20
Voltage (mV)	±80



Figure 29- Gustav-Klein 100 kW Power cycler

4.2.2 Data Acquisition System

The Greenlight Innovations Data Acquisition System (DAQ), shown in Figure 30, is an external measurement device closely interlinked with the power cycler. It is used to independently measure voltage and temperature. It reports all its values directly to the Emerald software for control and data collection. It has 16 measurement channels for voltage and 16 for temperature. Its specifications are given in Table 5.

Table 5- DAQ specifications

General System Specifications	
Timestep (ms)	100
Voltage Channel Specifications	
Channels 1-14	
Voltage Range (V)	-75 to +75
Resolution (mV)	1
Accuracy (mV)	± 37.5
Channels 15-16	
Voltage Range (mV)	-100 to +100
Resolution (mV)	0.001
Accuracy (mV)	± 0.1
Temperature Channel Specifications	
Channels 1-16	
Measurement Device	T-Type Thermocouple
Temperature Range (°C)	-270 to 370
Temperature Resolution (°C)	0.1
Temperature Accuracy (°C)	± 1

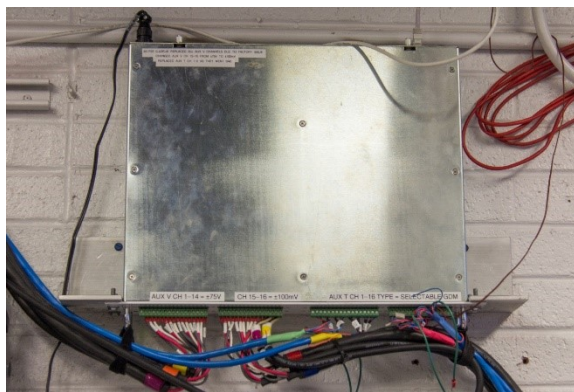


Figure 30- Greenlight Innovations DAQ

Temperature Measurement

Calibration

Some batteries (i.e., Volt, Leaf, EnerDel, Lishen) have built-in thermistors for measuring temperatures closer to cells than side-mounted sensors. These sensors were used where possible, for better accuracy due to their preferred location. In most cases, the thermistor coefficients were not available, so calibration tests were performed to identify the beta and R_{inf} values. The resistances of the thermistors were measured at 3 temperatures, and the results linearly regressed. The slope of the line is the beta value, and the log of the intersect is the R_{inf} value, as per equation 1.

$$\ln R = \frac{\beta}{T} + \ln r_{\infty} \tag{1}$$

The results of the calibrations are shown below, in Figure 31.

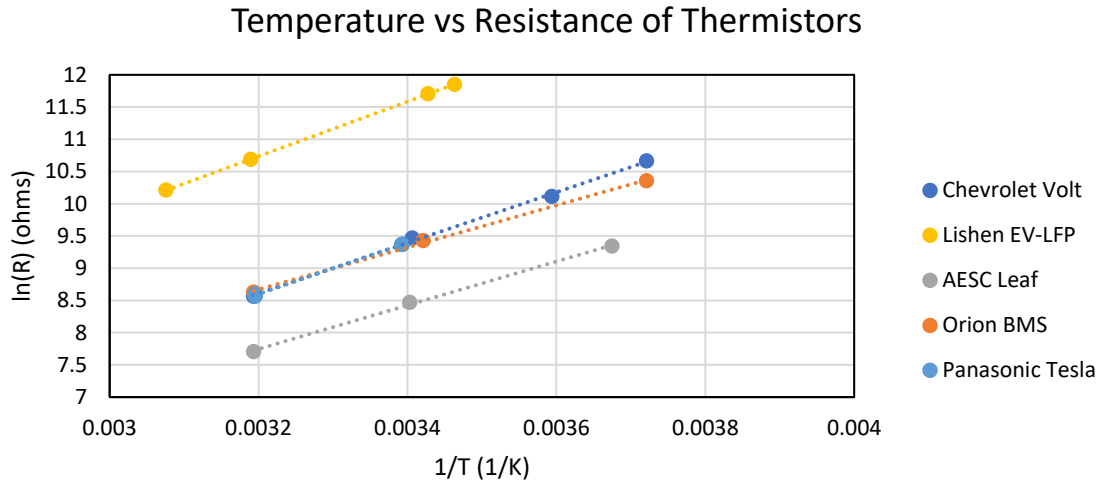


Figure 31- Thermistor Calibration- Linearized Resistance vs. Temperature

These results are summarized below in Table 6.

Table 6- Summary of Thermistor Calibration

Thermistor Source	β	r_{∞}
Chevrolet Volt	3919.9	0.019563
Lishen EV-LFP	4382.2	0.046617
AESC Leaf	3394.0	0.044392
Orion BMS	3261.6	0.170896
Panasonic Tesla	4000.2	0.014952

The Orion BMS thermistor values are for comparison, and to verify the accuracy of the method. The Orion specifications give the β 50/25 value at 3380K, therefore the validation measurement is within 4% of the known value.

Ballast Circuit

The thermistors were wired in a ballast circuit, as per Figure 32 below.

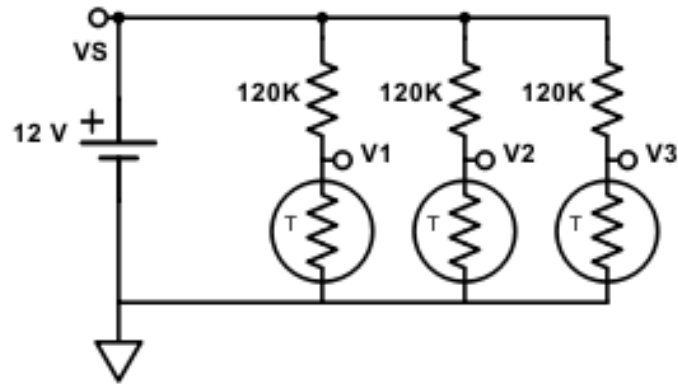


Figure 32- Ballast Circuit Diagram

The ballast circuit voltage measurements were made using the DAQ voltage channels 1-14, and the equation 1 above was used to calculate the corresponding temperatures. The measurements were checked against a reliable T-type thermocouple, and found to be within ± 1 °C.

Current Shunt

At low currents, the power cycler current measurement uncertainty is significant. Because the resolution of the power cycler can cause the current values to be off by 0.2 A, the relative accuracy of the power cycler's current measurement is much higher at low current values. To remedy this, a resistive current shunt is used. This shunt is constructed of e.g., a 100 A/100 mV resistor, through which the current passed. Other sizes in use include 300 A/100 mV and 500 A/50 mV, depending on the maximum expected current. The voltage drop across the shunt is measured by a DAQ voltage channel (15 or 16), which measures the value up to ± 100 mV. This change is used to calculate the current through the shunt and is used in place of the power cycler current value. The shunt specifications are given in Table 7.

Table 7- Current Shunt Specifications

Shunt	Accuracy
100 A/100 mV	0.25% ± 0.1 A
300 A/100 mV	0.25% ± 0.3 A
500 A/50 mV	0.25% ± 1 A

4.2.3 Control Software

The Emerald software controls the power cycler and records values from all peripheral measurement devices. Two scripts are used for each test: a battery parameter script, which defines the limits and setup of a particular test, and a cycling script which is used for all tests of the same type and controls the power cycler logic. These two scripts are called in sequence by a master control script. Example scripting logic is shown in Figure 33.

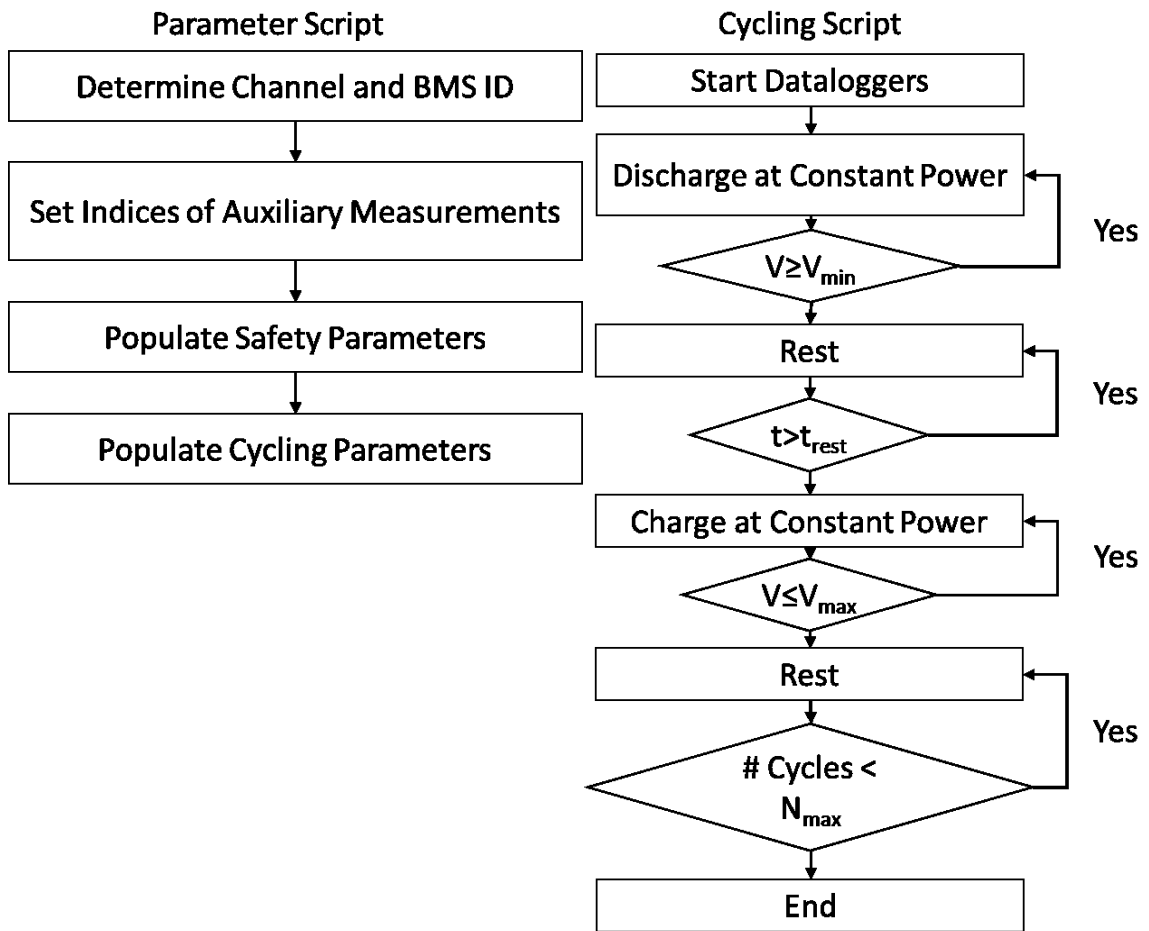


Figure 33- Example Control Flowchart with a CP Cycle

4.2.4 Battery Management System

The Orion Battery Management System¹² (BMS) is used on all the batteries under test. It serves three functions:

1. Cell voltage measurement
2. Cell balancing
3. Temperature measurement for safety

Cell Voltage Recording

The cell group voltage measurement is made and transmitted by a rolling broadcast over CANBUS. The BMS observes the voltages of all cells, and broadcasts them one at a time, in order, every 30 milliseconds. Ergo, the minimum refresh period for any single cell is no more than 1 second, and in practice is closer to 0.5 seconds.

Cell Balancing

Top-of-charge cell balancing is the procedure of removing charge from the highest voltage cells in a pack, until all cells are within a certain tolerance of the same voltage. The Orion BMS performs cell balancing as follows:

1. Check which cells are above a certain voltage (e.g., 4.2 vpc for a Li cell) *and* more than e.g., 0.05 V above the lowest-voltage cell.
2. Discharge those cells at 200 mA for 30 seconds.
3. Stop discharge for 30 seconds, go back to 1.

This forces all cells to have an even final charge voltage. Therefore, when cycling, all cells should be within the same band of voltage and will not deviate near the end of charge or discharge, which would cause early termination or unsafe voltages.

Temperature Measurement

The Orion BMS has 4 thermocouples which were used as redundant temperature measurements during testing to obtain highest and lowest temperatures for safety purposes.

¹² <https://www.orionbms.com>.

Table 8- BMS Specifications

Cell Voltage Measurement	
Voltage Resolution (mV)	1.5
Cell Broadcast period (ms)	30
Cell Balancing	
Balancing current, max (mA)	200
Balancing Duty Cycle (s)	30
Temperature Measurement	
Resolution (°C)	1
Timescale (ms)	<100

4.2.5 Thermal Conditioning

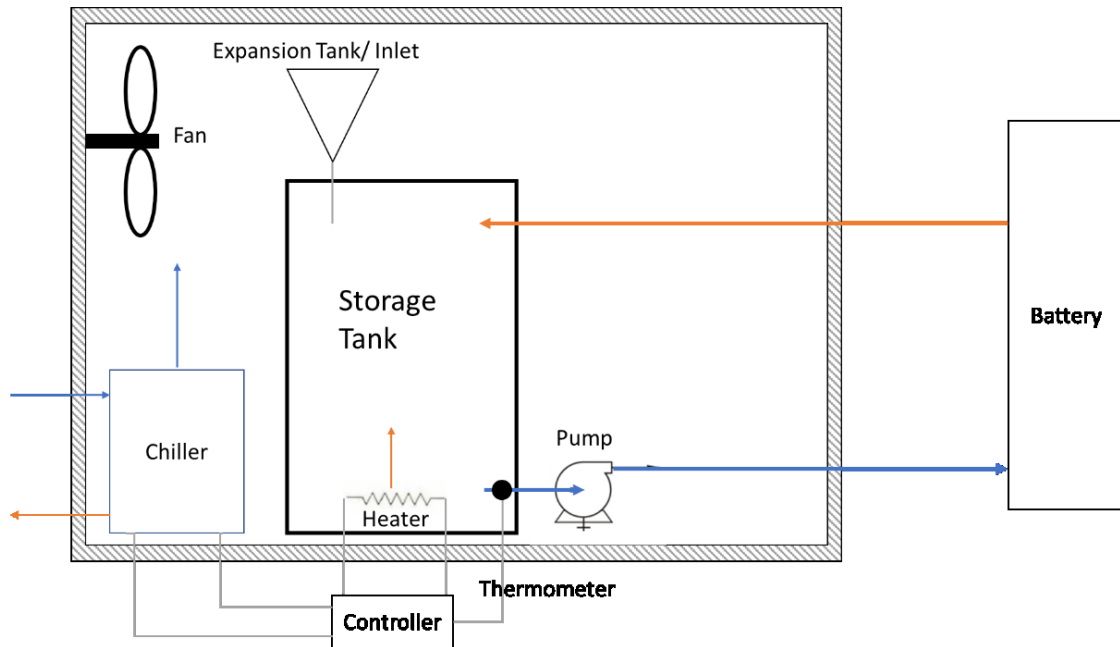
Air Cooling

The AESC Leaf, EnerDel and Lishen EV batteries are actively or passively air cooled. The lab is maintained at a steady temperature of 20 °C ± 1°C. The Leaf and Lishen EV packs are passively cooled with lab air without a fan, and the EnerDel batteries are cooled using the metal cooling plates and a simple fan distributor, using lab air, and shown in Figure 28.

Liquid Cooling Loop

The *Volt* and *Tesla* batteries require liquid cooling. The *Liquid Thermal Conditioning Loop* uses a chiller, a heater, a circulation pump, and a temperature controller to provide a constant temperature coolant supply. Figure 34 below outlines the system.

a)



b)

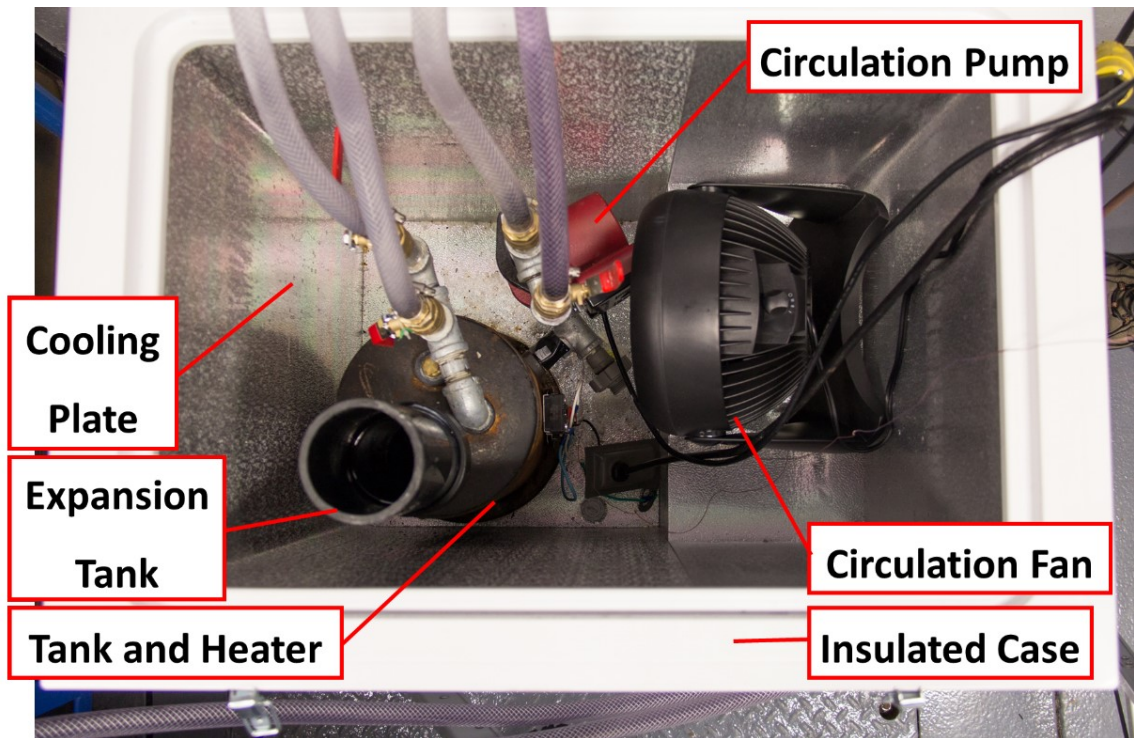


Figure 34- Liquid Cooling Loop a) Line diagram of LCL. b) Photograph of LCL from above. Shown are the heater tank, lower left, circulating pump, red, and circulating fan. The LCL is completely contained inside an insulated shell in normal operation.

The logic of the controller is as follows, for a 30°C setpoint:

- If the temperature of the coolant loop falls below a set value (27°C), turn the heater on until the working fluid rises above a certain temperature (30°C).
- If the temperature of the coolant loop rises above a set value (31°C), turn on the chiller until the working fluid falls below a certain temperature (30°C).

The heater is needed in normal operation to maintain the battery at optimal temperatures for charge and discharge response.

4.2.6 Overall Testing System

Figure 35 gives a line diagram of the whole system. Figures 36 through 40 give details of a typical battery hookup and measurement.

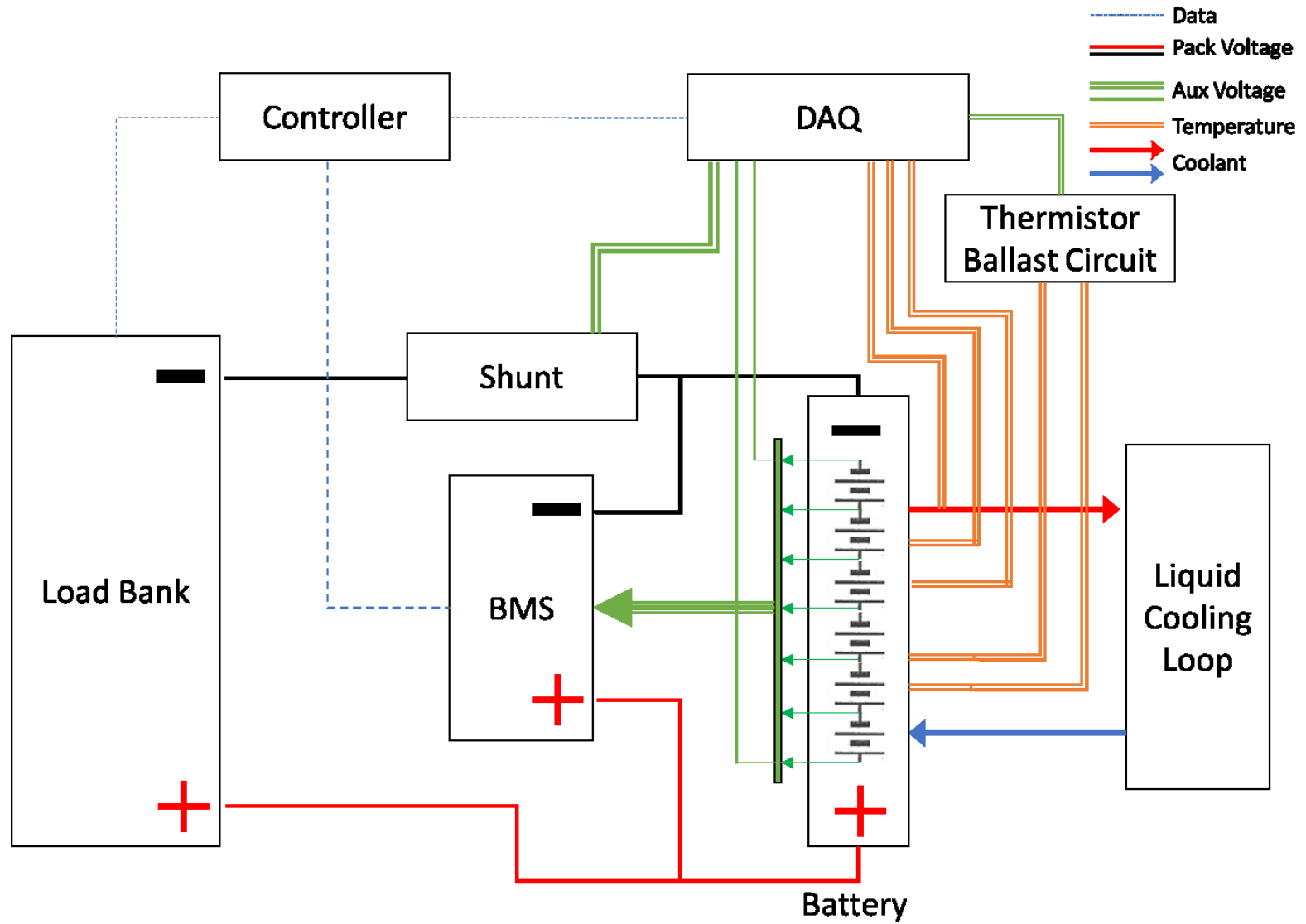


Figure 35- System Line Diagram. Blue dashed lines indicate communications, green lines indicate voltage taps, and orange lines indicate temperature measurement

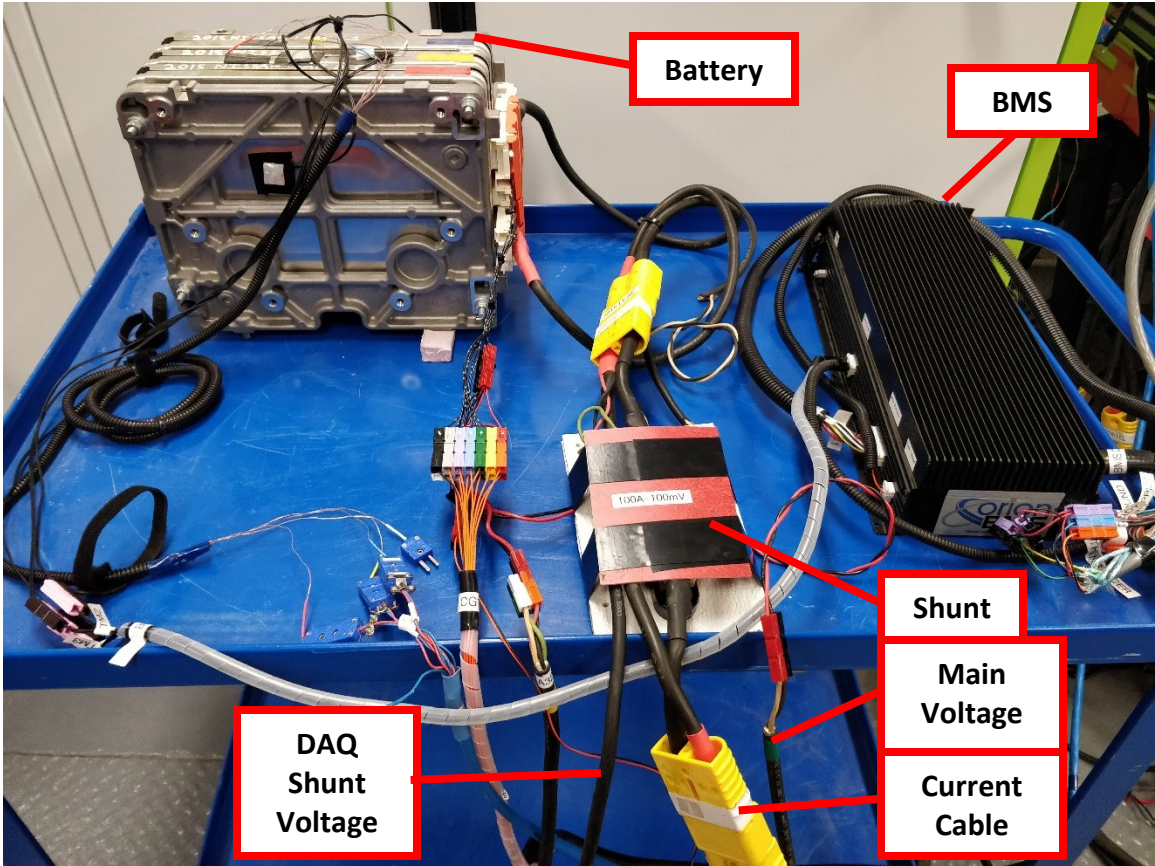


Figure 36- Full Testing Overview

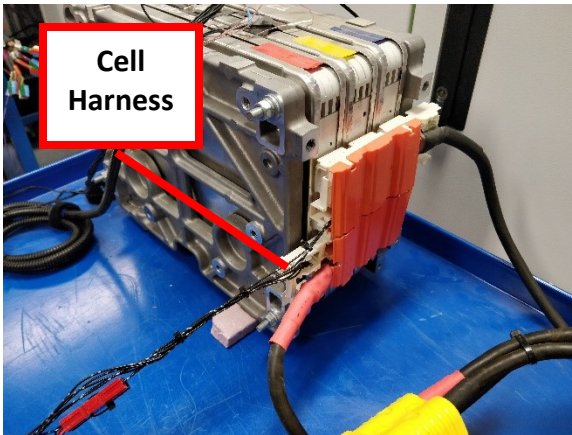


Figure 37- Leaf cell harness and main terminals

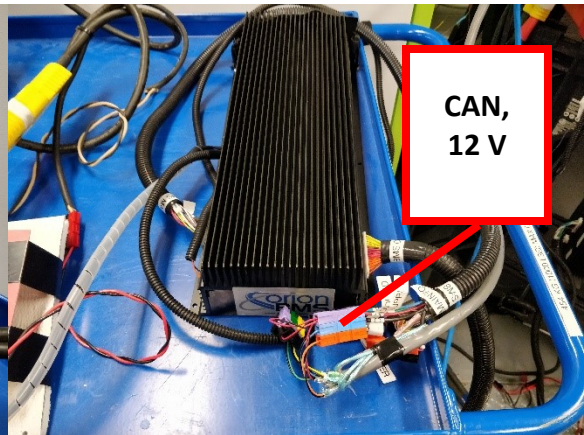


Figure 38- Orion BMS and CANbus channels

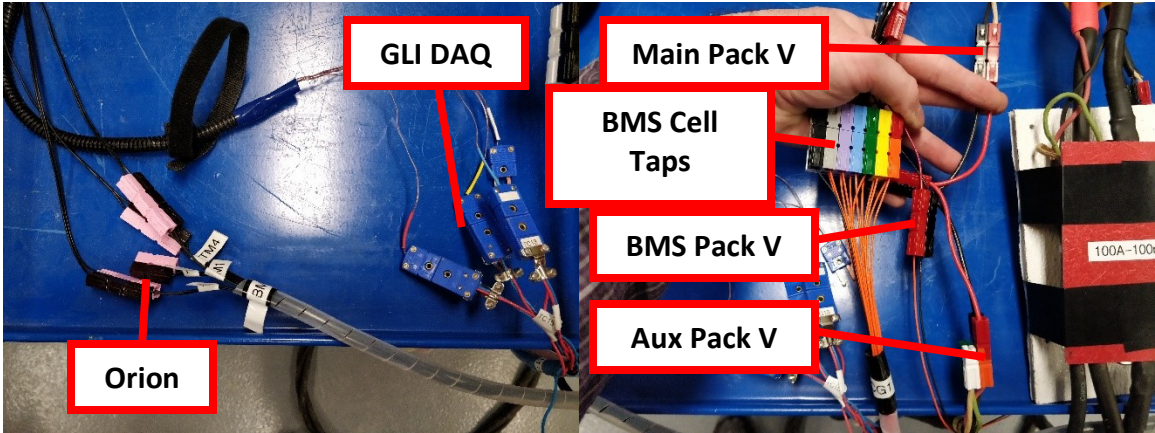


Figure 39- Orion Thermocouples and GLI DAQ Thermocouples

Figure 40- Cell Harness Interconnect with BMS and other voltages

4.3 Test Protocols

The tests performed are derived from the Pacific Northwest National Labs proposed *Protocol for Uniformly Measuring and Expressing the Performance of Energy Storage Systems* [16].

The protocol is designed to compare the performance of different energy storage technologies in electricity grid services.

All tests collect the following information:

- Current
- Voltage
- Temperatures
- Cell Voltages
- Elapsed Time

From these, all other variables are calculated, notably coulombic capacity, energy capacity, energy efficiency and overcharge.

The tests are chosen to determine the performance characteristics of the batteries (constant current and power), and to demonstrate the ability of the batteries to perform services (frequency regulation).

Each of the following tests (4.3.1 to 4.3.3) were performed on each battery to compare performance over the range of services.

Hour Rates

The testing protocols and results will describe current and power values in terms of *hour rates*. Normally, an hour-rate is intended to be the value of constant discharge which would deplete the battery in that timeframe, i.e., a 1 hour rate should deplete the battery in 1 hour. When dealing with aged batteries, or rates that are not as specified, the actual discharge time will vary. When reading this document, all hour rates are in reference to the specifications in Table 3. For example, the Leaf has a rated coulombic capacity of 60 Ah. A 1 hour rate would be a CC discharge at 60 A, a 0.5 h rate would be a CC discharge at 120 A.

Sign Convention

Discharge is specified to be a negative value in all measurements. Because the tests begin with discharge, this means Amp-hour depletion will fall, then climb back to zero when fully recharged, assuming 100% coulombic efficiency, which is validated in testing. This is consistent with SOC starting at 100% and declining with discharge.

Cycling Parameters

The parameters in Table 9 are used to determine the rates and limits of the tests presented in this section.

Table 9- Cycling Parameters

Manufacturer	Battery	1 Hour Rate Cycle Parameter				
		V _{max} (vpc)	V _{min} (vpc)	i _{max} (A)	P (kW)	T _{rest} (°C)
Chevrolet	Volt	4.2	2.5	45.0	6.0	35
Panasonic	Tesla	4.2	2.5	222.0	4.8	35
AESC	Leaf 2012	4.2	2.5	60.0	15.0	30
AESC	Leaf 2015	4.2	2.5	60.0	1.4	30
Enerdel	Moxie+	4.1	2.5	31.5	3.9	30
Lishen	EV-LFP	3.55	2.85	115.5	37.3	30

For ½ h and 4 h i_{max} and P rates, multiply by 2 or divide by 4, respectively.

4.3.1 Constant Current- Constant Voltage Capacity

The primary purpose of the constant-current constant-voltage (CC-CV) test is to determine the coulombic capacity of the battery under test at different current rates. An example cycle is shown below in Figure 41.

The duty cycle is as follows:

1. Wait 36 seconds to record initial values.
2. Enter constant-current mode at a rate i_{\max} , discharging until a battery minimum voltage, V_{\min} is reached.
3. Enter rest for 10 minutes, and until the highest temperature cools to a threshold value T_{rest} (e.g. 30 °C).
4. Enter constant-current mode, charging at a rate i_{\max} until a battery maximum voltage, V_{\max} is reached.
5. Change to constant-voltage mode, holding the voltage to V_{\max} and continue charging until the current is below a threshold value, i_{cutoff} (e.g. 3 A).
6. Enter rest for 10 minutes, and until the highest temperature cools to a threshold value T_{rest} .
7. Repeat 2 to 6 until 3 cycles have completed. This yields the initialization cycle, the data collection cycle, and the confirmation cycle.
8. Enter rest for 36 seconds to collect the end-of-test values.

Repeat the whole process three times total, once each for a 4 h, 1 h, and 0.5 h current rate i_{\max} , based on the rated coulombic capacity of the battery.

Energy efficiency is calculated at the end of charge, by dividing the time integral of power in discharge mode by the time integral of power in charge, i.e., by dividing the discharge energy by the charge energy.

This test is not in the PNNL protocol but was added because it is an industry standard test, used to determine the coulombic capacity of a battery for comparison between different chemistries, cell formats, etc., and is therefore of interest to third-party operators. However, it does not directly measure the usable energy of the battery under a grid service, which is the more practical statistic for grid storage.

4.3.2 Constant Power Capacity

The primary purpose of this test is to determine the usable energy capacity of the battery at different power rates. An example cycle is shown below in Figure 41.

The duty cycle is as follows:

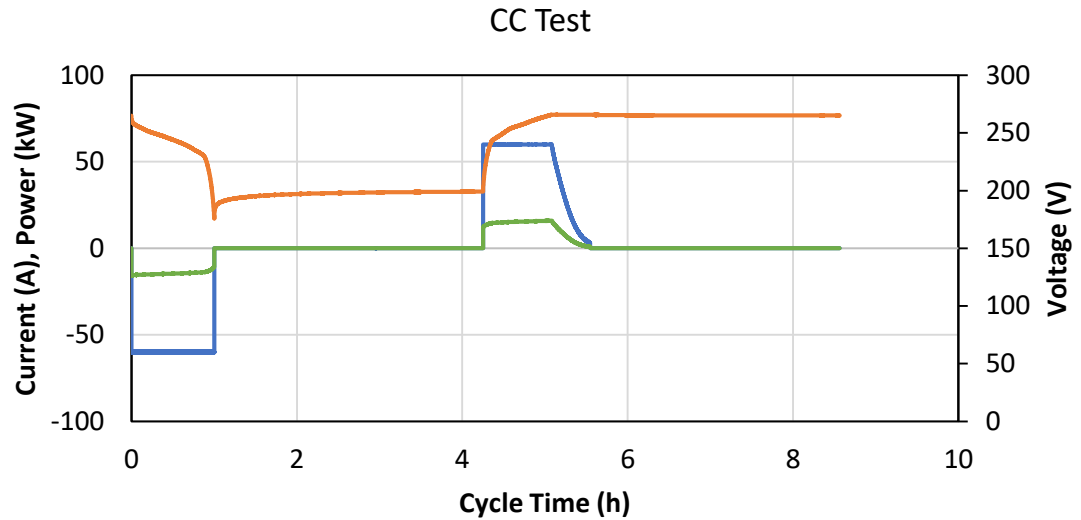
1. Wait 36 seconds to record initial values.
2. Enter constant-power mode, discharging at a rate P until a battery minimum voltage V_{\min} is reached.
3. Enter rest for 10 minutes, and until the highest temperature cools to a threshold value T_{rest} .
4. Enter constant-power mode, charging at a rate P until a battery upper voltage V_{\max} is reached.
5. Enter rest for 10 minutes, and until the highest temperature cools to a threshold value T_{rest} .
6. Repeat 2 to 5 until 3 cycles have completed.
7. Enter rest for 36 seconds to collect the end-of-test values.

Repeat the whole process three times total, once each for a 4 h, 1 h, 0.5 h power rate P based on the rated energy capacity of the battery.

The coulombic capacity of the battery under this test regime will be lower than under CCCV testing due to the lack of CV charging, but this is a more useful measure of what the battery can provide, given that contracting and service specifications are in terms of power and energy, not current and coulombs.

In the original PNNL protocol, one rate was used for three cycles, but the others were only cycled once. The test in this work has been expanded to three cycles at each rate so the capacity of the battery can stabilize through repeated cycling in accordance with the initialization, data collection, and validation methodology.

a)



b)

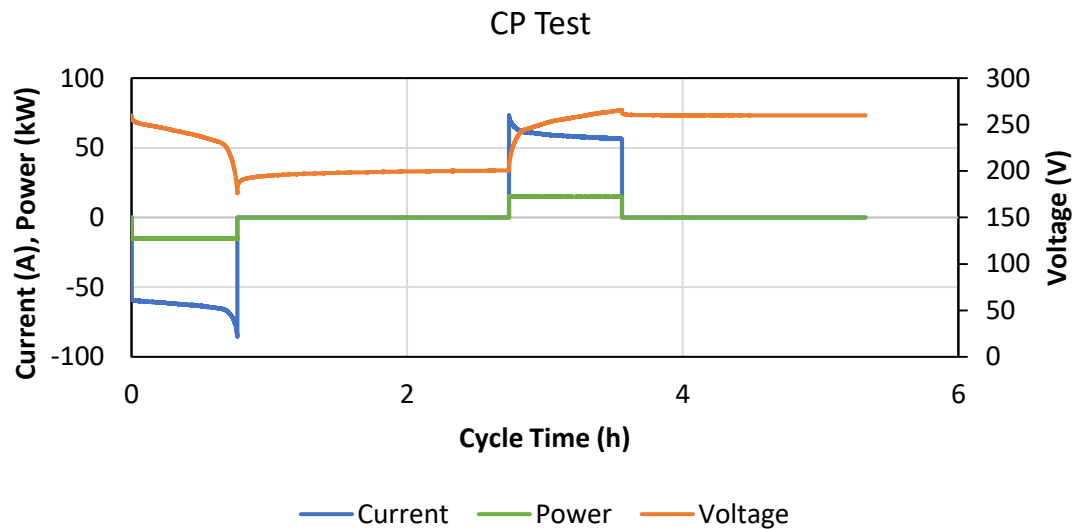


Figure 41- Example a) Constant-Current and b) Constant-Power Test Cycles from a 2012 Leaf, 1h rates on both.

Constant-current tests reach peak power at the start of discharge, and the end of CC charging, before stepping into CV charging. Peak temperatures are reached in discharge because the charge step takes longer to pass the same amount of charge. Constant-power tests reach peak currents at the end of discharge. Peak temperatures are reached in discharge, as current rises at the end of discharge, increasing heat dissipation, where in charge current starts high and stays lower than discharge due to higher battery voltage. The CC charge will always restore more charge than CP testing due to taper charging, and in real-world applications, a CPCV test which includes a taper charge, for example, on overnight charging, would be advised.

4.3.3 Frequency Regulation

The primary purpose of this test is to determine the greatest power the battery can offer in contract for frequency regulation.

The duty cycle is as follows:

1. Begin with the batteries fully charged, according to a CC-CV charge at V_{\max} .
2. Discharge at constant current at a 1 h rate until the batteries are at 50% of their *rated capacity* by amp-hour depletion.
3. Begin measuring charge and discharge values from this point.
4. Enter power-control mode and follow the signal timeseries given in Appendix C, where the signal is a unit scale signal, and should be multiplied by a rate R such that R is the highest power the timeseries will call on in its duration.
5. If the timeseries could not be completed due to the battery reaching minimum or maximum voltage, reduce the value of R and start from step 1.
6. If the timeseries was successfully completed, increase R until it can no longer finish the timeseries successfully.
7. Iterate this process until a peak rate is identified.
8. When the battery completes the timeseries, charge or discharge it at a 1 h constant-current rate until it is returned to the 50% amp-hour depletion mark (i.e., from step 3 there should be no net Ah depletion). Efficiency is calculated from this step.
9. Recharge the battery in CC-CV mode at a 1 h maximum rate until it is taper charged to V_{\max} .

Sections of the timeseries are shown below in Figure 42.

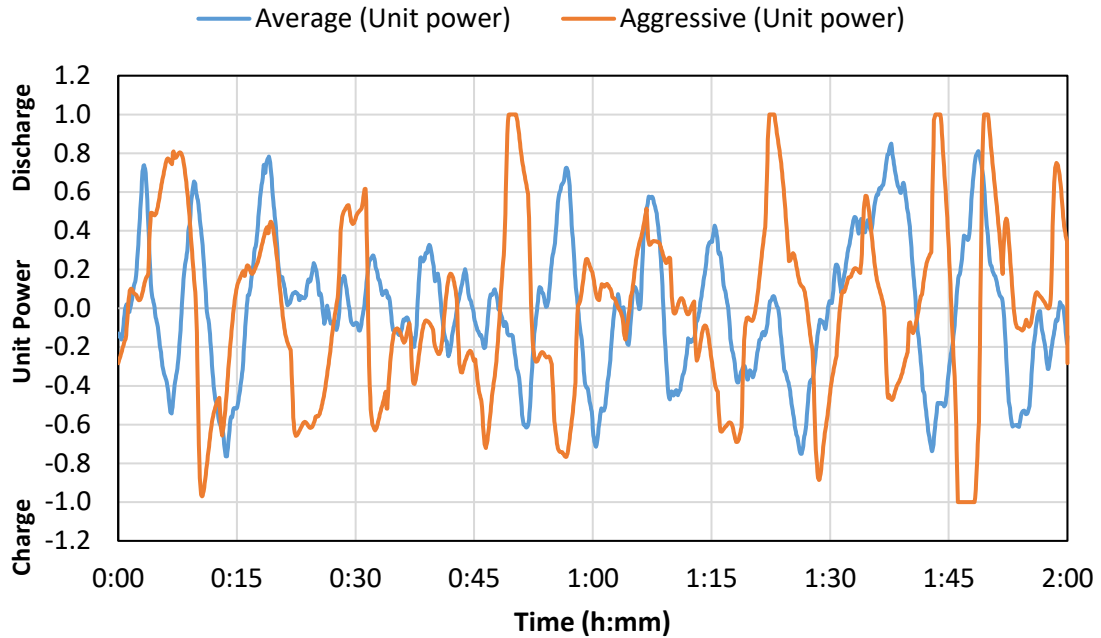


Figure 42- Example FR Signals from PNNL Protocol. Total cycle is composed of 10 average periods and 2 aggressive periods.

The efficiency and performance values shall be calculated from step 8, when the battery is returned to its operating state of charge.

Frequency regulation was chosen as a test because it is an economically feasible service. Also, frequency regulation is a fast-changing duty cycle, and represents the power end of the power-energy dichotomy that energy storage technology can be viewed with.

The FR signal is use is sourced from the PNNL protocol, which drew from the PJM regulation district for its source data. The authors of the protocol selected the component parts of the signal based on the following characteristics:

- The timeseries should be energy neutral in throughput.
- The power signal must reach symmetric boundaries for normalization.
- The signal must resemble a “typical” signal for the area.

Given their success with the above, and the scope of this thesis, the PNNL signal was found to be satisfactory.

This test was modified from the PNNL original in a critical way: R was previously fixed at the rated power capacity of the battery, and the battery either passed or failed the test. In the case of second-life batteries that may have no official rating, this new method allows for more useful results than simple pass/fail and allows for comparing different batteries by their R values than by whether they passed or failed a single test, and the remaining coulombic capacity at the end of the 24 h signal.

Chapter 5 Results and Analysis

The results and analysis are organized by test, covering constant-current and constant-power capacity tests, followed by frequency regulation grid service.

- The constant-current test is performed by discharging the battery at a constant current to a lower voltage limit, resting, then charging at a constant rate until an upper voltage limit, followed by holding it at a constant voltage until the current tapers to a specific value. The results and analysis show the coulombic capacity of each battery, and how it compares with the rated capacity, and the availability of that capacity at different current rates.
- The constant power testing is performed by discharging, resting and charging at a constant rate of power, stopping at upper and lower voltage limits, without a taper charge. The results and analysis will show the energy capacity, energy efficiency, cycle durations, and thermal responses.
- The frequency regulation test is performed by positioning the battery at 50% amp-hour depletion, then following a predefined timeseries of power values, then repositioning at 50% amp-hour depletion and then fully recharging. This section will discuss the relative performance of the batteries, their best performance, their energy efficiency in regulation services, and their operating temperature.

Usage of Third Cycle Data

The test procedure uses three cycles for data collection- initialization cycle, data collection cycle, and validation cycle. If a battery had previously been used for a different service, the available capacity can change with successive cycling, and the series of cycles allows the available capacity and thermal response to stabilize. The driving mechanism for this behavior is the dependence of voltage on the driving rate.

For the purposes of this testing, the voltage of a battery at any instant depends on its coulombic state of charge, temperature and the present current load, plus some time-dependent transient lag effects. Higher rates in constant-current or constant-power mode causes voltage to be more negative or positive in discharge or charge respectively, at the same state of charge. Because test termination is governed by voltage thresholds, a faster rate test will terminate at a more

restricted coulombic capacity for a higher rate. This causes the available capacity of the battery to be less than theoretically extractable.

Assuming the first cycle begins at an arbitrarily charged state, discharge will terminate at a characteristic state of charge for that rate and mode. Take this state as the lower limit of availability for that rate and method.

In charge, termination depends on the cycling method. With CCCV charging, all rates terminate at a fully charged state because the CV step allows the rate to slowly taper off, maintaining the upper voltage limit. Because all rates use the same taper current cutoff, they reach the same upper state of charge. In CP testing, charging will terminate at a characteristic state of charge for the rate.

The available capacity is bracketed between these upper and lower states for a given mode and rate. In the first cycle, discharge will terminate at its lower bracketing value and then charge to the upper bracketing value. The second cycle begins at the upper value and ends at the lower value, capturing the available capacity for that rate and mode. The third cycle should have the same capacity and is used to validate the measured capacity from the second cycle.

5.1 Constant Current Test (CC)

The primary purpose of CC testing is to compare the test results to the manufacturer's specifications, across a range of hour rates. This informs on the available coulombic capacity of the battery.

5.1.1 Summary

Table 10 summarizes the results of the CC capacity test at 3 separate hour rates. Capacity is the discharge capacity on the third cycle of the given test. Rated capacities are the values from Table 3, repeated for comparison.

Table 10- CC Coulombic Capacity Summary (Cycle 3)

Manufacturer	Battery	Capacity by Hour Rate (Ah)			
		4 Hour	1 Hour	0.5 Hour	Rated Cap.
LG Chem	Volt	48.4	49.0	46.5	45
Panasonic	Tesla	209.8	207.2	205.8	222
AESC	2012 Leaf	59.2	60.0	58.3	60
AESC	2015 Leaf	62.2	61.7	61.7	60
EnerDel	Moxie+	30.4	28.2	29.0	31.5

Table 11 summarizes the peak temperatures observed during CC testing. All temperatures are from the discharge step, which has the highest measured temperatures. Peak temperatures occur during discharge because the current during discharge is held for the whole step, whereas charge current tapers at the end of charge. Because an equal number of Ah must be discharged and then charged, and the charge step includes a CV section with current taper, the discharge step at constant current will run for more time than the constant-current segment of charge. This assumes the battery has perfect coulombic efficiency, which is a valid simplification, per [64]. Thus, the resistive losses, being proportional to the square of current, are greater in discharge, because it runs at the fixed current for longer than during charge. This is confirmed by checking the data for charge vs. discharge peak temperatures.

Table 11- CC Peak Temperatures during Test

Manufacturer	Battery	Peak Temperature by Hour Rate (°C)		
		4 Hour	1 Hour	0.5 Hour
LG Chem	Volt	28.2	34.1	42.0
Panasonic	Tesla	28.4	40.0	60.3 ¹³
AESC	2012 Leaf	23.0	43.7	44.0
AESC	2015 Leaf	26.4	38.5	45.5
EnerDel	Moxie+	22.0	31.7	37.9

In Figure 43 the solid lines give capacity results from Table 10 as normalized by dividing the result of discharge coulombic capacity by the specified coulombic capacity given in Table 3. The maximum temperatures are plotted as dotted lines in Figure 43 to complement observed

¹³ LCTL set to 20 °C for this test.

capacity gains, and suggest cycling hour-rate limits given a maximum allowable temperature of 50 °C.

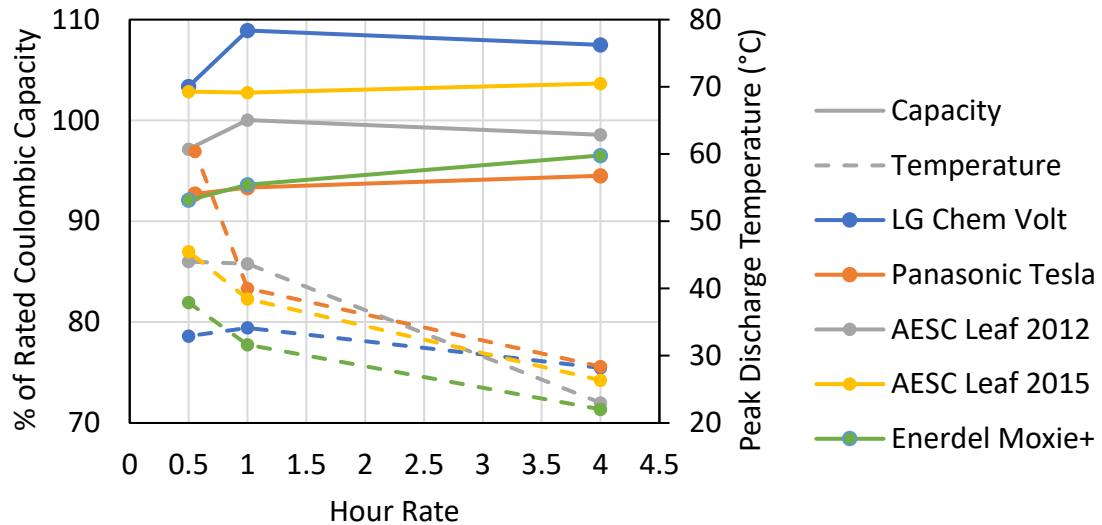


Figure 43- Scaled Capacity and Temperature vs. Hour Rate . Solid lines indicate capacity, dashed lines indicate temperatures.

All batteries remain within 10% of rated values for all tested hour rates. The EnerDel Moxie+ has the lowest final capacity, at 92%. This suggests the batteries are in reasonable and normal condition and justifies their continued testing.

The Volt, 2012 Leaf and 2015 Leaf do not trend monotonically downward in capacity as hour rate increases. This may be because the higher temperatures increase the capacity of the battery by accelerating the electrochemical reaction rate.

The highest temperature reached was 60.3 °C, by the Panasonic Tesla during 0.5 h testing. This exceeds the safety limit of 50 °C, suggesting that a 0.5 h rate is past the maximum performance limit of this battery, with the given cooling system. The second highest temperature was 45.5 °C, by the 2012 Leaf during 0.5 h testing. This is close to the safety limit of 50 °C, suggesting that a 0.5 h rate is near the maximum performance limit of this battery in ambient conditions.

5.2 Constant Power Test (CP)

CP testing yields the discharge energy capacity of the battery. While CC testing is an industry standard for specifying batteries, CP testing provides information on the energy capacity an operator can use in typical grid storage applications. This is more relevant than coulombic

capacity, because electrical service is provided in terms of power and energy, not currents and amp-hours.

Three different hour-rate tests were performed for each battery, and the discharge energy capacity and round-trip energy efficiency from the third cycle are displayed in Table 12.

Table 12- CP Energy and Efficiency (Cycle 3)

Hour Rate	Manufacturer	Battery	Rate (kW)	Energy Efficiency (%)	Discharge Energy (kWh)	Rated Energy (kWh)
4 hour	LG Chem	Volt	1.5	98.8	6.2	6.0
	Panasonic	Tesla	1.2	94.6	4.0	4.8
	AESC	2012 Leaf	3.8	97.5	13.9	15.0
	AESC	2015 Leaf	0.4	98.0	1.4	1.4
	EnerDel	Moxie+	1.0	98.7	3.8	3.9
1 Hour	LG Chem	Volt	6.0	96.6	5.7	6.0
	Panasonic	Tesla	4.8	87.1	3.4	4.8
	AESC	2012 Leaf	15.0	94.0	11.6	15.0
	AESC	2015 Leaf	1.4	94.7	1.2	1.4
	EnerDel	Moxie+	3.9	96.6	3.6	3.9
0.5 Hour	LG Chem	Volt	2.0	94.4	0.94	1.0 ¹⁴
	Panasonic	Tesla	6.0	82.4	2.9	4.8
	AESC	2012 Leaf	30.0	88.4	7.8	15.0
	AESC	2015 Leaf	3.0	92.3	0.7	1.4
	EnerDel	Moxie+	7.8	95.8	2.7	3.9

5.2.1 Energy Capacity

Figure 44 presents the normalized discharge energy capacity as a function of hour rate and adds charge energy as well. Normalization is performed by dividing the results of Table 12 by the energy capacity specifications in Table 3.

¹⁴ The 0.5 h Volt CP test was performed with a reduced module of 6 cells in series

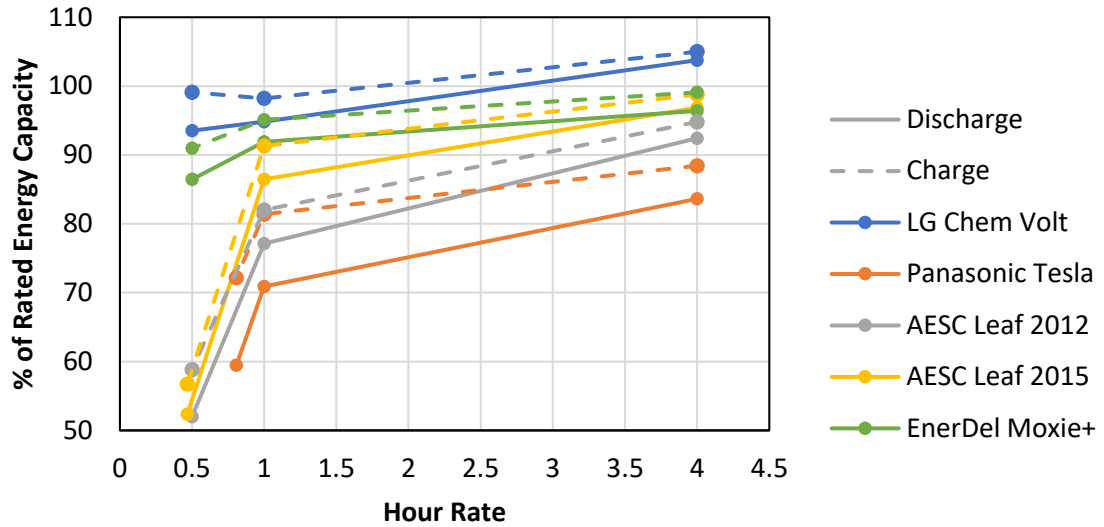


Figure 44- Discharge and Charge Energy Capacity during Constant-Power Testing. Solid lines are discharge capacity, dashed lines are for charge capacity.

The tests terminate based on the voltage of the pack reaching a lower or upper limit. The voltage of the cell will drop in discharge, or rise in charge, when under load, as a function of the current draw, at the same depletion, as shown in Figure 45.

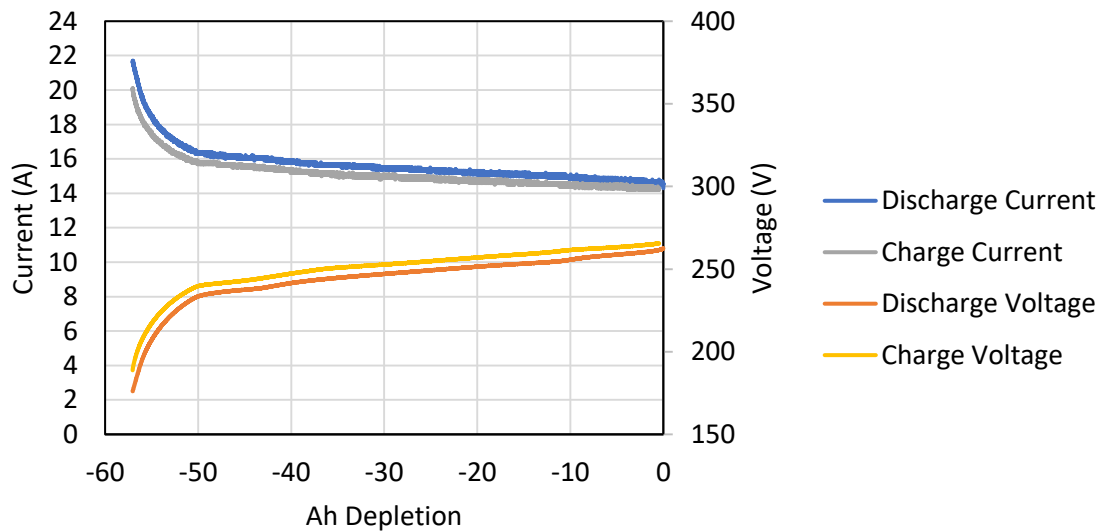


Figure 45- Ah-Depletion, Current, Voltage Relationship at Constant Power Data drawn from a 4 h Leaf 2012 CP test

For the same voltage, drawing more power will require drawing more current. Thus, as a higher power test depletes the energy in the battery, it will trigger the test limit where a lower power test at the same depletion would not. This early termination leaves a portion of the full capacity

inaccessible at this rate and voltage threshold. The same process applies in charge mode, restricting the amount of recharge. With successive cycling, this restricted energy capacity stabilizes, and is reported as the available discharge capacity in the third cycle. Going past the voltage limits would allow the use of the restricted capacity, but voltage excursion can damage the electrodes and electrolyte of the cell [65], even though the voltage change is load induced, rather than because of charge depletion. This phenomenon of available capacity reduction is demonstrated in Figure 44.

This restriction in capacity is most pronounced at 0.5 h rates, where the Moxie+, Leaf 2012 and 2015 lose 20 percent of their full energy capacity available compared to a 1 h rate.

Between 4 h and 1 h, all batteries lost less than 15% of their full capacity. For operators, this indicates that energy capacity is stable for 2+ hour rates. Even at the high rates, the batteries can perform the service, though less capacity is available.

5.2.2 Cell Voltage and Efficiency

Figure 46 shows the average cell group voltages of each pack in charge and discharge, as a function of hour rate.

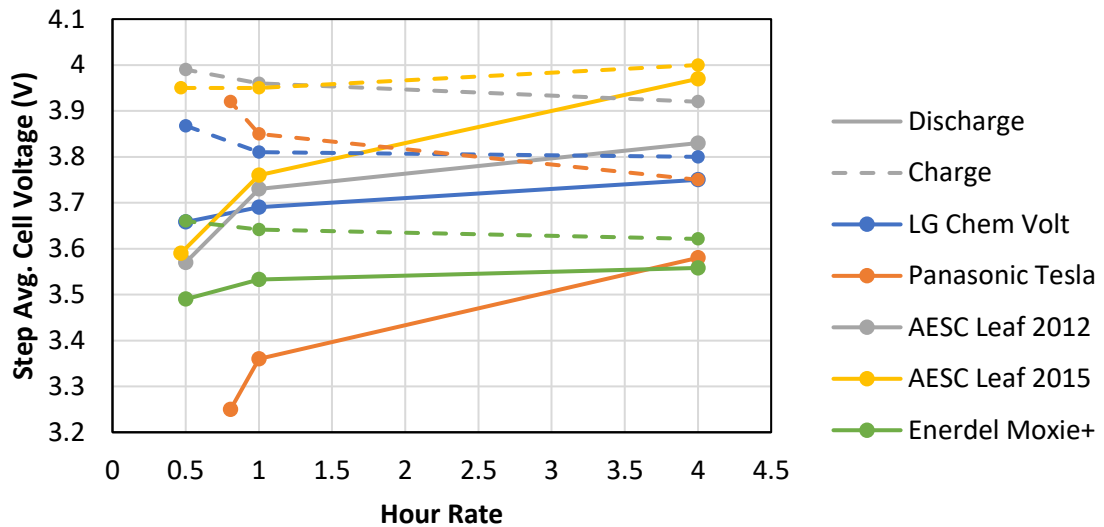


Figure 46- Average Step Cell Voltage vs. Hour Rate. Solid lines are discharge cell voltage, dashed lines are charge cell voltage.

Two main trends can be identified in Figure 46. The discharge voltage drops slowly from 4 h to 1 h, then from 1 h to 0.5 h, the Leaf 2015 and 2012 all drop by 0.2 to 0.4 VPC. The average charge voltage of all batteries remains mostly flat as a function of hour rate, only gradually increasing.

Figure 47 presents the energy efficiency from Table 12 by battery and hour rate.

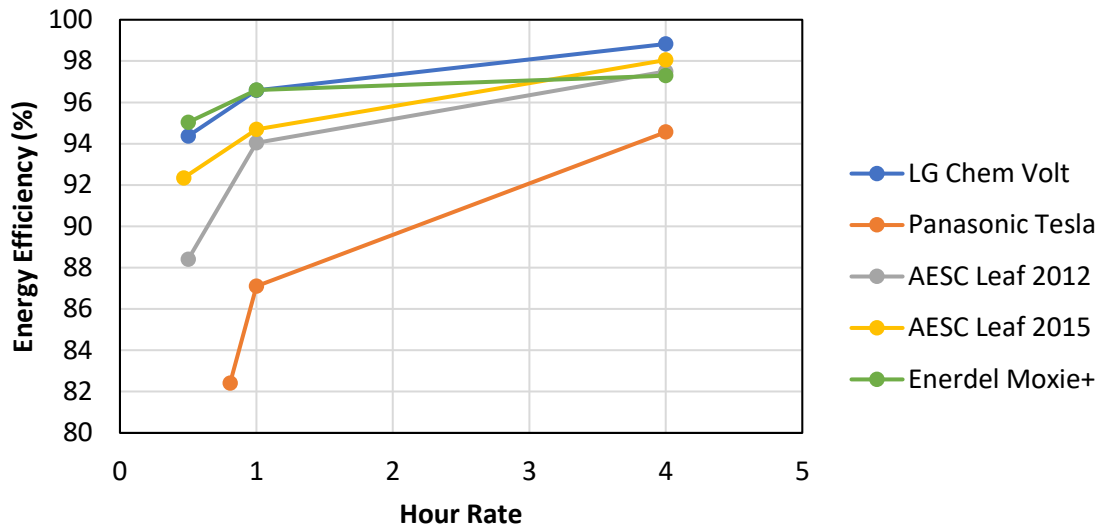


Figure 47- Constant Power Round Trip Energy Efficiency Test Results

Efficiency values begin closely clustered together, and except for the Tesla, stay clustered as hour rate increases to 1 h. The Moxie+ remains very efficient up to 0.5 h, which is consistent with its HC negative electrode.

The 4 h energy efficiency values are all near or above 95%. Assuming a 96% converter efficiency for example [66], this would be 87.5% AC-AC energy efficient. Compared to other energy storage technologies, this is excellent performance, against benchmarks of 70%-90% [67]. As the hour rate increases, the lowest DC-DC energy efficiency is still high, at 88.4% for the 2012 Leaf.

The 2012 Leaf efficiency of 88.4% is substantially lower than the 2015 Leaf efficiency of 92.3%, for the same hour rate and capacity of battery. This may indicate a substantial improvement in the electrochemical material composition of the cells, or the effects of aging.

5.2.3 Cycle Time and Temperature

Table 13 below presents the time required to perform each step of the CP cycle, along with the peak temperature reached in each portion of the cycle. This is useful to grid operators for scheduling and knowing what temperatures to expect from cycling batteries of this type. The peak discharge temperature is always higher than the peak charge temperature because the currents reached in discharge are higher than those in charge. To achieve the same power, the discharge current must be higher than the charge current at the same state of coulombic depletion. The higher currents dissipate more energy to resistive losses, leading to higher temperatures. This cause of peak discharge temperature is different in nature from the constant-current test, which was because of different durations of operation in discharge and charge modes at the same current rates.

Table 13- CP Step Duration and Temperatures

Hour Rate	Manufacturer	Battery	Dis. Duration (h)	Dis. Temperature (°C)	Dis. Rest Duration (h)	Chg. Duration(h)	Chg. Peak Temperature (°C)	Chg. Rest Duration (h)
4 Hour	LG Chem	Volt	4.16	27.3	0.16	4.21	27.0	0.16
	Panasonic	Tesla	3.37	29.7	0.17	3.57	27.8	0.17
	AESC	2012 Leaf	3.65	23.0	0.16	3.74	24.0	0.16
	AESC	2015 Leaf	3.32	29.3	0.16	3.41	28.7	0.16
	EnerDel	Moxie+	3.79	25.8	0.17	3.84	25.7	0.17
1 Hour	LG Chem	Volt	0.95	31.4	0.16	0.98	30.0	0.16
	Panasonic	Tesla	0.72	44.5	1.49	0.85	35.9	1.14
	AESC	2012 Leaf	0.77	36.0	1.97	0.82	35.0	1.76
	AESC	2015 Leaf	0.87	38.7	1.24	0.93	37.2	0.88
	EnerDel	Moxie+	0.92	31.3	0.27	0.95	26.9	0.17
0.5 Hour	LG Chem	Volt	0.47	33.3	0.17	0.51	31.4	0.17
	Panasonic	Tesla	0.48	50.6	2.75	0.60	41.3	2.51
	AESC	2012 Leaf	0.26	39.0	2.37	0.30	35.0	1.79
	AESC	2015 Leaf	0.25	43.3	1.34	0.27	38.6	0.89
	EnerDel	Moxie+	0.34	32.3	0.27	0.36	30.7	0.17

By summing the time in each step the total time to perform a whole cycle is found, including rest time to cool down prior to discharge or charge. These results are presented in Figure 48, along with peak temperature achieved during the cycle.

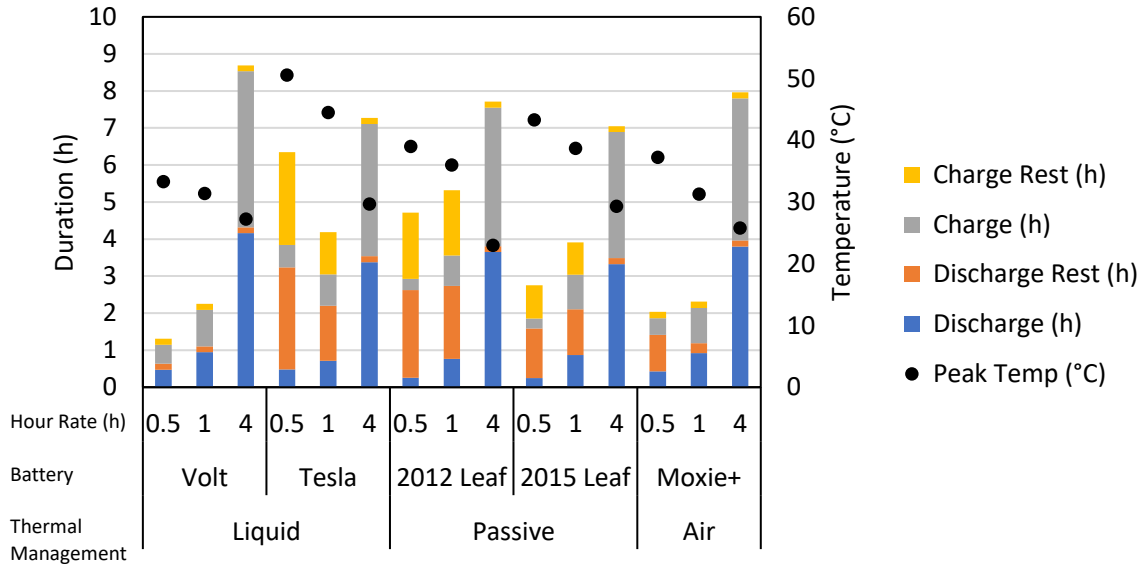


Figure 48- Constant Power Step Time and Peak Discharge Temperature by Battery and Hour Rate

Figure 48 is useful for predicting the thermal recovery rates for various service hour rates, particularly for peak shaving. Once the discharge has completed, the battery must cool before recharging. At a 4 h discharge rate, all batteries are ready for charge immediately as their temperature has not risen by any appreciable amount. At 1 h rate, the passively cooled batteries require up to one hour of cooling time before charging. At 0.5 h rates, the passively cooled packs require up to three hours to cool. As peak shaving services usually charge overnight, all batteries are capable of any rate of discharge when given a multi-hour cooling window. The Tesla experiences a large temperature rise, reaching 50 °C in discharge. This is higher than the passively cooled packs reach for the same hour rate, which is unexpected, given the Tesla is liquid-cooled. This temperature rise may be explained by the much lower energy efficiency of the Tesla at 0.5 h rates- it falls to 82% vs. approximately 90% for the two Leaf packs.

The grid may also require peak shaving services at two points during the day (double peak), in the morning and evening, with an interval where solar generation depresses energy prices, such as in the California grid, as shown in Figure 49. In this situation, the ability to thermally recover in a short period is necessary to prepare for the evening peak. Only actively cooled batteries are shown to have this cooling rate, taking less than 0.5 h to cool for the Moxie+, Tesla and Volt at 1

h rates. Being able to provide a service twice as often increases revenue potentials, and this would advantage the actively-cooled batteries.

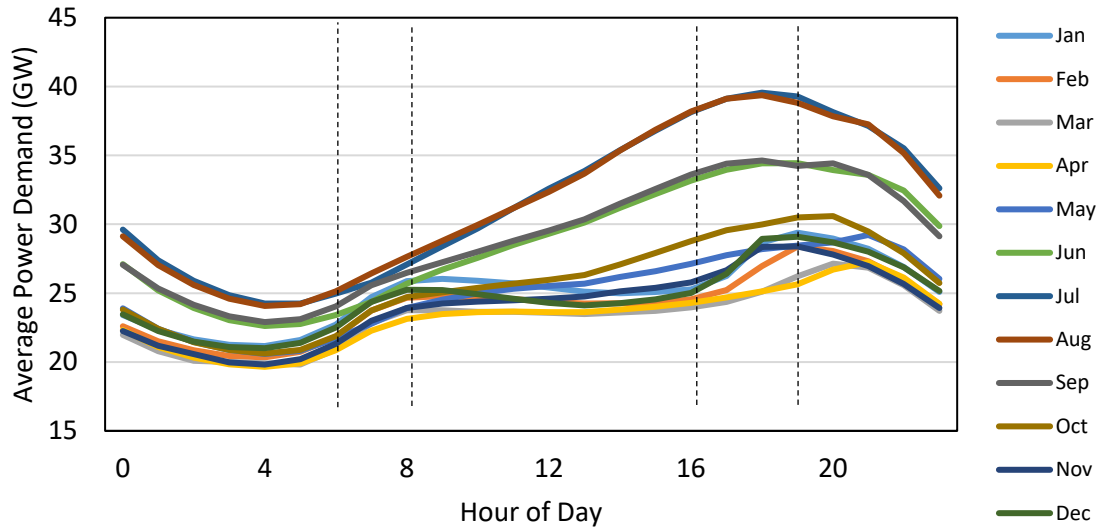


Figure 49- CAISO electricity hourly demand average by month. Drawn from CAISO hourly 2017 information [17]. Peak hours are bracketed by dotted lines.

5.2.4 Peak Shaving Applicability

Peak shaving is a duty cycle which discharges during the peak of electric grid power consumption in a day, capitalizing on the high price of electricity during that period. The example duty cycle from PNNL has a CP discharge period lasting from 2,4 or 6 hours, with a 12 h CP recharge which would be run overnight to take advantage of lower nighttime pricing [16]. This duty cycle was tested, and the results were within 1% variation to those of regular CP testing as performed above. This suggests that the CP test protocol used in this thesis is a faster method of determining peak shaving potential than the unmodified PNNL protocol.

For operators, the results presented in 5.2 are applicable to peak shaving operation, with similar or better efficiency from the battery.

5.3 Frequency Regulation Test (FR)

The purpose of the FR testing is to find rate (bid) limits and energy efficiency of batteries providing FR services. FR services are contracted with a maximum power that an operator can provide through a window of time, and the grid operator will send a signal for the storage

operator to follow, up to a maximum of the contracted power value. The PNNL standard provides a 24-h normalized cycle, such that the peak power values are ± 1 units. This signal is multiplied by a peak power value for testing, and this peak power value is increased until the battery can no longer complete the 24 h cycle. In the market, three factors influence the peak power bid selection. Revenue is directly proportional to the peak power value contracted, so optimizing it is a necessary goal when providing regulation services. The inefficiency of the battery and converter systems requires that the operator be able to recharge the battery in operation, and a power signal may be asymmetric for some time, from hours to days, leading to a slow charge or discharge of the battery without repositioning near 50%. In the last scenario, bidding a lower peak power value would permit the operator to safely contract for a longer period of time. The metrics of performance are the maximum peak power, minimum remaining coulombic capacity, the energy throughput of the duty cycle, the peak temperature reached during the cycle, and the energy efficiency of the duty cycle.

5.3.1 Maximum Rate and Throughput

The FR duty cycle is a scaled timeseries where the peak power is user-specified. The peak power column in Table 14 is the highest value of power that was successfully tested. Data from that test is presented alongside the power value in Table 14. The hour rate is calculated from the rated energy capacity of the battery. The lowest SOC in test is calculated as shown below. The 24 h energy throughput is the sum of all discharge and charge energy through the 24 h timeseries. The number of equivalent cycles is found by dividing the former by twice the rated energy of the battery, to evenly compare the battery's energy throughput¹⁵.

The Volt test results are based on a reduced 6-cell module from the original pack.

¹⁵ Twice the rated value because a full cycle would involve a discharge followed by a charge, hence twice the capacity

Table 14- FR Throughput and Equivalent Cycles

Manufacturer	Battery	Peak Power (kW)	Peak Equivalent Hour Rate (h)	Lowest SOC in test (%)	24 h Energy Throughput (kWh)	Number Equivalent Cycles by Rated Energy
LG Chem	Volt	2.0	0.50	32.6	14.4	7.2
Panasonic	Tesla	6.0	0.84	5.2	43.5	4.5
AESC	2012 Leaf	30.0	0.46	5.5	215.8	7.2
AESC	2015 Leaf	2.6	0.52	14.2	18.6	6.7
Enerdel	Moxie+	7.8	0.39	25.2	56.0	7.2

The lowest State of Charge (SOC) is calculated with Equation 2, using Lowest AhD as shown below in Figure 50.

$$Lowest\ SOC = \left(1 + \frac{Lowest\ AhD}{Rated\ Coulombic\ Capacity}\right) * 100\% \quad (2)$$

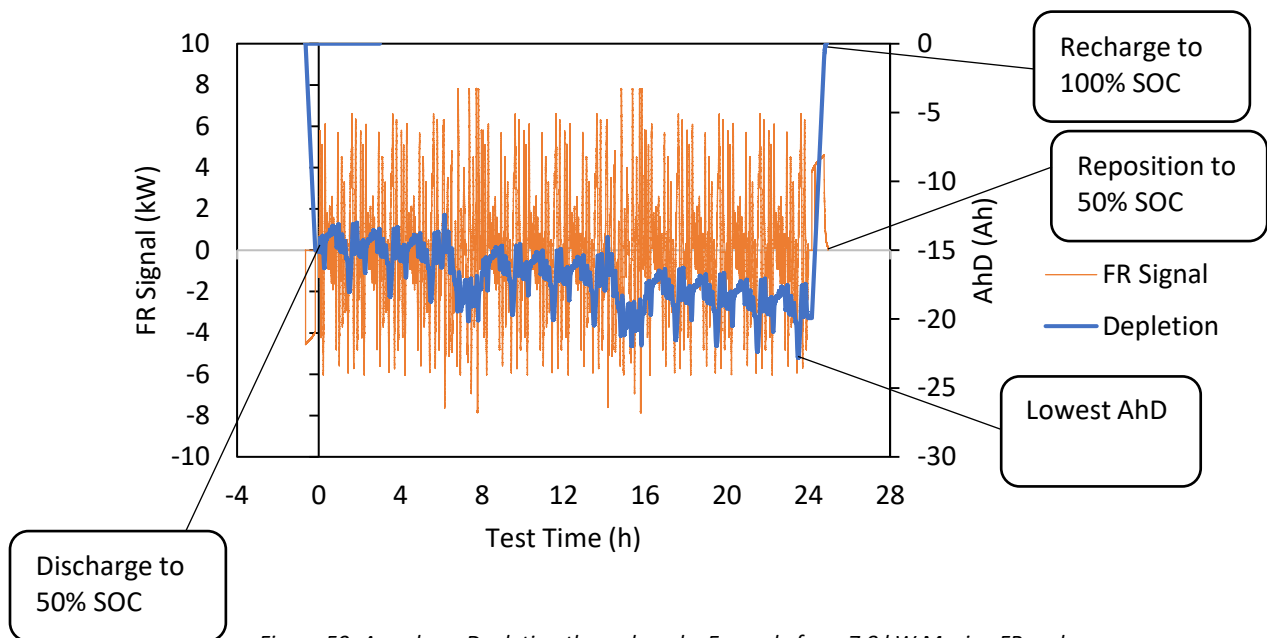


Figure 50- Amp-hour Depletion through cycle. Example from 7.8 kW Moxie+ FR cycle.

Lowest SOC is used as a metric to evaluate how close to failure (Complete discharge or charge) the cycle was. Once it reaches 5-15%, the battery reaches the lower voltage limit of the pack on peak discharge pulses, and the timeseries ends early, failing to complete the test. Part of the objective of testing is to determine the highest peak power that can be used without this occurring.

Energy throughput is a performance metric used to estimate the impact of regulation services on the health of the battery, and to compare the intensity of FR service with nominal deep-discharge cycling. By dividing the energy throughput by twice the rated value, an equivalent number of deep discharge cycles can be obtained. The batteries under testing performed 4 to 7 equivalent deep-discharge cycles over a 24 hour period. If the same batteries were used for peak shaving, only one cycle could be completed in the same timeframe.

Because revenue is a function of the power bid in the window, high energy throughput in regulation is not an advantage. Rather, the more throughput, the faster the battery will degrade. Comparing the cycling frequency of peak shaving and regulation, the FR service will deplete the available lifetime throughput of the battery 4 to 7 times faster- implying that the revenue per day must also be at least that much higher.

5.3.2 Efficiency and Peak Temperature

The secondary test results inform operators about the implications of long-term provision of FR services. In the primary results, the timeseries can terminate early because the battery state of charge will gradually deplete due to the asymmetry of charge and discharge voltages at the same state of charge under constant-power service calls per Figure 45. This means that the primary results are limited to only powers that can be sustained in 24 hours without recharging. In sustained operation, the state of charge will be maintained by periodic recharging or by biasing the charge power to be larger than the discharge power. Periodic interruptions are not paid services, so operators will stay in FR operation for as much time as possible. By calling for more peak power in charge than discharge, or by biasing using a charge baseline, the battery will be slightly recharged continuously, allowing indefinite operation. Therefore, the secondary test statistics inform the long-term operation of the battery in FR service. Efficiency values inform an operator of how much more the peak charge power needs to be than peak discharge power, and temperature is an upper limit to power, according to how hot the operator is willing to permit the batteries to run. Table 15 summarizes the results of the same tests as Table 14, presenting energy efficiency, peak temperature, and the lowest average cell voltage recorded during the cycle. The recharge factor is found by inverting the fractional efficiency, representing the persistent offset which would be required to continuously maintain SOC.

Table 15- FR Cycle Efficiency and Temperature

Manufacturer	Battery	Energy Efficiency (%)	Recharge Factor (%)	Lowest Average Cell Voltage (V)	Highest Temperature (°C)
LG Chem	Volt	97.8	102.2%	3.52	31.3
Panasonic	Tesla	92.9	107.6%	3.22	37.3
AESC	2012 Leaf	95.8	104.4%	3.51	38.0
AESC	2015 Leaf	96.7	103.4%	3.51	34.0
Enerdel	Moxie+	98.0	102.0%	3.07	27.0

Efficiency for all batteries under test was greater than 92% DC-DC, meaning that recharge multipliers are less than 1.1, which should be manageable. This may be because the batteries are operating in partial state of charge operation, which is the easiest state for accepting varying charge and discharge current. This can be verified by observing the average cell voltage. The lowest average cell voltage is 3.07 V for the Moxie+, but most batteries were closer to 3.5 V. This confirms that operations mostly occurred in the mid-range of voltage for the pack. Therefore, long-term operation should in fact be operating at efficient voltages. The highest temperature reached was 38°C, which, is within normal operating bounds. Batteries with more advanced thermal management systems were as much as 10°C cooler.

Overall, this supports the idea that EV batteries can be used to provide continuous, high-power services.

5.3.3 Operational Impact

In sustained operation, it is important to understand the envelope of possible peak power coefficients. During primary testing, the battery had net coulombic depletion due to inefficiency, gradually lowering its average SOC. This loss reduces power capability, until the required power exceeds the capability, and the test fails. If the battery is dynamically recharged, the power capability should not be reduced.

Temperature Control

Higher temperatures pose two obstacles:

1. Operation at high temperatures accelerates capacity loss.
2. High temperatures increase the risk of a thermal event.

Depending on the economic profile, the first point may not be of much concern. The second is always a subject of concern. Each battery will have a temperature past which it is not safe to operate; therefore, a peak power which causes a temperature higher than this in steady-state is not feasible. This can be seen in the Leaf 2012, which has a peak temperature of 38 °C. If dynamic recharging were used, a higher power rate could be used, but still not be feasible with this battery, because its steady-state temperature is already near the upper limit of safe operation, which can range from 40°C to 50°C depending on operator discretion. Thus, it may already be at its power limit, even with dynamic recharging.

Contrast this with the Moxie+ which reached 25 °C and has much more tolerance to increase its peak power.

Because FR service is constantly changing its power setpoint, the battery has a chance to cool off between high power calls. Figure 51 shows the temperature trend on a Leaf 2012 FR cycle, demonstrating that the temperature has stabilized overall. Because this was the warmest pack, with the worst cooling profile, it represents the worst-case scenario. This means the 24 h timeseries is sufficient to determine the temperature reached by the battery in continuous service with this signal.

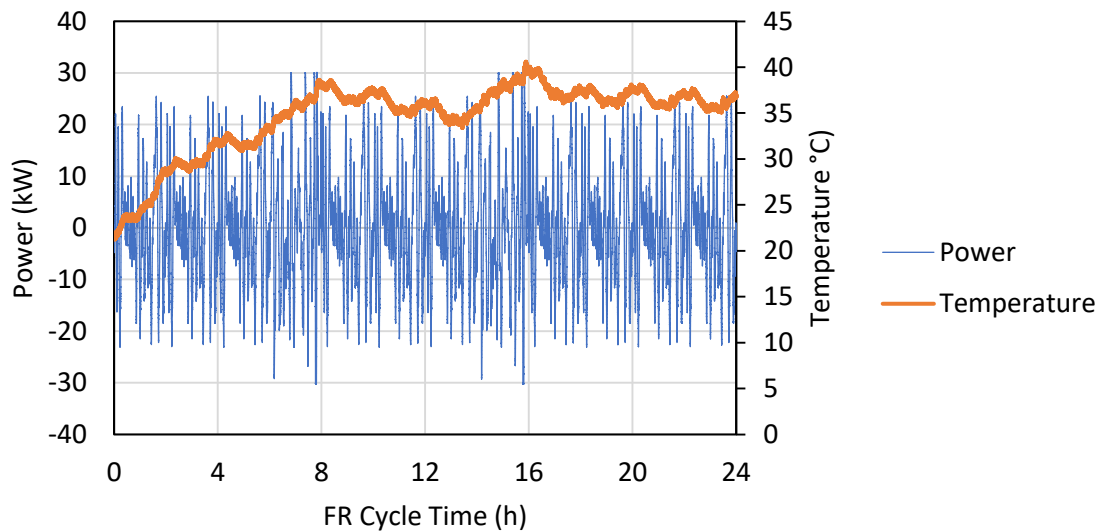


Figure 51- Demonstrating Steady-State Temperature in Leaf 2012 FR Operation

The impact of this analysis is that cooling is a necessary consideration when running higher power rate FR cycles, that better cooling enables more power, and consequently some packs

may be restricted at power levels below their peak power output because of this. Therefore, the specifications of the battery are not sufficient predictors of FR performance capabilities.

Dynamic Recharging

Dynamic recharging refers to the practice of adjusting the peak power factor or biasing the signal slightly upwards such that the battery is recharged during charge calls. This may be done in three ways:

1. The battery efficiency at a certain power rate and SOC is known, and the charge power is multiplied by a recharge factor (i.e., divided by its efficiency) such that on average, the charge calls will bring the battery back up to its nominal SOC. This practice is called an asymmetric bid and is used in the CAISO region.
2. Coulomb-counting is used to track the Amp-hour depletion of the battery, and a bias is used only when this drops below the desired SOC threshold. The bias may vary in proportion to how undercharged or overcharged the battery is.
3. Bias the received power signal upwards by a fixed value, calculated to continuously offset inefficiency losses.

Both options assume that periodic re-zeroing may be needed to re-set the known SOC. The objective is to minimize these disruptions.

Option 1 is the easiest to implement but requires having a good estimate of the battery's efficiency, or else the pack will gradually overcharge or deplete, neither of which is desirable. Option 2 will broadly work but depends on an accurate bulk coulomb-counting ability, and an estimate of what recharge factor is needed.

Option 3 is similar to Option 1, in that it depends on an accurate estimation of the battery's efficiency. If the efficiency is variable, or the signal is asymmetric, this can lead to overcharge or undercharge.

The results of the FR tests are therefore applicable in two ways: They provide an estimate of what recharge factor will be required, which is relevant to both options 1 and 2, and with Figure 52, a look at the dependency of the recharge factor on the hour rate of the battery.

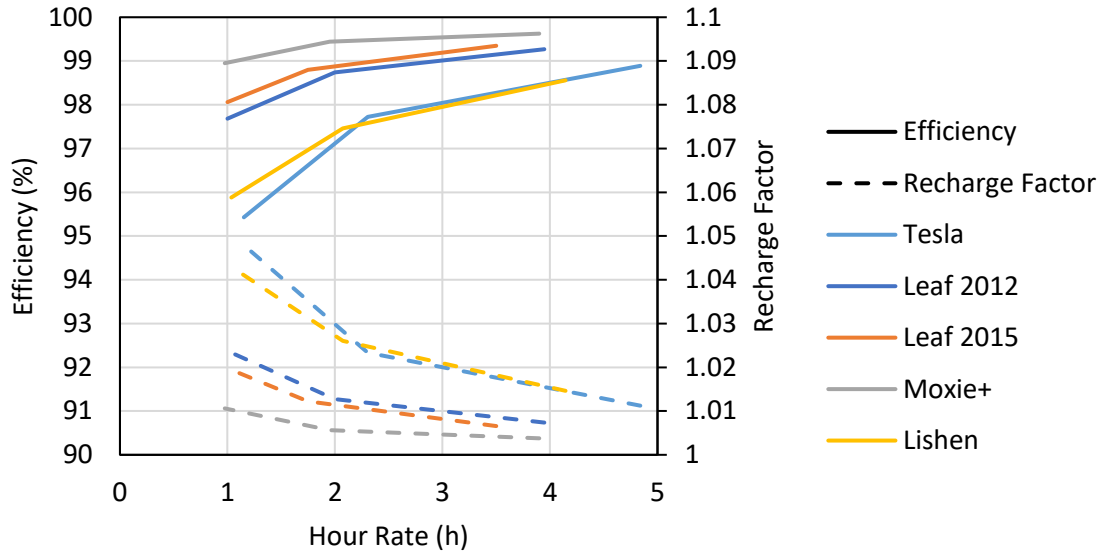


Figure 52- FR Efficiencies and Recharge Factor. Efficiency in solid lines, Recharge Factor in dashed lines

The recharge factor varies from 1% recharge to 3.5% at 2 to 0.5 h rates, for the 2015 Leaf. The highest recharge factor in testing was 4.4%, at an equivalent 0.46 h rate. Operators may safely assume recharge factors from 1-5% nominally, at the DC terminals. If a nominal 97.5% efficient converter¹⁶ is used, the AC-AC recharge factor will be approximately 8.5%-14.2%.

¹⁶ AC-DC, DC-AC.

Chapter 6 Discussion

The discussion of results covers three main topics:

1. A detailed examination of the thermal performance of each battery, and how their temperature management systems influence their relative performance, with the objective of predicting the performance of prospective battery purchases.
2. The relative energy density and specific energy metrics of each battery, with commentary on implicit design decisions and task-specific optimization.
3. Refinement of FR metrics and peak power prediction based on reduced energy capacity.

6.1 Influence of Thermal Design on Operational Performance

The thermal management capacity of a battery is a significant factor of its performance limits.

Rates of 1-4 h do not generally produce substantial temperature rises, but high-intensity discharge, and sustained FR operation can lead to risky temperatures if not controlled.

Additionally, the capacity and voltage limits of a battery can be relatively easily identified by deep-discharge cycling, but temperature response is a function of intensity of use, thermal inertia, and cooling type and design. Batteries which cannot manage the temperature peaks of high intensity services are ill-suited to provide them, independently of their electrochemical ability or condition. Therefore, predicting and characterizing the thermal response of a battery is important for grid storage operators.

This section is divided into a description of the temperature response of each pack individually, along with a detailed description of its cooling mechanisms, and a comparison of temperature responses to determine the effectiveness of cooling types. The results of this analysis will assist operators in predicting and controlling their battery's temperature response.

Cooling vs. Heating

In observation of the Tesla Model X's battery thermal management behavior, and charge behavior, it should be noted that the default temperature of a battery in a vehicle may be above ambient conditions- that is, the battery is artificially heated [69]. This may be to improve the impulse-response performance or improve charge receptivity. Supercharging behavior heats the battery to reach 40-48 °C before active cooling is applied, or the power rate is reduced.

In the MBA concept described in Chapter 3, no provision was made for heating the batteries. This is because a) the by-product heat of operation can be used to elevate the temperature of the facility as needed, in either air temperature or liquid cooling, and b) adding heating is a relatively simple concern if required.

6.1.1 Battery Thermal Profiles

Summary

This section will repeat the testing parameters used for each battery and proceed to a profile of each battery’s thermal characteristics, including instrumentation and example temperature measurements inside the battery.

Table 16 gives the testing parameters and cooling type of each battery. The Rest Temperature Threshold is the maximum temperature for every temperature sensor to report before the controller will exit rest and enter the next cycling step. The cooling medium temperature refers either to the ambient air temperature of the lab, which is independently conditioned to 20 °C, or the cooling loop, which circulates a water-glycol mixture conditioned to a particular temperature. Exceptions to these testing parameters will be noted on a case-by-case basis.

Table 16- Summary of Experimental Thermal Parameters per Battery

Battery	Cooling Type	Cooling Medium	Rest Temperature Threshold (°C)	Cooling Medium Temperature (°C)
AESC Leaf 2012	Passive	Air	30	20
AESC Leaf 2015	Passive	Air	30	20
Lishen EV	Passive	Air	30	20
EnerDel Moxie+	Air	Air	30	20
Chevrolet Volt	Liquid	Glycol-Water	35	30
Panasonic Tesla	Liquid	Glycol-Water	35	30

The following sections describing each battery will include a detailed description of the cooling process and an example temperature-time response chart showing all temperature sensors, demonstrating the internal distribution of temperature. **All graphs use CC deep discharge data.**

2012 Leaf

The 2012 Leaf is a passively cooled battery. It is separated into two modules, one above the other. It is instrumented with 4 thermocouples mounted externally, and 3 OEM thermistors installed internally. The locations of these sensors are shown in Figure 53.

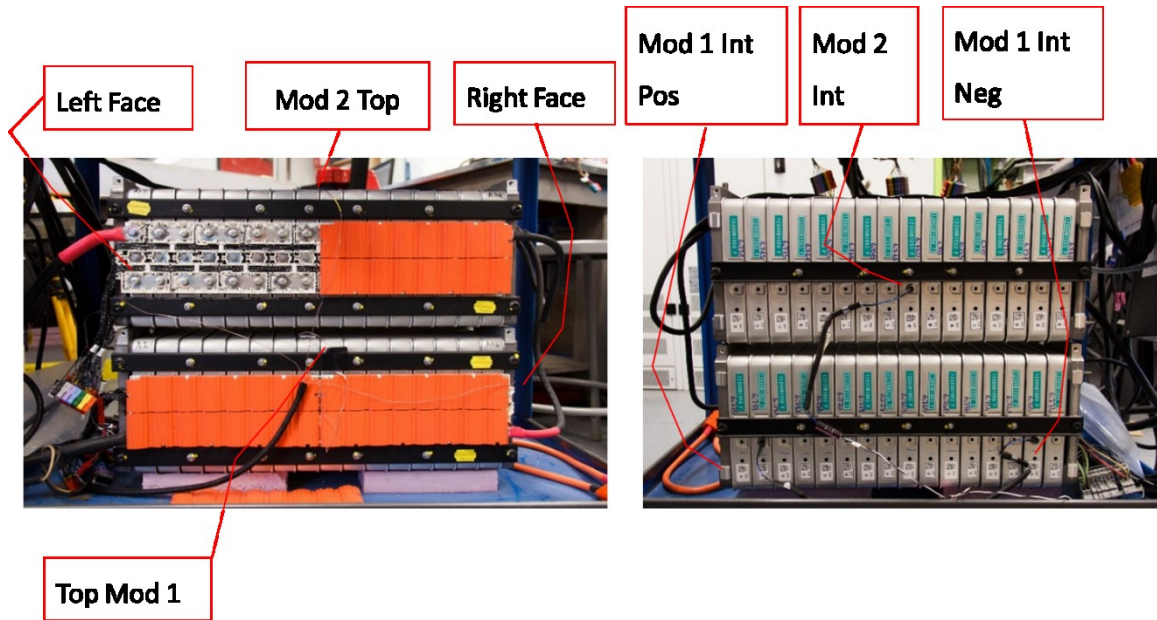


Figure 53- Leaf 2012 Temperature Sensor Nomenclature

The cooling medium is the ambient air of the laboratory, which is conditioned to 20 °C. The thermistors were calibrated as having a β value of 3394, and an r^{inf} value of 0.0444. Figure 54 shows the temperature response of the Leaf 2012.

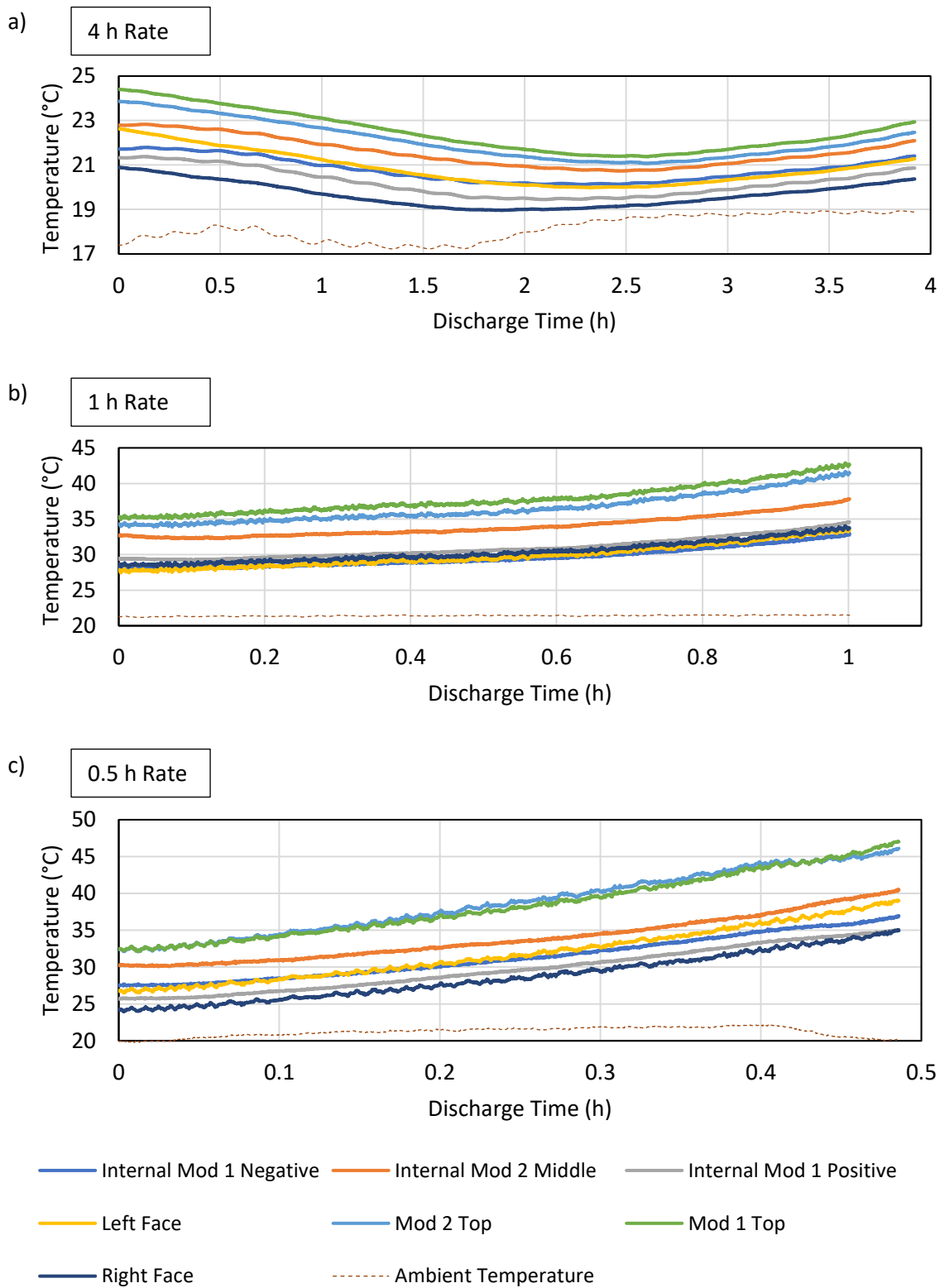


Figure 54- Temperature Response of 2012 Leaf.

The curve in Figure 54a may be explained by a combination of two factors: The temperature at the start of discharge will be the temperature from the end of the previous rest step, which may be elevated, and that temperature rise is greatest at the ends of discharge due to the rise in internal resistance.

The warmest parts of the pack measured were the tops of the modules. The internal measurement of module 2 was warmer than the internal measurements of module 1, as expected, as module 2 has its thermistor mounted in the middle of the stack, versus mounts near the ends of the stack.

2015 Leaf

The 2015 Leaf is a passively cooled pack. It is composed of 3 modules, with 4 thermocouples. One is mounted to the side, one on top, and two sandwiched internally between modules two and three. The sensor locations are shown in Figure 55.

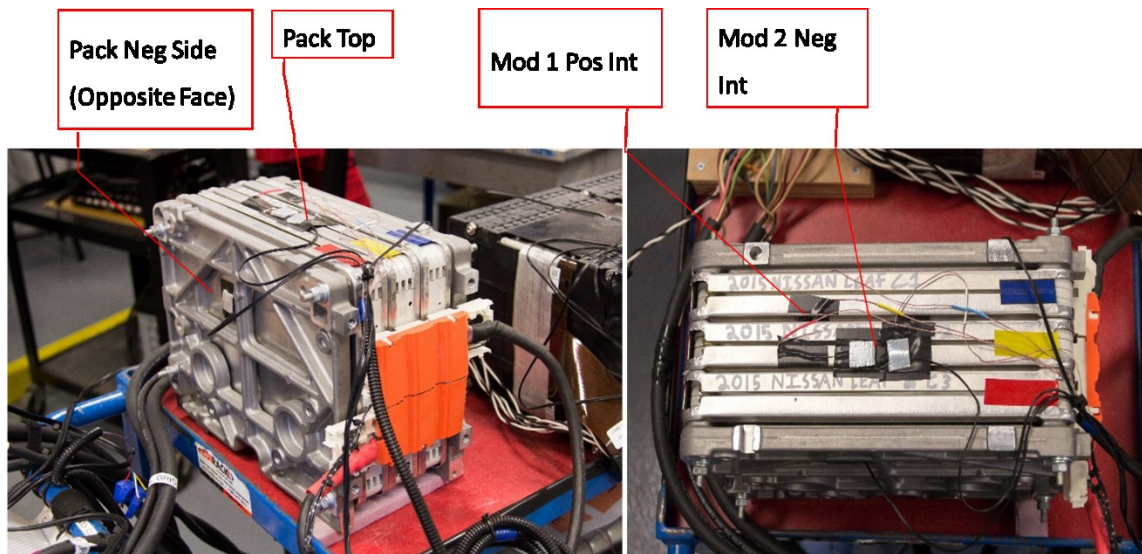
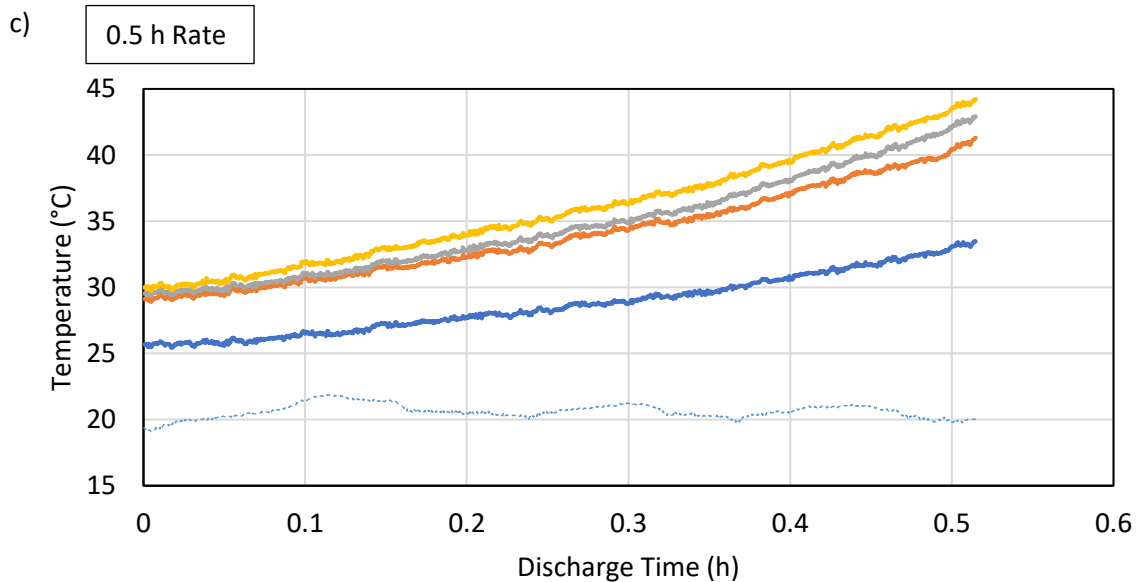
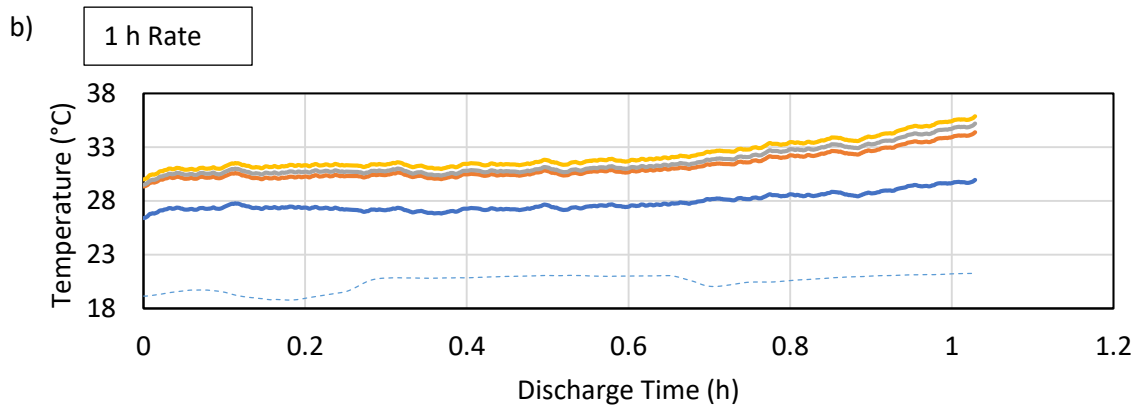
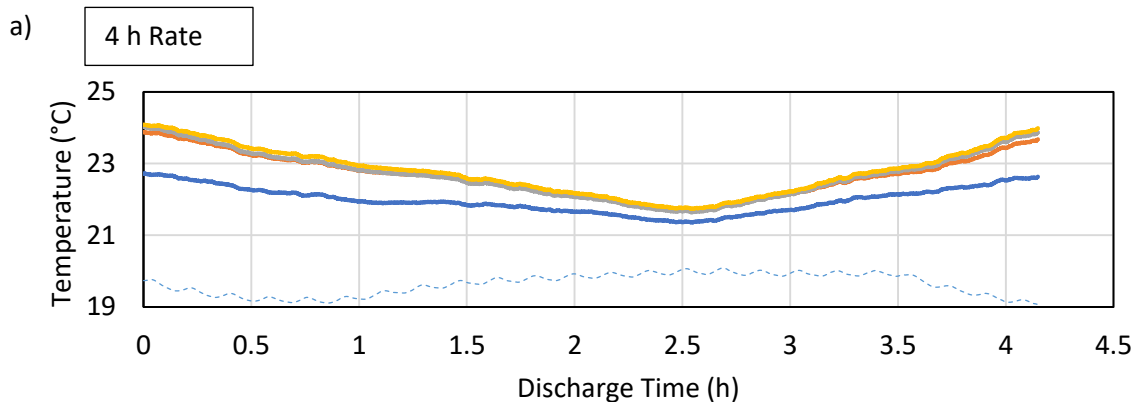


Figure 55- Leaf 2015 Temperature Sensor Nomenclature

The cooling medium is the ambient air of the laboratory, which is conditioned to 20 °C. The temperature response of the Leaf 2015 can be found in Figure 56.



- Pack Negative Side
- Pack Top
- Mod 1 Positive Internal
- Mod 2 Negative Internal
- - - Ambient Temperature

Figure 56- Temperature Response of 2015 Leaf.

The internal temperatures are highest, and the side temperature is lowest, as expected.

EnerDel Moxie+

The EnerDel Moxie+ is an actively air-cooled battery. It uses aluminum fins sandwiched between its cells to carry heat to the outside, where a fan is used to force air through channels in the fins. The cooling system makes use of a fan driving ambient lab air, cooled to 20 °C, into a flat, open plenum. Each module's air channels open into this plenum and are hence at equal pressure. The opposite sides of the channels are open to the lab. The aluminum fins fit between every other cell, and extend out one side, where they are folded into a closed vertical air channel.

The battery is instrumented with 6 thermistors out of the original set, with each module having one near its end, and one in its middle. The thermistor coefficients were taken from the manufacturer's specifications. The sensor locations are given in Figure 57.

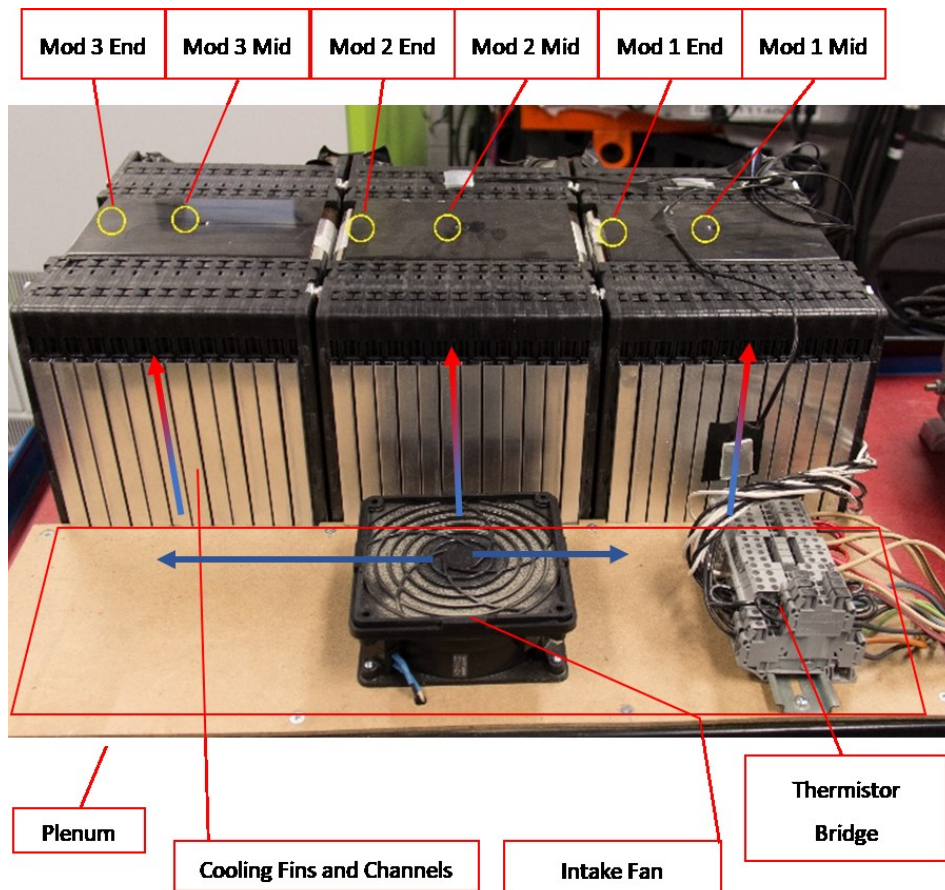


Figure 57- Moxie+ Temperature Sensor Nomenclature

The temperature response of the EnerDel Moxie+ at the three hour rates under test is shown in Figure 58.

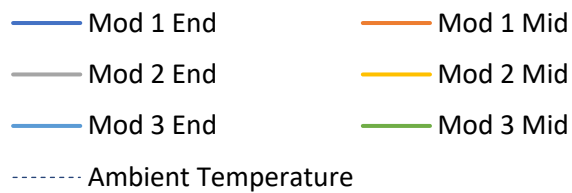
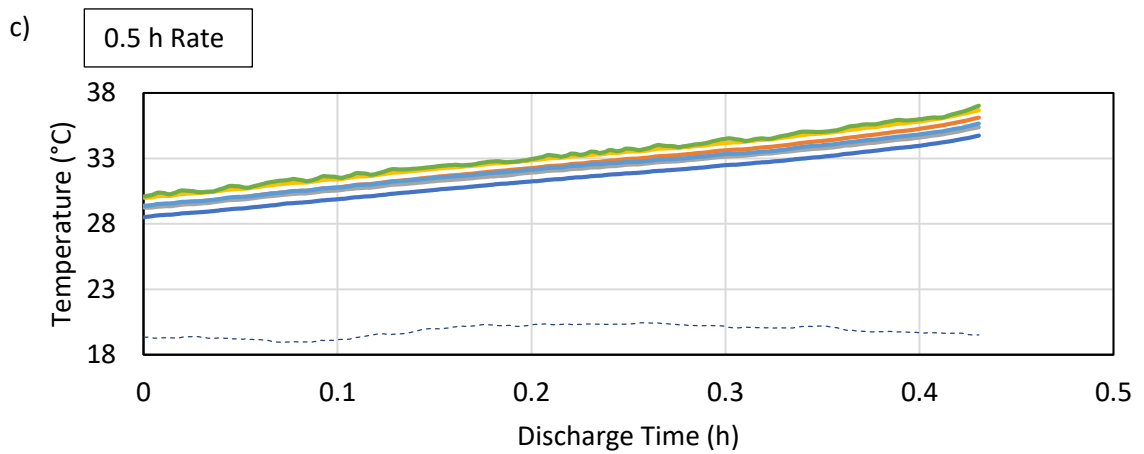
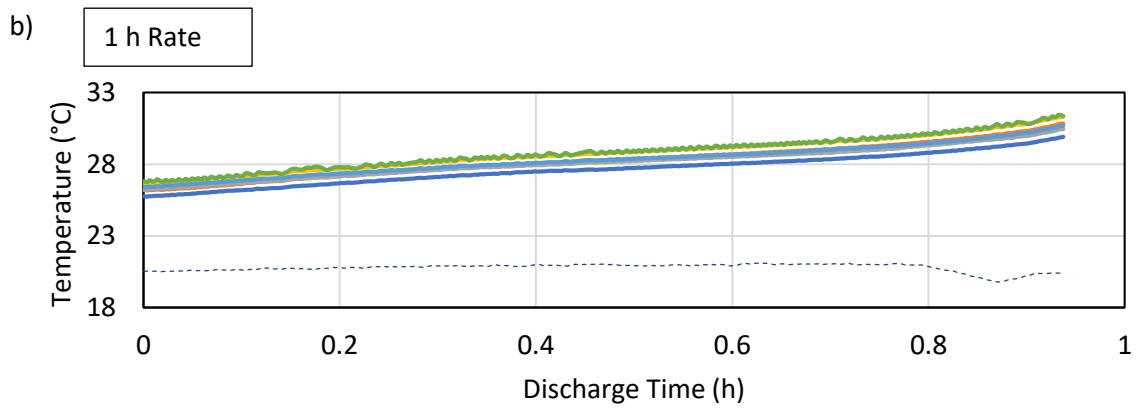
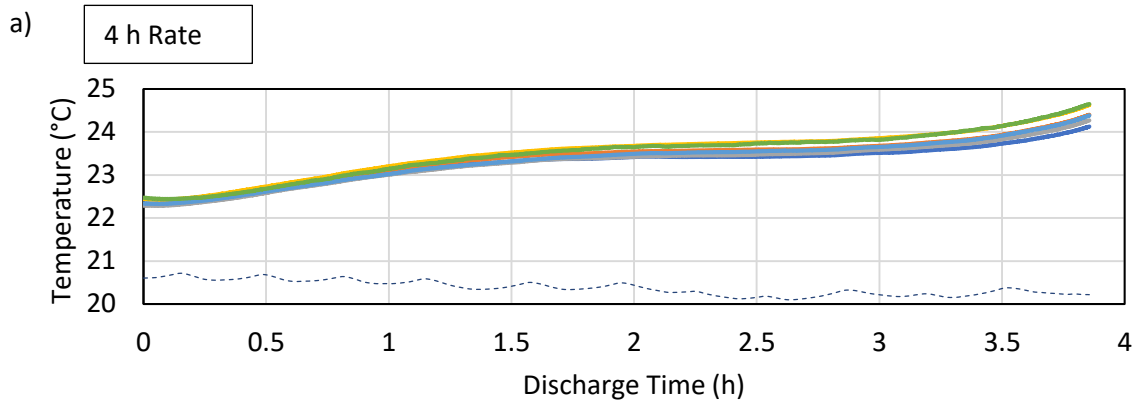


Figure 58- Temperature Response of EnerDel Moxie+.

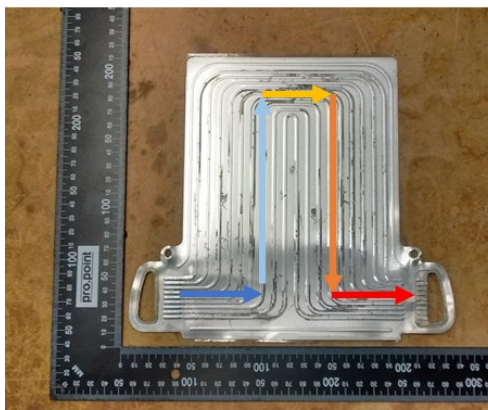
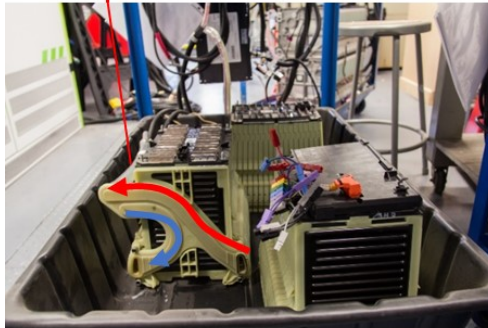
All cells track each other closely in temperature within a given test, indicating a very effective and homogenous thermal management system.

The 0.5 h test starts discharge at approximately 30 °C, which is expected as the pack must cool down to 30 °C in rest before proceeding to the next cycling step. The starting temperature in 4 h discharge is lower because it would have ended charge below 30 °C, thus as soon as the minimum 10 minutes of resting time elapsed, the test would proceed, being under the temperature threshold of 30 °C.

Chevrolet Volt

The Chevrolet Volt has a liquid-cooled thermal management system. The battery has two long manifolds, one extending down each side of the pack, on opposing faces. The coolant manifold distributes coolant into sandwiched cooling plates between cells. The fins are a thin, two-layered plate of aluminum, with small stamped channels. The coolant is carried through these channels, across the face of the battery, and then enters the return path to the coolant manifold. Therefore, each coolant plate has equal pressure, and hence equal flow rates. The cross-flow design ensures each cell receives coolant at an equal temperature, and the channels in the plate maximize the flux over the warmest part of the cell- the middle, approximately 1/3 of the height of the cell, down from the tabs. The system is held together with O-rings on every interface, and 4 steel rods that hold the pack in tension using the metal plates on either end. The flow rate through the cooling manifold of the reduced 6-cell module (rated 1 kWh) was approximately 0.5 L/min, of a glycol-water mixture. The short-circuit coolant flow is more than 6 L/min, so the coolant pump can safely be assumed to be of sufficient capability to supply. With 0.5 L/min/kWh capacity, normalizing based on the rated energy capacity of the module, a full Volt pack (rated 16 kWh) would likely operate near 7 L/min. The cooling system is shown in detail with flow directions in Figure 59.

Coolant Temperature Sensor



Module Thermistor



Figure 59- Chevrolet Volt Coolant Flow

One thermistor is located at the end of every module, and have been calibrated to the following values: β of 3920, and r_{inf} of 0.0196.

For some tests (4 h and 0.5 h), the pack was reduced to a single module of 6 cell groups, and thermocouples were placed on the face of those cells, away from the cooling fin, inside the pack. These tests have lower overall temperatures due to the increased surface area to volume ratio for heat dissipation, and the higher expected coolant pressure from constricting the same flow through fewer channels. The thermal response is shown in Figure 60.

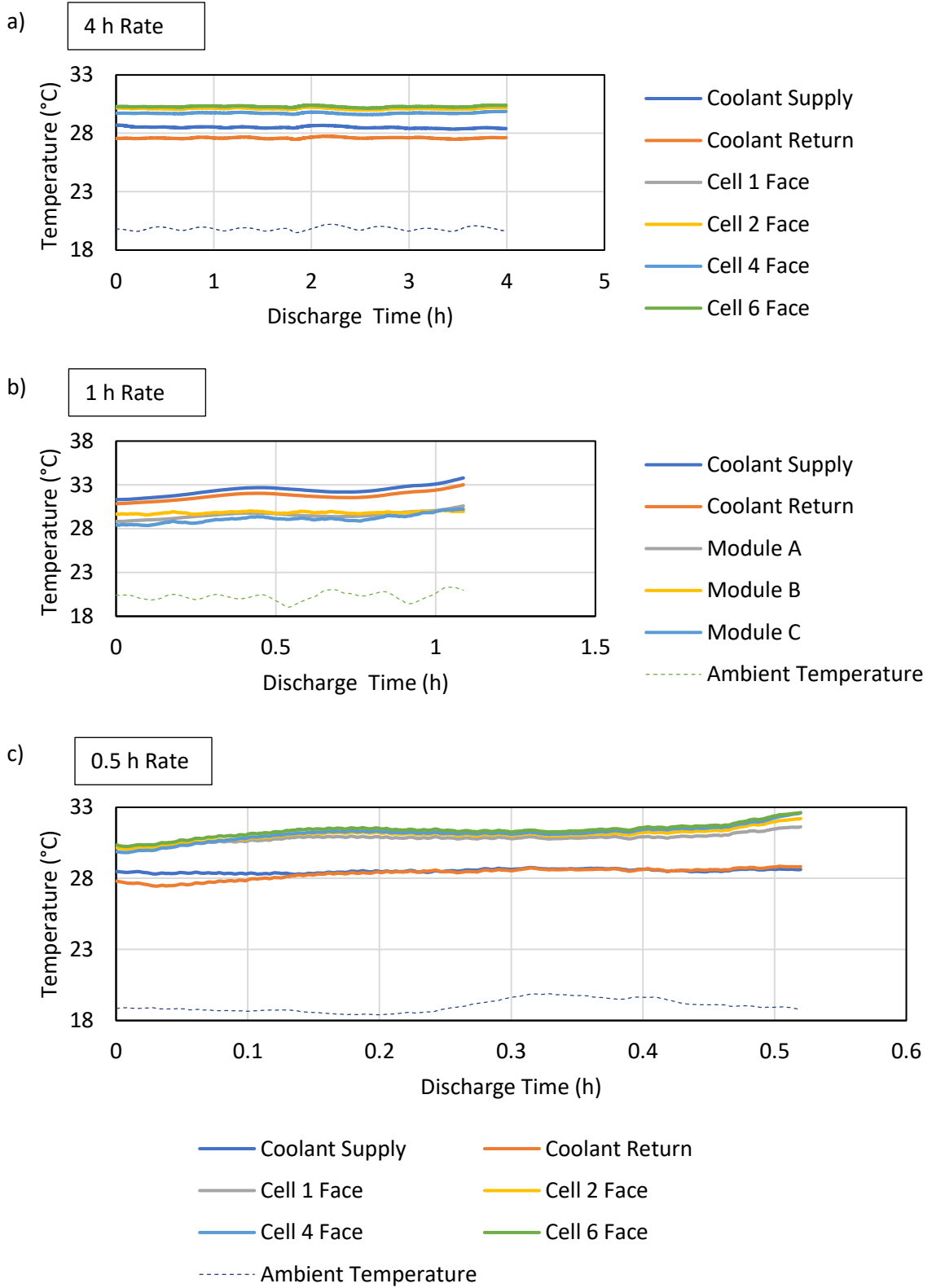


Figure 60- Temperature Response of Chevrolet Volt. Clockwise from top left: 4 h, 1 h, 0.5 h. 4 h and 0.5 h data from 6-cell reduced module, 1 h data from 3-module pack.

From the 4 h and 0.5 h tests, it is observed that the cell temperatures are closely matched. From the 1 h test, the modules remain close in temperature, implying that the coolant is being well-distributed. During the 1 h test, near the 0.5 h mark, the coolant temperatures begin to decline. This is likely due to the cooling unit in the thermal conditioning loop activating.

Panasonic Tesla

The Panasonic Tesla is a liquid-cooled battery. It uses a long, flattened tube which is threaded in between the strings of cells to make tangential contact with each cell on one face. It is separated from the cells by a thin rubber sheet, for safety. Because it is a continuous pipe, the coolant inside will rise in temperature as it passes, and the last cells in contact will not receive the same cooling as the earlier cells. It is instrumented with five thermocouples, one mounted to the inlet and outlet directly on the aluminum, and three mounted on the bare face of the cells, in order: The cell nearest to the inlet, a cell on the back approximately in the middle, and on the cell nearest to the outlet. The coolant flow rate was measured to be 0.5 L/min for a 4.84 kWh module. With 0.1 L/min/kWh capacity, normalizing based on the rated energy capacity of the module, a full Tesla battery pack of 16 modules (rated 85 kWh), approximately 8 L/min would be required. The details of the cooling system are shown in Figure 61.

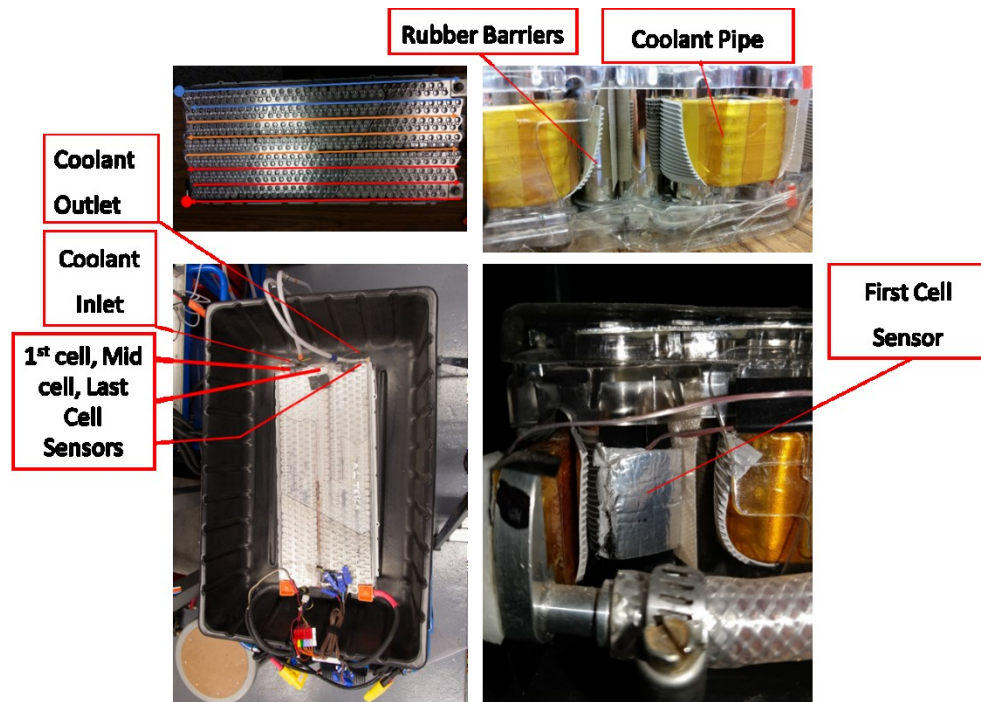


Figure 61- Tesla Temperature Sensor Nomenclature

The temperature response of the Tesla under the three hour rates is displayed in Figure 62.

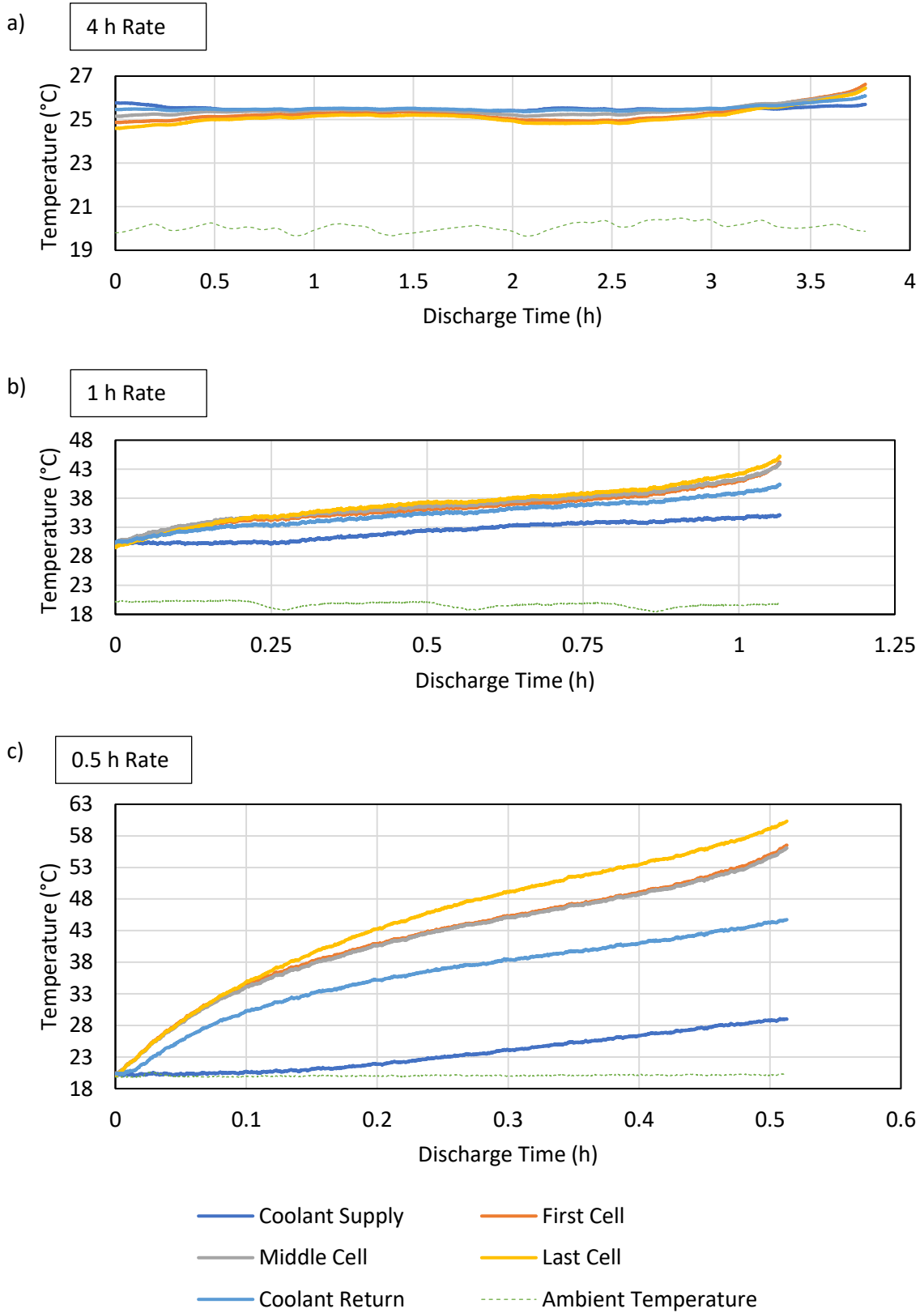


Figure 62- Temperature Response of Panasonic Tesla. The 0.5 h test made use of a 20 °C setpoint on the cooling loop.

From Figure 62 it is observed that the last cell is always the warmest, and there is a substantial rise in coolant temperature between the inlet and outlet. This large difference suggests a long lag time between coolant entering the battery and exiting.

6.1.2 Comparison of Responses

To compare the effectiveness of the battery’s thermal management systems, the peak temperature of the battery is plotted, and the difference between that peak and 1) The rest threshold temperature, the “starting gate” value for discharge to begin from, and 2) the temperature of the cooling medium setpoint are also shown. Both values are given in Table 16.

Table 17 Tabular Peak Temperatures by Battery and Hour Rate

Passively Cooled Air Cooled Liquid Cooled	Peak Temperatures in CC			Peak Temp over Rest			Peak Temp over Cooling		
	Testing by Hour Rate			Temperature Threshold			Medium by Hour Rate		
Battery	4	1	0.5	4	1	0.5	4	1	0.5
AESC Leaf 2012	23.0	43.7	44.0	0	13.7	14.0	3.0	23.7	24.0
AESC Leaf 2015	26.4	38.5	45.5	0	8.46	15.5	6.4	18.5	25.5
EnerDel Moxie+	22.0	31.7	37.9	0	1.7	7.9	2.0	11.7	17.9
Chevrolet Volt	28.2	34.1	32.9	0	0	0	0	4.1	2.9
Panasonic Tesla	28.2	40.0	60.3	0	5.0	38.8	0	10.0	40.3 ¹⁷

Values of zero in Table 17 indicate the battery never rose above that temperature.

Peak Temperature Comparison Charts

Table 17 tabulates the peak temperatures of the batteries, their temperatures above rest threshold, and temperature above the cooling medium. These values are shown in Figures 63 through 65.

¹⁷ The cooling loop setpoint for this test was 20 °C.

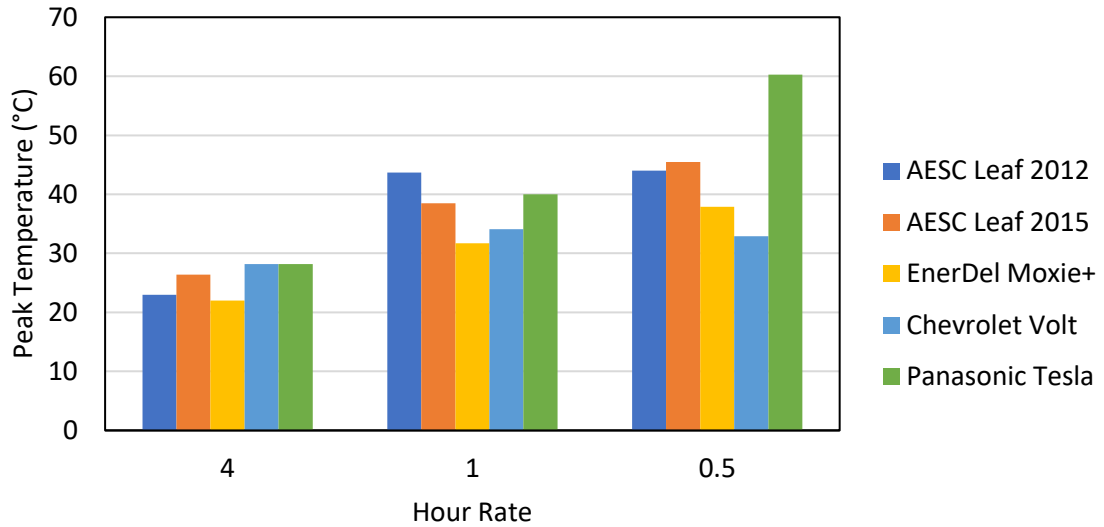


Figure 63- Peak Temperature by Battery and Hour Rate

Comparing temperatures directly in this way does not evenly compare the peak temperatures. The forced-air and passively cooled batteries are cooled by a different medium than the liquid-cooled batteries, and are permitted to leave rest at different temperatures. The following charts compare the batteries by subtracting the rest threshold temperature and the cooling medium temperature, respectively, from the peak temperature overall.

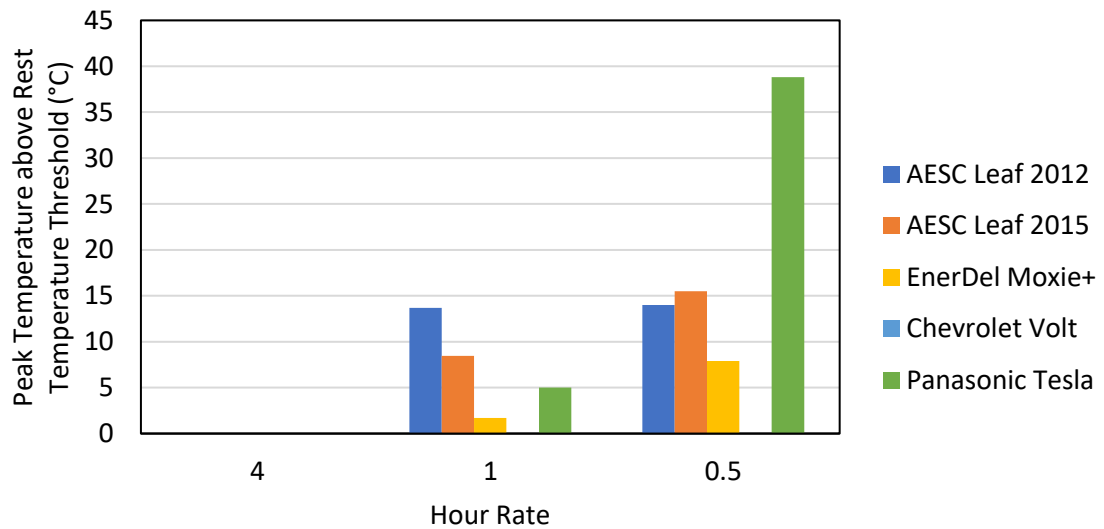


Figure 64- Peak Temperature Rise above Rest Threshold Temperature

At 4 h rates, no battery rose above the rest threshold temperature, and the Volt did not at any rate. This makes relative comparisons difficult, through a lack of contrasting values.

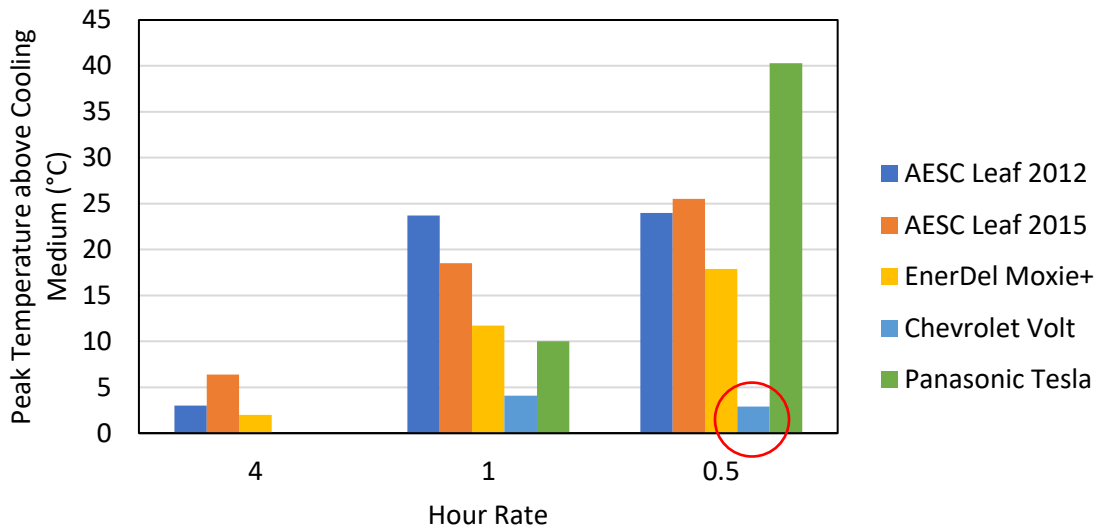


Figure 65- Peak Temperature Rise above Cooling Medium

In Figure 65 it is observed that there is divergence between temperatures at all hour rates. At the 4 h rate, the liquid-cooled batteries do not rise above their cooling medium temperature. As the rate increases, the temperatures diverge according to the effectiveness of their cooling system. The data presented in Figure 65 will be used for the rest of the analysis.

6.1.3 Thermal Performance Factor Analysis

The batteries performed as follows:

- The Volt performed the best in all tests, maintaining less than a 5 °C rise in temperature.
- The Tesla performed second best in the 4 h and 1 h tests, then worst in the 0.5 h test.
- The Moxie+ performed well in all tests, finishing with an 18 °C rise on a 0.5 h rate.
- The Leaf 2012 and 2015 performed similarly, with the 2012 being slightly cooler on a 0.5 h test than the 2015.

The Tesla cooling system was insufficient to compensate for the heat rejection on the 0.5 h test. The tangential cell contact has been noted previously, but the series configuration may have a different influence on cooling. The tube length and pump pressure together govern the length of time the coolant spends in the system, i.e., independent of discharge rate. As the discharge rates increase, the fixed amount of coolant in the system must absorb more heat, and thus exits

at a higher temperature. While this is also true of the Volt and Moxie+, the path lengths are so short that the effect is negligible. This effect can be seen in Figure 60 and Figure 62, where the inlet and outlet temperatures behave differently. With the Volt, the inlet and outlet temperature quickly become uniform, meaning the coolant has short residency period, and instead the overall average thermal conditioning system temperature is rising. With the Tesla, it takes 12+ minutes for the reservoir temperature to begin to rise, and the inlet and outlet temperatures never stabilize. In half that time, the Volt coolant has reached nearly steady-state operation, with the inlet and outlet temperatures being nearly equal. This means that despite being liquid-cooled, the configuration of the Tesla can cause it to underperform an air-cooled battery with a parallel thermal conditioning configuration.

Both the Moxie+ and Volt had low peak temperatures during cycling, despite using different cooling medium (air and liquid, respectively). They both use parallel-format cooling, in the case of the Volt with parallel coolant liquid flow, and with the Moxie+, with parallel cooling fins and airflow. This means each cell experiences the same inlet and outlet temperature, and thus very similar heat transfer rates, with short path lengths for coolant.

For an operator, this means that thermal performance is not simply a function of being air or liquid cooled, but rather by the coolant flow configuration.

For passively cooled batteries, the peak temperatures reached during testing were near 50 °C, the lab's selected temperature limit. Depending on the operator's selection of upper temperature limits, this means the passively cooled batteries are limited in their ability to provide high-rate discharge by cooling, not electrochemistry. Similar limitations were also noted in FR service.

6.2 Energy Density and Specific Energy

Energy density and specific energy are important metrics in battery design. In mobile applications, they become critically important, but in stationary usage they lose some significance. Nonetheless, higher density of storage will lead to a better usage of the space of the plant. In addition, the implicit design choices of the batteries may be of interest. This section will discuss these metrics with the tested batteries and compare the test results with findings from the literature.

The energy density and specific energy of a battery are, at minimum, determined by its chemistry. Typical values for some battery chemistries are shown in Table 18.

Table 18- Literature Values for Energy Efficiency, Specific Energy, and Energy Density [68,70,71]

Cathode	Example Battery	Energy Efficiency (%)	Manufacturer Specific Energy (Wh/L)	Energy Density (Wh/kg)
NCA	Tesla	93.2	554	250
NMC	Moxie+	95.1	154	200
LFP	Lishen EV	90.8	220	120
LMO	Leaf	97.5	317	140

Table 19 summarizes the resultant energy capacity metrics, using the energy capacity, mass and volume of the batteries under test in this thesis. CP testing is used for these metrics because this should provide the best estimate of useful energy capacity, and hence useful density.

Table 19- Measured Values for Energy Efficiency, Density and Specific Volume by 4 h CP testing energy capacity

Manufacturer	Battery	Volume (L)	Mass (kg)	Energy (kWh)	Specific Energy (Wh/L)	Energy Density (Wh/kg)
LG Chem	Volt	32.6	53.4	6.22	191	117
Panasonic	Tesla	15.9	25.4	4.05	255	159
AESC	2012 Leaf	75.6	121.6	13.86	183	114
AESC	2015 Leaf	7.1	11.4	1.36	191	119
EnerDel	Moxie+	27.3	48.0	3.76	138	78

Given the high performance and cost of the Tesla battery pack, its efficiency is notably lower than that of the other batteries. This may be because Tesla has made a design decision to focus on other performance parameters, namely, energy density. As seen in Figure 66, the Tesla module has a specific energy 30% higher than its nearest competitor. The energy density is also higher, 33% above nearest competitor.

Figure 66 contrasts the efficiency values with the energy density and specific energy.

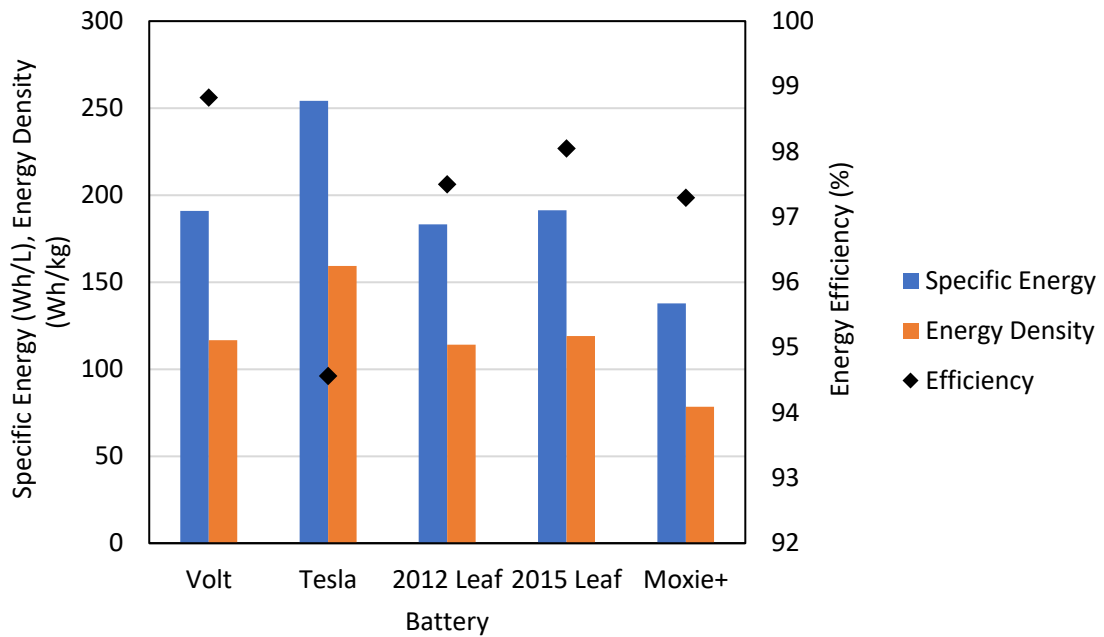


Figure 66- Energy metrics contrasted with Energy Efficiency

The Tesla appears to have focused on high energy density, making a trade-off for efficiency. The Moxie+ efficiency is not substantially different than the other three mid-range batteries, but its energy density and specific energy are 70% and 67% of the mid-range average; as much of a drop as the Tesla is an increase. This may be because the Moxie+ is a design being prepared for heavy trucking usage, where space and weight are less constraining than domestic automobiles. It is possible they are prioritizing cost, thermal performance, or power density instead.

The measured values are compared to the literature values in Figure 67.

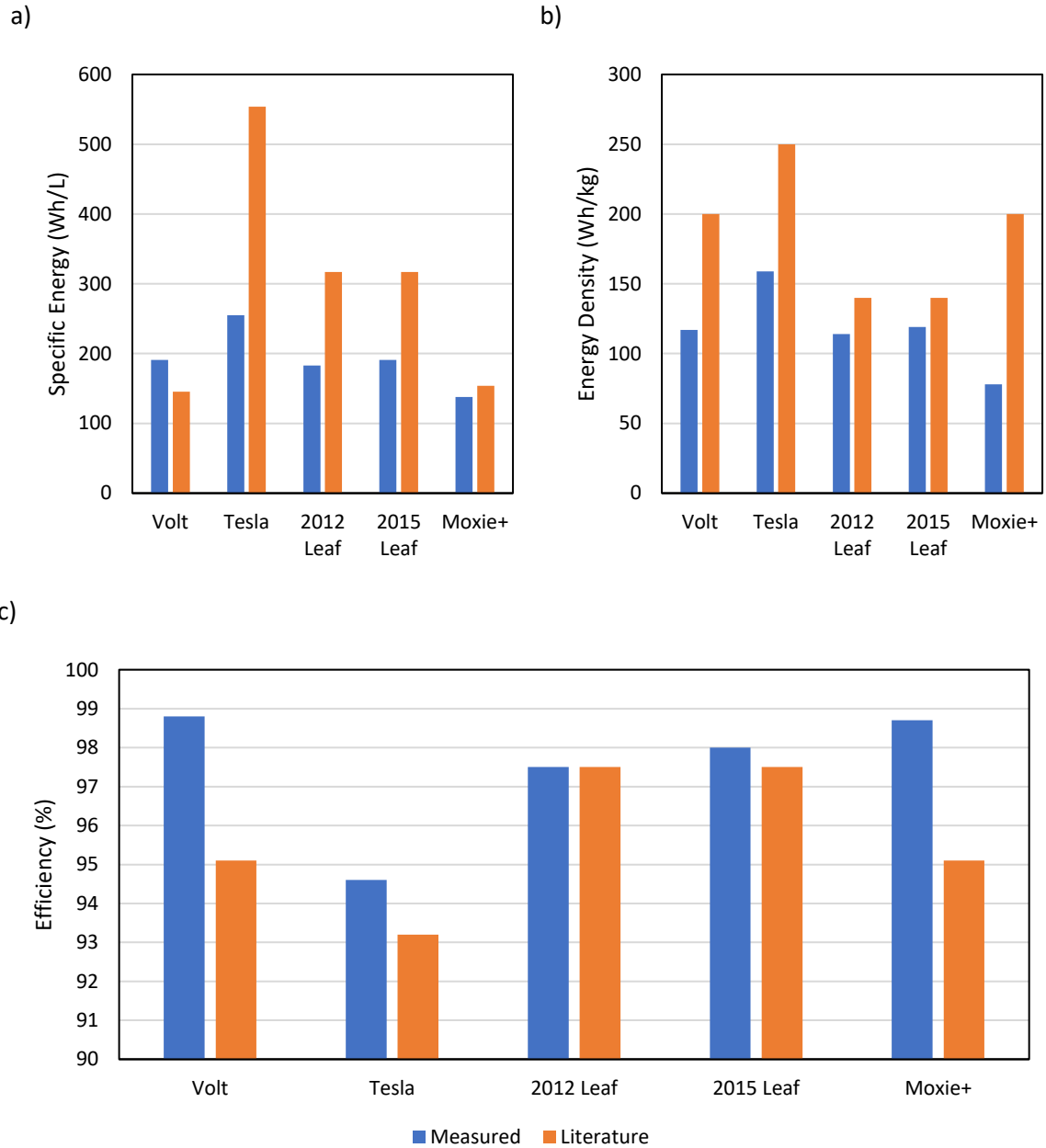


Figure 67- Literature and Measured Value of Energy Density, Specific Energy, and Energy Efficiency [61,62,63,68]

For specific energy and energy density, all batteries under test report less than the literature-expected values, except the Volt specific energy. This is at least in part because the literature values are on a per-cell basis, whereas the measured values include the weights and volumes of the module and pack casings, and the cells are aged.

The Tesla measured specific energy is 46% of the manufacturer's reported value. This is close to the approximate packing factor, taking the total volume of the cells of the pack and dividing it by the volume of the pack, which is 49%.

The measured energy efficiency of the batteries is equal to or higher than the literature values in all cases, with differences of 0-3.7 percentage points. This may be because the electric vehicle batteries tested are of higher quality than the cells tested in literature, or because the hour-rate of this work's calculations is slower than that used in the literature. Operators using electric vehicle batteries for storage can justifiably expect >90% energy efficiency from their batteries.

The specific energy value is a useful predictive quantity for prospective operators. Modern EV battery designs are limited by the size of the car, and most new designs optimize the space under the floor of the car. For this reason, modern EV batteries are expected to be convergent on a size envelope. Assuming this to be the case, and a racking system that is specified for this convergent design with a high packing factor, then the energy density of the plant will primarily be dependent on the energy density of the batteries. Thus, for operators seeking to prioritize energy capacity, batteries with a high specific energy will best satisfy that need. Consequently, specific energy will be used in this analysis as a proxy for energy capacity, to unify the comparisons of batteries. Energy density is not useful in the same way because the MBA will not be constrained by weight as heavily as space, being a stationary application.

By the trend in the measured and literature data, prioritizing a high specific energy capacity implies a trade-off in energy efficiency.

Power density and specific power were not calculated because they are primarily functions of what the manufacturer deems the highest rated power or nominal power of the pack. Power rates could be calculated based on the power of a given hour rate, but this would be a linear transformation of the existing energy measurement.

6.3 FR Performance Metrics using Measured Capacity

In Section 5.3, the peak power factor was normalized for comparison by dividing the rated energy capacity by the peak power factor to obtain the equivalent hour rate. In practice, batteries arriving at the plant will have varied coulombic and energy capacities. If the real battery coulombic capacity is significantly lower than its rated capacity due to aging effects, positioning the battery at 50% SOC by rated coulombic capacity would position it much lower

than intended, ultimately limiting its possible power factor by reaching a fully discharged state earlier.

If the objective of the plant operator is to maximize revenue by bidding the highest possible power provision for FR service, slowly iterating the power value upwards with every battery connected until it reached its performance limit would be time consuming, as each iteration would take a day or more¹⁸.

It is suggested that an operator with a newly arrived battery perform a 4 h CP test to determine the present energy capacity of the battery and start FR services at a 0.5 h peak power factor based on the 4 h capacity test. Iterating from there would save time compared to starting at a slow rate, and in some cases may already be near the power limit¹⁹. Table 20 compares the peak power factor and minimum SOC by rated values and by tested values. The measurement-based hour rate is found by dividing the 4 h CP energy capacity by the peak power factor, and the measurement-based minimum SOC is found with the 4 h CC coulombic capacity.

Table 20- FR Metrics comparison of Rated Values vs. Tested Values

Manufacturer Battery		FR Power Factor Hour Rate by:			
		Manufacturer Rating (h)	Constant Power Test (h)	Lowest SOC by Rating (%)	Lowest SOC Measurement (%)
Chevrolet	Volt	1.50	1.56	44.5	44.8
Panasonic	Tesla	0.81	0.67	5.2	2.6
AESC	2012 Leaf	0.50	0.46	6.8	6.2
AESC	2015 Leaf	0.54	0.52	11.1	12.4
Enerdel	Moxie+	0.50	0.48	25.2	24.3

It is observed from the comparison that the metrics do not differ greatly. This is because the batteries under test are still quite close to their rated capacity. The Tesla has a 20% difference in hour rate, the highest compared to the next highest at 10%, the 2012 Leaf.

6.4 Ranking of Batteries for Storage Services

It is the principal research objective of this thesis to determine the capability, performance, and practice of repurposed EV batteries in grid electricity storage services. Utilities constructing a

¹⁸ In addition to the uncertainty of how much will be demanded per at a given power rating.

¹⁹ No battery under test was at a dangerous temperature at the half hour rate, so this is expected to be a safe starting value for power-bid seeking.

mixed battery array require a method to identify strengths and weaknesses of the tested EV batteries for providing given services. An example method is the experimental investigation performed in this work, identifying the performance of the batteries in CP discharge and FR service. In this chapter, the performance results will be ranked according to the requirements of each service.

This method is intended to assist prospective storage operators in either purchasing batteries to meet an intended service provision, or in assigning different duties to each battery in a mixed array, possibly via an advanced or stacked control method.

This section will compare the performance of the batteries side-by-side using appropriate crucial metrics for each service. Peak shaving and frequency regulation will be the focus of the comparisons, as they are presently the most common and profitable services on the market.

6.4.1 Peak Shaving

Peak shaving is a service designed to meet peak electricity demand or to avoid purchasing electricity at the costliest time of day²⁰. It requires the steady discharge of energy over a fixed window of time, usually between 1-4 hours. This is followed by a slow overnight charge, when electricity prices are low. This analysis will investigate the suitability of batteries for the 1 h and 4 h scenarios separately.

For all peak shaving cases energy efficiency and energy capacity are primary performance characteristics. The higher the energy capacity of the battery, the higher the power and longer the duration that can be discharged, and this directly increases the performance capability of a mixed battery array. Because the batteries tested are of different absolute size, specific energy is used instead of absolute energy capacity, per the argument in Section 6.2 that this is a better reflection of the normalized capacity of a battery. Energy efficiency is significant because the energy required for charge is assumed to be purchased from the grid, and low efficiency will increase this expense, impacting the profitability of the service, and requiring additional alternative generation to be procured.

For 4 h peak shaving, temperature management was not found to be a significant factor. All batteries had minimal temperature rise, up to 7 °C, and sufficient time is available before

²⁰ It has a similar usage profile to energy arbitrage.

charge for this residual heat to dissipate. Instead, thermal management complexity is penalized, as more complicated systems are expected to suffer more malfunctions or require more maintenance, due to having more active components, more seals, and more joints, etc.

For 1 h peak shaving, temperature rise becomes more significant, with up to 23 °C temperature rises and 2 h rest durations. Depending on the specifics of plant operation, 23 °C may be an acceptable temperature rise, but elevated temperatures will adversely impact the lifetime of the battery, and in any event, increases the thermal load on the cooling system requiring it to be more powerful. For comparison, the peak temperature above cooling medium metric from section 6.1 is used. Energy capacity retention, defined as the fractional reduction in energy capacity in going from a 4 h rate to a 1 h rate becomes relevant, with reductions of 5-15%.

0.5 h peak shaving is not considered as a service because of its rarity in practice. For high power batteries, frequency regulation may be a better service.

Table 21 presents the numerical performance ratings of each battery. Thermal complexity is a subjective evaluation of the thermal management system’s complexity, taking into consideration the risk of spills, hose couplings, number of seals, and potential of failure. Capacity retention is a unitless fraction of the CP discharge energy at a 1 h rate and the discharge energy at a 4 h rate of the same battery.

Table 21- Peak Shaving Performance Values

Battery	4 h			1 h			
	Specific Energy (Wh/L)	Energy Efficiency (%)	Thermal Complexity	Specific Energy (Wh/L)	Energy Efficiency (%)	Capacity Retention	Peak Temperature (°C)
Volt	191	98.83	High	190.96	96.58	0.91	4.1
Tesla	254	94.56	High	254.18	87.10	0.85	10.0
Leaf 2012	183	97.50	Low	183.28	94.04	0.83	23.7
Leaf 2015	191	98.05	Low	191.24	94.69	0.89	18.5
Moxie+	138	97.29	Medium	137.72	96.60	0.95	11.7

Table 22 presents the rankings of each battery in each category, ordered by their performance from best to worst.

Table 22- Peak Shaving Performance Rankings. Sorted vertically, descending from best to worst.

4 h			1 h			
Specific Energy	Energy Efficiency	Thermal Complexity	Specific Energy	Energy Efficiency	Capacity Retention	Peak Temperature
Tesla	Volt	Leaf 2015	Tesla	Moxie+	Moxie+	Volt
Leaf 2015	Leaf 2015	Leaf 2012	Leaf 2015	Volt	Volt	Tesla
Volt	Leaf 2012	Moxie+	Volt	Leaf 2012	Leaf 2015	Moxie+
Leaf 2012	Moxie+	Tesla	Leaf 2012	Leaf 2015	Tesla	Leaf 2015
Moxie+	Tesla	Volt	Moxie+	Tesla	Leaf 2012	Leaf 2012

With 4 h peak shaving, the Leaf 2012 and 2015, and the Volt occupy the leading places. The Leaf models benefit from simplicity and high energy efficiency, and the Volt from a middle-of-range ranking of specific energy, and the best energy efficiency. The Tesla appears at the top of the specific energy rankings but occupies low rankings in the other two categories. Based on these outcomes, it appears that passively cooled bulk packs are most suitable for 4 h peak shaving services.

In the 1 h peak shaving category, actively cooled packs displace passively cooled packs, with the Volt and Moxie+ occupying the top rankings. The Tesla has the highest specific energy, but poor capacity retention, and the Moxie+ and Tesla performed very similarly (10, 11°C). This suggests that 1 h peak shaving can best be fulfilled by batteries with active cooling, for its subsidiary effects on energy efficiency and capacity retention.

The Panasonic Tesla did not perform well in the peak shaving category overall using the given metrics.

6.4.2 Frequency Regulation

Frequency regulation is a service wherein a power generator or storage operator modulates their power output or input according to a signal provided by a grid operator. The operator receives payment dependent on the magnitude of their power bid and is penalized for not being able to follow the signal. This creates a complex set of requirements for providing this service. In some jurisdictions, and in the PNNL example cycle, the overall theoretical energy consumption is neutral. Again theoretically, this means a battery could operate near 50% state of charge indefinitely, but two factors prevent this. First, the inefficiency of the battery causes its state of

charge to deviate, slowly reducing with repeated charge and discharge cycles. This can be offset by a small positive bias in its power signal, which maintains the state of charge. Second, the actual signal may be greatly biased towards charge or discharge for hours at a time, likely completely discharging any battery during that brief period.

The first factor is offset by high efficiency, slowing the rate of loss. The second factor is reduced by having a greater energy capacity; but in a unified comparison, hour rates are used instead of absolute power values, and the analysis of Section 5.3 found convergence towards similar hour rates. Because any operator can voluntarily reduce their power bid, and hence their risk from the second factor, for a unified comparison the metric of success in this factor is not energy capacity but greatest hour rate-equivalent bid which was successful.

Finally, continuous FR operation causes a rise in temperature, up to 18 °C above the cooling medium. Higher temperatures lead to reduced lifetime and increased cooling costs. Table 23 summarizes the numerical performance values of the batteries under test.

Table 23- FR Service Numerical Performance Values

Battery	Energy Efficiency (%)	Peak Temperature Above Medium (°C)	Highest Hour Rate
Volt	97.8	7.3	0.5
Tesla	92.9	18.0	0.8
Leaf 2012	95.8	14.0	0.5
Leaf 2015	96.7	7.0	0.5
Moxie+	98.0	0.0	0.5

Table 24 presents the rankings of each battery in each category, ordered by their performance from best to worst.

Table 24- Frequency Regulation Performance Ranking. Sorted vertically, descending from best to worst.

Energy Efficiency	Peak Temperature	Highest Hour Rate
Moxie+	Moxie+	Volt
Volt	Leaf 2015	Moxie+
Leaf 2012	Volt	Leaf 2012
Leaf 2015	Leaf 2012	Leaf 2015
Tesla	Tesla	Tesla

The Volt and Moxie+ are leaders in this service, taking 5 of the top 6 rankings. The Leaf batteries take the remaining rankings, with the Tesla occupying the lowest rankings in all columns. This would suggest that actively cooled batteries are the best candidates for high-performance services, except for batteries which have notably low efficiency.

6.4.3 Summary of Ranking Results

The general trend of the ranking suggests that high-power applications such as frequency regulation are best served by batteries with active cooling, while low-power applications such as peak shaving are served by batteries with passive cooling.

Cofactor Analysis

The performance of batteries in various services appears to be heavily influenced by its efficiency and cooling mechanism. These metrics influence each other by the mechanism of increased heat generation at lower efficiency, and higher efficiency at higher temperatures. To evaluate the efficiency independently with each battery, more effort would need to be taken to test at identical temperatures.

Simplification of Cooling System

Given the outcomes of 6.4.1 and 6.4.2, a facility which is providing a single service, e.g., peak shaving, may find it useful to eliminate either the liquid or air cooling systems. In the case of peak shaving, the AESC Leaf, and likely other passively-cooled batteries are the most suited to medium-rate sustained discharge. If the service case is known in advance, the MBA could be composed mostly or wholly of these batteries, removing the need for a liquid conditioning loop, which would greatly simplify the plant. Alternatively, if the Volt and Tesla are available, the liquid cooling could be eliminated because there is no significant temperature rise during 4 h rated discharge with these batteries. The converse would hold for a FR service provider focusing

on high-power, liquid cooled batteries- no fans would be required to drive cooling air through the plant.

This is partially a compromise on the advantage of the MBA's ability to accept any locally available battery but is still more flexible than being restricted to a single model or brand.

Stacking of Services

The results of 6.4 suggest a limited region of overlap for the provision of stacked services. The requirements of 4 h rate peak shaving and frequency regulation are at odds and imply different battery profiles. With the case of 1 h peak shaving and frequency regulation, the same batteries were found to be well suited, suggesting that those batteries could be used flexibly to perform both services, namely, the actively cooled batteries with good efficiency.

Chapter 7 Conclusions and Recommendations

This thesis investigates the re-purposing of used electric vehicle (EV) batteries for grid energy storage, creating a new mixed-battery-array concept and ranking the experimental performance of present day EV batteries according to their ability to provide energy storage services.

This is an important field of research because of the confluence of several important factors:

1. The growing share of renewable energy in the electricity grid which necessitates bulk energy storage to compensate for the generation variability.
2. The high cost of new batteries which presently render them uneconomical except for certain use cases (E.G., Transmission upgrade deferral, area regulation, backup services, demand charge management).
3. The forecasted growth of the EV market which is expanded worldwide and includes every major automotive manufacturer. Large lithium ion batteries are deployed in each EV.
4. The high probability of significant remaining capacity and functionality of EV batteries after the vehicle is retired due to age, use, corrosion, or accidents.
5. The limited recoverable value from recycling lithium-ion batteries.

The combination of the points 3 and 4 leads to a large potential supply of cheap storage in the form of re-purposed EV batteries as a solution to the problem of grid energy storage.

The decision to investigate used EV batteries was supported by:

1. Technoeconomic analyses by national research labs that concluded re-purposing of EV batteries for grid storage was potentially profitable.
2. The existence of pilot projects by original equipment manufacturers (OEM) that demonstrated technical functionality of single EV pack types.
3. Other preliminary studies of practical usage of used EV batteries for non-automotive purposes.

The existing usage scenarios were either: a) performed by the OEM internally, or b) performed by third-party operators without a unifying framework. In most cases little or no technical performance data was reported. OEMs are presumed to not require external testing of their own batteries, but third-party operators and grid operators would benefit. A gap was identified

in the literature for a practical implementation of a re-purposed EV battery for grid storage concept, and that little experimental performance data was available.

7.1 Conclusions

Mixed battery array

This thesis develops the Mixed Battery Array concept. It enables third-party operators, who would by necessity deal with a supply of batteries consisting of various brands, operating environments, ages, models, and past-usage to flexibly integrate a diverse local supply into a coherent whole plant providing storage services.

The Mixed Battery Array (MBA) concept is described. It consists of a tray-and-bay warehouse shelving system designed to accommodate the major EV battery pack sizes, focusing on ease of use and safety. The concept includes the need for an initial calibration cycle for arriving batteries to create an expectation of useful performance and preprocessing to identify and remove bad cells. Several designs concepts were elaborated described with varying electrical architecture and control logic.

Experimental testing

To support the MBA concept, a compilation of experimental tests was conducted to create a characteristic performance ranking. This involved rigorous comparative testing of EV batteries in a series of standard, replicable tests. The tests were: 1.) Constant-current tests to identify coulombic capacity and compare against manufacturer specified values, 2.) Constant-power tests to identify usable energy capacity, energy efficiency and temperature response in a grid storage peak shaving application, 3.) Frequency regulation tests to determine the maximum power bid of the pack and its energy efficiency while accounting for state of charge and thermal limitations. Various hour rates were used in each test to account for the range of energy and power services required by the electricity grid.

Constant Power Results

The CP test results validated the fundamental premise that EV batteries are technically capable of being repurposed for use outside of their automotive life. The energy capacities measured were within 10% of manufacturer ratings for batteries at a 4 h rate, with typical voltage limits.

Round-trip DC-DC energy efficiency was 94%+ at 4 h rates on all batteries, with an average of 97%. All batteries were run at up to half-hour rates, maintaining at least 50% of rated capacity

and an average of 90% efficiency. As the capacities are well within specification, and efficiencies are high, the batteries are applicable for deep discharge uses.

Temperature management was a major factor in the cycling frequency of the batteries. Passively cooled batteries were as much as 10 °C warmer than actively cooled batteries, leading to longer cooling times, which caused the overall duty cycle duration to grow to nearly five hours for a half-hour discharge/charge rate in the case of the 2012 Leaf. At 4 h rates, all batteries were near ambient temperature due to high efficiency and gradual heat dissipation.

As temperature is a limiting factor in short duration performance, this suggests passive packs should not be used in applications where short, intense, sustained bursts of power may be called upon, nor for consecutive high power deep discharge cycles. Peak shaving over several hours is a common service which passively cooled packs are well suited for. Actively cooled packs would be applicable for high-intensity services such as frequency regulation and voltage support.

Peak shaving tests were performed as an extension of the CP testing, with the result that peak shaving tests deliver nearly indistinguishable results from CP tests, which take less time to conduct. Therefore, given functionality with CP performance, peak shaving is within the performance abilities of EV batteries tested.

Frequency Regulation results

FR testing consisted of a 24 h power-signal timeseries, with the highest peak power factor determined by iterative testing. All batteries, when the power bid value was pushed as high as possible, converged on approximately a half-hour equivalent rate before suffering charge depletion in the 24 period. This is a satisfactory starting power bid for operators providing FR services.

If dynamic recharging is used, thermal management is the limiting factor for how hard the battery may be driven. Passively cooled packs approach the limit of safe temperatures in steady-state operation during testing near half-hour equivalent rates, but actively cooled packs were not, and could be operated at a higher power. Dynamic recharge factors of 1.01-1.08 are expected for continuous operation to compensate for inefficiency due to charge/discharge voltage differences.

Thermal Management Results

Thermal management systems were found to be most effective when using high surface area, parallel heat transfer designs. The two batteries with the best thermal response were the Moxie+ (Air-cooled) and Volt (Liquid-cooled), the next being the tangential-contact Tesla (Liquid-cooled), and the worst being the Leaf (Passively cooled). The practical conclusions are that cooling performance is best predicted by parallel and uniformly applied cooling, not by liquid cooling alone. Passively cooled packs will take as long or longer than the active period to cool down at higher rates (<1 h).

Performance Ranking of Repurposed EV Batteries in Grid Storage Application

The ranked comparison of battery performance in providing specific services supports the hypothesis that passively cooled packs are well-suited to providing peak shaving services, up to 1 h rates, when actively cooled packs gain advantage. Similarly, for frequency regulation, actively cooled, efficient packs are found to perform well compared to passively cooled packs.

Characterization Testing for Receiving and Processing Repurposed EV Batteries

Third-party operators receiving a new battery will need to perform characterizing tests to determine its abilities for optimal control. Identifying and demonstrating such tests is an objective of this work, and was done through constant-current, constant-power, and frequency regulation testing. To save time on intake, the testing process may be simplified somewhat. Half-hour deep discharge performance was not found to be a key factor in and storage service discussed. For deciding between peak shaving and frequency regulation services, a single 4 h test and FR test may suffice to identify the relative strengths of the battery. The FR test may also be shortened from its original 24 h, considering that energy efficiency was found to be the most significant performance factor in FR service, and efficiency can be calculated with modest amount of discharge and charge energy. Overall, the testing time could be reduced to 28 hours²¹ for identification. 8 hours could be saved on this if a single cycle of constant power discharge is acceptable, leading with a CV charge to ensure full capacity.

7.2 Recommendations

The findings lead to several recommendations for future research and commercial implementation of the mixed battery array concept.

²¹ 8 * 2 hours for two deep discharge CP cycles + 12 h for FR testing

Whole Pack Testing

Testing complete packs, instead of partial packs, would give a holistic performance picture. A whole pack would capture a more complete temperature response, instead of having exposed modules which dissipate heat faster by being exposed and having a higher surface-area-to-volume ratio. Individual cells would have less influence on the operation of the whole pack, compared to the minimum 6 cell groups in this thesis. Operating a whole pack would also reveal practicalities of the mixed battery array concept as it is the most granular level.

Frequency Regulation Signal

The FR power signal used in this thesis is from PNNL, which is based upon the PJM grid in 2011-2012. A cursory examination of recent FR signal data (2017) reveals significant differences between the idealized testing cycle and actual implementation, primarily in energy throughput per bid size. Future testing should use a variety of signals from more recent sources, so long as the signals follow the test guidelines in Section 4.3.3. Further considerations are given in Appendix D.

Battery Age and Wear

This thesis confirmed the functionality of “lightly-used” batteries. As the EV market develops, used batteries will become available that have experienced a wide variety of conditions. Energy throughput (i.e. km of travel) and age (vehicle year model) will strongly affect performance and this must be characterized to increase confidence in the mixed battery array concept viability.

Stacked Electricity Services

Stacking of electricity services is broadly viewed as necessary for battery energy storage economic viability. By stacking services, a single storage element can provide more than one revenue stream. Service stacking affects thermal performance and SOC positioning, which affects regulation power bid values and wear. Experimental results indicate that actively cooled batteries with high energy efficiency are suitable candidates for experimentation. Therefore, experimental testing of re-purposed EV batteries providing stacked services is a strong candidate for investigation.

Bibliography

- [1] United Nations. "Paris Agreement," U.N.T. Collection, 2015. Available: http://unfccc.int/paris_agreement/items/9485.php
- [2] J.G.J. Oliver, G. Janssens-Maenhout, M. Muntean and Peters, Jeroen A H W, "Trends in global CO2 emissions: 2016 report," PBL Netherlands Environmental Assessment Agency, The Hague, The Netherlands, 2016.
- [3] B. Plumer and N. Popovich, "Here's How Far the World Is From Meeting Its Climate Goals," *The New York Times*, Nov 6, 2017.
- [4] Christiana Figueres, "Three years to safeguard our climate," *Nature*, vol. 546, no. 7660, Jun 29, pp. 593.
- [5] "Global Greenhouse Gas Emissions Data," U.S.A. EPA, Wash., WA, U.S.A., 2017. [Online]. Available: <https://www.epa.gov/ghgemissions/global-greenhouse-gas-emissions-data>
- [6] IRENA, "REthinking Energy 2017: Accelerating the Global Energy Transformation," *International Renewable Energy Agency*, Abu Dhabi, U.A.E., 2017.
- [7] M.I.M. Ridzuan, I. Hernando-Gil, S. Djokic, R. Langella and A. Testa, "Incorporating regulator requirements in reliability analysis of smart grids. Part 1: Input data and models," presented at *ISGTEurope*, Istanbul 2014.
- [8] Mark Z. Jacobson, Mark A. Delucchi, Mary A. Cameron and Bethany A. Frew, "Low-cost solution to the grid reliability problem with 100% penetration of intermittent wind, water, and solar for all purposes," *Proceedings of the National Academy of Sciences*, vol. 112, no. 49, pp. 15060-15065, Dec 2015.
- [9] W.F. Pickard, "Massive Electricity Storage for a Developed Economy of Ten Billion People," *IEEE Access*, vol. 3, pp. 1392-1407, Aug 2015.
- [10] W. T. Jewell, "Electric industry infrastructure for sustainability: Climate change and energy storage," *2008 IEEE Power and Energy Society General Meeting - Conversion and Delivery of Electrical Energy in the 21st Century*, Pittsburgh, PA, 2008, pp. 1-3. doi: 10.1109/PES.2008.4596181
- [11] C. Budischak, D. Sewell, H. Thomson, L. Mach, D.E. Veron and W. Kempton, "Cost-minimized combinations of wind power, solar power and electrochemical storage, powering the grid up to 99.9% of the time," *Journal of Power Sources*, vol. 225, pp. 60-74, Oct 2012.
- [12] M. Aneke and M. Wang, "Energy storage technologies and real life applications – A state of the art review," *Applied Energy*, vol. 179, pp. 350-377, Jul 2016.

- [13] M. Lave and A. Ellis, "Comparison of solar and wind power generation impact on net load across a utility balancing area," *2016 IEEE 43rd Photovoltaic Specialists Conference (PVSC)*, Portland, OR, 2016, pp. 1837-1842. doi: 10.1109/PVSC.2016.7749939
- [14] F. Monforti, T. Huld, K. Bodis, L. Vitali, M. D'Isidoro and R. Lacal-Arantequi, "Assessing complementarity of wind and solar resources for energy production in Italy. A Monte Carlo approach," *Renewable Energy*, vol. 63, pp. 576-586, Oct 2014.
- [15] B. P. Swaminathan, V. Debusschere and R. Caire, "Intelligent day-ahead scheduling for distribution networks with high penetration of Distributed Renewable Energy Sources," *2015 IEEE Eindhoven PowerTech*, Eindhoven, 2015, pp. 1-6. doi: 10.1109/PTC.2015.7232718
- [16] D.R. Conover, A.J. Crawford, V.V. Viswanathan, S. Ferreira and D. Schoenwald, "Protocol for Uniformly Measuring and Expressing the Performance of Energy Storage Systems," PNNL, Richland, Wash., U.S.A., 2010, Apr 2016
- [17] M. Delleny, "Historical EMS Hourly Data," CAISO, Folsom, CA, U.S.A., Mar 8. [ONLINE] Available: <https://www.caiso.com/Documents/HistoricalEMSHourlyLoadDataAvailable.html>
- [18] M. van der Houten, "IEA World Energy Outlook," *International Energy Agency*, Paris, France, 2015.
- [19] J.S. Neubauer, A. Pesaran, B. Williams, M. Ferry and J. Eyer, "A Techno-Economic Analysis of PEV Battery Second Use: Repurposed-Battery Selling Price and Commercial and Industrial End-User Value," presented at SAE World Congr. and Exhibition, Detroit, MI., Apr 2012.
- [20] "RePower America." Internet: <http://repoweramerica.solar/>, Mar 2018.
- [21] E. Cready, J. Lippert, J. Pihl, I. Weinstock And P. Symons, "Technical and Economic Feasibility of Applying Used EV Batteries in Stationary Applications," Sandia National Labs, Livermore, CA, U.S.A., SAND2002-4084, Mar 2003.
- [22] N. Pearre S and L. Swan, "Technoeconomic feasibility of grid storage: Mapping electrical services and energy storage technologies," *Applied Energy*, vol. 1, no. 137, pp. 501-510, May 2014.
- [23] A.F. Ghoniem, "Needs, resources and climate change: Clean and efficient conversion technologies," *Progress in Energy and Combustion Science*, vol. 37, pp. 15-51, Apr 2010.
- [24] L.E. Doman, V. Arora, L.E. Singer, V. Zaretskaya, A. Jones, T. Huetteman, M. Bowman, N. Slater-Thompson, B. Hojjati, D. Peterson, P. Gross, P. Otis, M. Lynes, P. Lindstrom, "International Energy Outlook," U.S. E. I.A., Washington, D.C., U.S.A., DOE/EIA-0484(2016), May 2016.
- [25] "Key World Energy Statistics 2016," International Energy Agency, Paris, France, 2016.
- [26] "Energy Storage Exchange." U.S. Dept. Energy, Internet: <http://www.energystorageexchange.org/>, Mar 2018.

- [27] Z. Shahan. "Big Auto's Fully Electric Car Sales Up 102% In USA." Internet: <https://cleantechnica.com/2017/07/05/big-autos-fully-electric-car-sales-102-usa/>, Jul 5, 2017.
- [28] K.B. Naceur, J.F. Gagné. "Global EV Outlook 2017," IEA, Paris, France, June 2017.
- [29] J. Cobb, "Hybrid Cars: December 2017 Dashboard," HybridCars, Internet: <http://www.hybridcars.com/december-2017-dashboard/>, Jan 4, 2018.
- [30] J. Neubauer, "Battery Lifetime Analysis and Simulation Tool (BLAST) Documentation," NREL, Golden, CO, U.S.A., NREL/TP-5400-63246, Dec 2014.
- [31] Z. Shahan, "Tesla's Battery Prices Falling Faster Than Everyone Else's — Who Knew? (+ Cool EV Battery Charts)," CleanTechnica, Internet: <https://cleantechnica.com/2016/06/08/teslas-batteries-cheaper-everyone-elses-knew-cool-ev-battery-charts/>, Jun 8, 2016.
- [32] "Electromobility Analysis and News," EMValley, Internet: <http://www.emvalley.com/>, Mar 2018.
- [33] G. Crabtree, E. Kócs L. Trahey, "The energy-storage frontier: Lithium-ion batteries and beyond," *Materials Research Soc. Bulletin*, vol. 40, no. 12, pp. 1067-1078, Dec 2015.
- [34] "Batteries." Office of Energy Efficiency and Renewable Energy, Washington, DC, U.S.A. Mar 2018 [Online] Available: <https://www.energy.gov/eere/vehicles/batteries>.
- [35] J. Neubauer, K. Smith, E. Wood and A. Pesaran, "Identifying and Overcoming Critical Barriers to Widespread Second Use of PEV Batteries," NREL, Golden, CO, U.S.A., NREL/TP-5400-63332, Feb 2015.
- [36] J. St. John, "Nissan, Green Charge Networks Turn 'Second-Life' EV Batteries Into Grid Storage Business," GreenTechMedia, Internet: <https://www.greentechmedia.com/articles/read/nissan-green-charge-networks-turn-second-life-ev-batteries-into-grid-storage#gs.xW4Vjp0>, Jun 15, 2015.
- [37] "Nissan and Eaton make home energy storage reliable and affordable to everyone with 'xStorage'," Nissan, Yokohama, Japan, ID: 145249, May 10, 2016. [Online] Available: <https://newsroom.nissan-europe.com/uk/en-gb/media/pressreleases/145249/nissan-and-eaton-make-home-energy-storage-reliable-and-affordable-to-everyone-with-xstorage>.
- [38] J. Parnell, "Renault-Nissan to build 100MW second-life battery project," Energy Storage News, Internet: <https://www.energy-storage.news/news/renault-nissan-to-build-100mw-second-life-battery-project>, Jun 8, 2017.
- [39] A. Colthorpe, "Storage system powered by used Nissan batteries installed at Japanese solar farm," PV Tech, Internet: https://www.pv-tech.org/news/battery_storage_powered_by_used_nissan_leaf_batteries_installed_at_japanese, Feb 7, 2014.

- [40] N. Gordon-Bloomfield, "Following Nissan, General Motors Announces Second-Life Program for Electric Car Batteries," *Transport Evolved*, Internet: <https://transportevolved.com/2015/06/18/following-nissan-general-motors-announces-second-life-program-for-electric-car-batteries/>, Jun 18, 2015.
- [41] E. Wesoff, "Chevy Volt Batteries to Get Second Life in Grid Storage," *GreenTechMedia*, Internet: <https://www.greentechmedia.com/articles/read/chevy-volt-batteries-to-get-second-life-in-grid-storage#gs.hTPrtYE>, Nov 15, 2012.
- [42] M. Kane, "BMW and Bosch's Second-Life 2.8 MWh Energy Storage Solution in Hamburg," *InsideEVs*, Internet: <https://insideevs.com/bmw-and-boschs-second-life-2-8-mwh-energy-storage-solution-in-hamburg/>, Oct 25, 2016.
- [43] N. Gordon-Bloomfield, "Toyota Repurposes Hybrid Batteries for Off-Grid Battery Storage System," *Transport Evolved*, Internet: <https://transportevolved.com/2015/05/19/toyota-repurposes-hybrid-batteries-for-off-grid-battery-storage-system/>, May 19, 2015.
- [44] "World's largest 2nd-use battery storage is starting up," Daimler, Lünen/Stuttgart, Germany, Sept. 13, 2016. [Online]. Available: <http://media.daimler.com/marsMediaSite/ko/en/13634457>.
- [45] Z. Shahan, "Tesla CTO JB Straubel On Why EVs Selling Electricity To The Grid Is Not As Swell As It Sounds," *CleanTechnica*, Internet: <https://cleantechnica.com/2016/08/22/vehicle-to-grid-used-ev-batteries-grid-storage/>, Aug 22, 2016.
- [46] Relectrify, Melbourne, Australia. [Online]. Available: <https://www.relectrify.com/>.
- [47] Spiers New Technologies, Oklahoma City, Oklahoma, U.S.A. [Online]. Available: <http://www.spiersnewtechnologies.com/>.
- [48] FreeWire Technologies, [Online]. Available: <https://freewiretech.com/>.
- [49] eCamion, Markham, Ont. Canada. [Online]. Available: <http://www.ecamion.com/company/>.
- [50] C. Narula K, R. Martinez, O. Onan, M. R. Starke, G. Andrews, "Economic Analysis of Deploying Used Batteries in Power Systems," ORNL, Springfield, VA. U.S.A., ORNL/TM-2011/151, June 2011.
- [51] J.S. Neubauer, E. Wood and A. Pesaran, "A Second Life for Electric Vehicle Batteries: Answering Questions on Battery Degradation and Value," presented at SAE 2015 World Congress & Exhibition, Detroit, Michigan, U.S.A., NREL/CP-5400-63524, Apr 2015.
- [52] B. Williams and T. Lipman, "Analysis of the Combined Vehicle and Post-Vehicle-Use Value of Lithium-Ion Plug-In-Vehicle Propulsion Batteries," PIER, Berkely, CA, U.S.A., 500-02-004, Apr 2011.
- [53] L. Ahmadi, M. Fowler, S.B. Young, R.A. Fraser, B. Gaffney, S.B. Walker, "Energy efficiency of Li-ion battery packs re-used in stationary power applications," *Sustainable Energy Technologies and Assessments*, vol. 8, pp. 9-17, Jun 18, 2014.

- [54] D. Strickland, L. Chittock, D. A. Stone, M. P. Foster and B. Price, "Estimation of Transportation Battery Second Life for Use in Electricity Grid Systems," in *IEEE Transactions on Sustainable Energy*, vol. 5, no. 3, pp. 795-803, July 2014. doi: 10.1109/TSTE.2014.2303572
- [55] S. Tong, A. Same, M. Kootstra and J. Park, "Off-grid photovoltaic vehicle charge using second life lithium batteries: An experimental and numerical investigation," *Applied Energy*, vol. 104, pp. 740-750, Dec 29, 2012.
- [56] R. Wachal, "Stationary Energy Storage System Using Repurposed Electric Vehicle Batteries," Presented at IEEE PES Winnipeg, Manitoba HVDC Research Center, Winnipeg, MA, Canada, Jan 28, 2014.
- [57] M. Starke, B. Ollis, P. Irminger, G. Andrews, O. Onar, P. Karlson, S. Thambiappah, P. Valencia, S. Massin, A. Goodson and P. Rosenfeld, "Community Energy Storage with Secondary Use EV/PHEV Batteries," ORNL, Oak Ridge, TN, U.S.A., DEAC05-00OR22725, 2014.
- [58] E. Martinez-Laserna et al., "Evaluation of lithium-ion battery second life performance and degradation," 2016 IEEE Energy Conversion Congress and Exposition (ECCE), Milwaukee, WI, 2016, pp. 1-7. doi: 10.1109/ECCE.2016.7855090
- [59] L. Gaines, "The future of automotive lithium-ion battery recycling: Charting a sustainable course," *Sustainable Materials and Technologies*, vol. 1-2, pp. 2-7, Nov 15, 2014.
- [60] "2016 Chevrolet Volt Battery System," Chevrolet. [Online]. Available: https://media.gm.com/content/dam/Media/microsites/product/Volt_2016/doc/VOLT_BATTERY.pdf.
- [61] "NCR18650A Specifications," Panasonic, 2012.
- [62] "Cell, Module and Pack for EV Applications," AESC, Zama City, Kanagawa Prefecture, Mar 2018. [Online]. Available: http://www.eco-aesc-lb.com/en/product/liion_ev/.
- [63] "CP160-365 Moxie+ Prismatic Cell Specifications," EnerDel, 2012.
- [64] J. Xia, M. Nie, L. Ma, J.R. Dahn, "Variation of coulombic efficiency versus upper cutoff potential of Li-ion cells tested with aggressive protocols," *Journal of Power Sources*, vol. 306, pp. 233-240, Dec 17, 2015.
- [65] S. Tobishima, K. Takei, Y. Sakurai, J. Yamaki, "Lithium ion cell safety," *Journal of Power Sources*, vol. 90, pp. 188-195, 2000.
- [66] G. Wang et al., "A Review of Power Electronics for Grid Connection of Utility-Scale Battery Energy Storage Systems," in *IEEE Transactions on Sustainable Energy*, vol. 7, no. 4, pp. 1778-1790, Oct. 2016. doi: 10.1109/TSTE.2016.2586941
- [67] Bruce Dunn, Haresh Kamath and Jean-Marie Tarascon, "Electrical Energy Storage for the Grid: A Battery of Choices," *Science*, vol. 334, no. 6058, pp. 928-935, Nov 18, 2011.

- [68] "Types of Lithium-ion," Battery University/Cadex Labs, Internet:
http://batteryuniversity.com/learn/article/types_of_lithium_ion, Nov 2017.
- [69] Swan, L, private communication, Sept 2017
- [70] G. Mulder, N. Omar, S. Pauwels, M. Meeus, F. Leemans, B. Verbrugge, W. De Nijs, P. Van den Bossche, D. Six, J. Van Mierlo, "Comparison of commercial battery cells in relation to material properties," *Electrochimica Acta*, vol. 87, pp. 473-488, 2013. doi:
<http://dx.doi.org/10.1016/j.electacta.2012.09.042>
- [71] P. Meister, H. Jia, J. Li, R. Kloepsch, M. Winter, T. Placke, "Best Practice: Performance and Cost Evaluation of Lithium Ion Battery Active Materials with Special Emphasis on Energy Efficiency," *Chemistry of Materials*, vol. 28, pp. 7203-7217, Sept 23 2016. doi:
[10.1021/acs.chemmater.6b02895](http://dx.doi.org/10.1021/acs.chemmater.6b02895)

Appendix A Example Parameter Script

```
\\ Battery: AESC Leaf 2012 16 Mod
\\ Configuration: 2P64S
\\ Created: Ben Thompson
\\ Modified:
STEP_TIME    10 msec
  \\ CRITICAL: MUST FILL OUT CORRECTLY
SET_VALUE    S_ChannelNumber_I =    1
SET_VALUE    S_BMSNum_I =    1
SET_STRING    S_TestName_S "AESC_Leaf_2012_RECHARGE"
  \\ Pack Voltage and Current Mapping
SET_VALUE
  S_Pack_Volt_Ch_I =    0
  S_Pack_Current_Ch_I =    15
  S_Shunt_A =    100
  S_Shunt_mV =    100
END_SET
  \\ Auxiliary Channel Mapping Indices, This is used only for equations and alarms. More
  Aux can be included in datalogger.
SET_VALUE
  S_Aux_Volt_ChStart_I =    0
  S_Aux_Volt_ChEnd_I =    0
  S_Aux_Temp_ChStart_I =    5
  S_Aux_Temp_ChEnd_I =    8
  S_Aux_TestTemp_Ch_I =    16
END_SET
  \\ Global Safety Values- MUST BE SET (If adding a new alarm, also add to SubScript
  SafetyLimitsReset
SET_VALUE
  L_Alarm_Pack_Volt_Max_V =    270
  L_Alarm_Pack_Volt_Min_V =    160
  L_Alarm_Pack_Current_Max_A =    120
  L_Alarm_Pack_Current_Min_A =    -120
  L_Alarm_Aux_Volt_Max_V =    4.3
  L_Alarm_Aux_Volt_Min_V =    2.42
  L_Alarm_Aux_Temp_Max_C =    50
  L_Alarm_Aux_Temp_Min_C =    0
END_SET
  \\ Test Limits
SET_VALUE
  S_Cycle_Num_Start_I =    1
  L_Cycle_Num_End_I =    1
END_SET
  \\ Rest Values
SET_VALUE
  L_Rest_TempHigh_C =    30
  L_Rest_TempLow_C =    15
```



```

L_RestBegin_Length_h = 0
L_RestEnd_Length_h = 0
L_Rest1_Length_h = 0
L_Rest2_Length_h = 0
L_Rest3_Length_h = 99999
L_Rest4_Length_h = 99999
L_Rest5_Length_h = 99999
END_SET
  \\ Global Discharge Values
SET_VALUE
  L_Dis_Cap_Ah = 99999
  L_Dis_En_kWh = 99999
END_SET
  \\ Discharge 1 Values
SET_VALUE
  L_Alarm_Dis1_Dur_Max_h = 1
  S_Dis1_CC_A = -0
  S_Dis1_CV_V = 0
  S_Dis1_CP_kW = -0
  L_Dis1_Volt_V = 800
  L_Dis1_Time_h = 0
  L_Dis1_Cap_Ah = 99999
  L_Dis1_En_kWh = 99999
  L_Dis1_Current_A = -0
END_SET
  \\ Global Charge Values
SET_VALUE
  L_Chg_Cap_Ah = 99999
  L_Chg_Cap_Overcharge_Ah = 99999
  L_Chg_Cap_Overcharge_pct = 99999
  L_Chg_En_kWh = 99999
  L_Chg_En_Overcharge_kWh = 99999
END_SET
  \\ Charge 1 Values
SET_VALUE
  L_Alarm_Chg1_Dur_Max_h = 1.5
  S_Chg1_CC_A = 60
  S_Chg1_CV_V = 269
  S_Chg1_CP_kW = 0
  L_Chg1_Volt_V = 268.8
  L_Chg1_Time_h = 99999
  L_Chg1_Cap_Ah = 99999
  L_Chg1_En_kWh = 99999
  L_Chg1_Current_A = 200
END_SET
  \\ Charge 2 Values
SET_VALUE
  L_Alarm_Chg2_Dur_Max_h = 1

```

```

S_Chg2_CC_A      =      60
S_Chg2_CV_V      =      268.8
S_Chg2_CP_kW     =      0
L_Chg2_Current_A =      3
L_Chg2_Time_h    =      99999
L_Chg2_Cap_Ah    =      99999
L_Chg2_En_kWh    =      99999
L_Chg2_Volt_V    =      0
END_SET
  \\    Link to the correct datalogger for the channel. This supports AuxMeas mapping.
IF      S_ChannelNumber_I = 1      THEN
DATALOG_CONFIG    MeasureLogger
  PROFILE = MeasureCh1.ini;
END_CONFIG
END_IF
IF      S_ChannelNumber_I = 2      THEN
DATALOG_CONFIG    MeasureLogger
  PROFILE = MeasureCh2.ini;
END_CONFIG
END_IF

  \\    Datalogger Parameters: must follow the loading of the Profile, because otherwise the
Profile defaults will overwrite the below
DATALOG_CONFIG    MeasureLogger
  TEST_NAME = S_TestName_S;
  USER_NAME = "Ben Thompson";
  TEST_COMMENT = " Aux temps X-X are pack side, pack side, pack middle, pack top. Aux
temperatures are from lower left, lower right, upper thermistors.";
  LOG_PERIOD = 1000 ms;
  PARTITION_METHOD = No Partition
END_CONFIG
END

```

Appendix B Example Cycling Script

```
\\ Cycle: Dis-CC-V_Chg-CC-CCCV-A
STEP_TIME    100 msec
SET_VALUE    M_Cycle_Num_I      =      S_Cycle_Num_Start_I
DATALOG_START MeasureLogger
  \\ Starting Rest
SET_VALUE    mode_set          =      Standby
SET_VALUE
  C_Ch_Current_A    =      0
  C_Ch_Power_kW     =      0
  C_Ch_Voltage_V    =      0
END_SET
DO
WHILE (M_Step_Time_h < L_RestBegin_Length_h) OR (M_Aux_Temp_Max_C >=
L_Rest_TempHigh_C) OR (M_Aux_Temp_Min_C <= L_Rest_TempLow_C)
  \ Discharge
CALL CyclingScripts\SubScripts\ComponentsChannelLimitsDischarge.aut
SET_VALUE    mode_set          =      Current
SET_VALUE
  C_Ch_Power_kW     =      0
  C_Ch_Voltage_V    =      0
END_SET
DO
SET_VALUE    C_Ch_Current_A    =      S_Dis1_CC_A
WHILE (M_Ch_Voltage_V > L_Dis1_Volt_V) AND (M_Step_Time_h < L_Dis1_Time_h)
SET_VALUE    mode_set          =      Standby
CALL CyclingScripts\SubScripts\ComponentsChannelLimitsReset.aut
  \\ Discharge Rest
SET_VALUE    mode_set          =      Standby
SET_VALUE
  C_Ch_Current_A    =      0
  C_Ch_Power_kW     =      0
  C_Ch_Voltage_V    =      0
END_SET
DO
WHILE (M_Step_Time_h < L_Rest1_Length_h) OR (M_Aux_Temp_Max_C >=
L_Rest_TempHigh_C) OR (M_Aux_Temp_Min_C <= L_Rest_TempLow_C)
  \\ Charge 1
CALL CyclingScripts\SubScripts\ComponentsChannelLimitsCharge.aut
SET_VALUE    C_Comp_VoltHigh_V =      S_Chg1_CV_V
SET_VALUE    mode_set          =      Current
SET_VALUE
  C_Ch_Power_kW     =      0
  C_Ch_Voltage_V    =      0
END_SET
DO
SET_VALUE    C_Ch_Current_A    =      S_Chg1_CC_A
```

```

WHILE (M_Ch_Voltage_V < L_Chg1_Volt_V) AND (M_Step_Time_h < L_Chg1_Time_h)
  \\ Note: no return to standby mode because a smooth current transition to Chg2
  \\ Charge 2
  \\ Modify the Component Limit current to give CCCV mode while in Voltage control
SET_VALUE C_Comp_PosCurrentHigh_A = S_Chg2_CC_A
SET_VALUE mode_set = Voltage
SET_VALUE
  C_Ch_Current_A = 0
  C_Ch_Power_kW = 0
END_SET
DO
SET_VALUE C_Ch_Voltage_V = S_Chg2_CV_V
  \\ Wait briefly to allow current to rise when leaving pause
WAIT 1 sec
  \\ While condition includes standby to account for delays in machine action (e.g.
emergency stop) where the mode is changed, causing current to goto zero, before the script is
paused
  \\ While condition check of momentary current is to allow for jumping into this step from
pause, giving rise time for current
  \\ While condition check of average current is to account for noise in the current signal at
low values.
WHILE (mode = 0) OR (M_Ch_Current_A > L_Chg2_Current_A) AND (M_Step_Time_h <
L_Chg2_Time_h) OR (M_Ch_Current_Avg_A > L_Chg2_Current_A) AND
(M_Step_Time_h < L_Chg2_Time_h)
  \\ Put the Channel in Standby Mode prior to restoring current limits
SET_VALUE mode_set = Standby
  \\ Reset the Component Limit current to full machine value as we have exited the CCCV
mode
CALL CyclingScripts\SubScripts\ComponentsChannelLimitsReset.aut
  \\ Call calculation and storage of cycle efficiencies and capacities
CALL CyclingScripts\SubScripts\CycleCapacityandEfficiency.aut
LABEL Rest2
SET_VALUE mode_set = Standby
SET_VALUE
  C_Ch_Current_A = 0
  C_Ch_Power_kW = 0
  C_Ch_Voltage_V = 0
END_SET
DO
WHILE (M_Step_Time_h < L_Rest2_Length_h) OR (M_Aux_Temp_Max_C >=
L_Rest_TempHigh_C) OR (M_Aux_Temp_Min_C <= L_Rest_TempLow_C)
  \\ Loop Check
SET_VALUE mode_set = Standby
IF M_Cycle_Num_I < L_Cycle_Num_End_I THEN
CALL CyclingScripts\SubScripts\CycleClear.aut
EQUATION M_Cycle_Num_I = M_Cycle_Num_I + 1
JUMP Discharge
END_IF

```

```

\\ End Rest
SET_VALUE mode_set = Standby
SET_VALUE
  C_Ch_Current_A = 0
  C_Ch_Power_kW = 0
  C_Ch_Voltage_V = 0
END_SET
DO
  WHILE (M_Step_Time_h < L_RestEnd_Length_h) OR (M_Aux_Temp_Max_C >=
  L_Rest_TempHigh_C) OR (M_Aux_Temp_Min_C <= L_Rest_TempLow_C)
  LABEL TestEnd
  SET_VALUE mode_set = Standby
  SET_VALUE
    C_Ch_Current_A = 0
    C_Ch_Power_kW = 0
    C_Ch_Voltage_V = 0
  END_SET
  DATALOG_STOP MeasureLogger
  \\ End the script (test stops)
END

```

Appendix C Frequency Regulation Unit Timeseries from PNNL

The timeseries used for FR control can be found at the following address:

<http://www.sandia.gov/ess/publications/SAND2013-7315P.xlsx>.

Appendix D Alternative Frequency Regulation Signals

Section 4.3.3. lays out the key requirements for a FR test signal, namely

- The timeseries should be energy neutral in throughput.
- The power signal must reach symmetric boundaries for normalization.
- The signal must resemble a “typical” signal for the area.

Given the diversity of signals, and the requirements of testing, and the results of the experiments, the following observations can be made:

1. This work used peak power factor as a primary metric, but energy efficiency was a better predictor of success at FR service provision.
2. A more consistent method would be to use fixed hour rate bid values, and compare remaining SOC at the end of the timeseries.
3. Given that the real-world FR timeseries may be very asymmetric, bids made must be conservative.

If a real-world timeseries simply discharges for the majority of the day, no storage device is going to provide service the entire time unless it is bidding a trivial hour rate. The factors influencing how difficult or easy a given frequency regulation are:

1. The width of the half-cycles, i.e., the time spent in a single mode of charge or discharge.
2. The energy deviation from neutral, which is the time-integral of the power call inside a half-cycle.
3. The maximum value of the half-cycle.

Assuming the maximum value of the signal is normalized and scaled by the bid made by the operator, a peak power call is only an issue if the battery has charged or discharged away from 50% SOC, and will experience a large voltage change from a maximum power call. Such an event can cause early termination, or failure to provide services. If the battery is at 50% SOC, then the power call should not present an issue, as its power call can only be the maximum expected by the operator.

If the signal calls for sustained discharge, any storage device will eventually deplete. For this reason, some ISOs have begun stating an intent to balance their FR signal to be energy-neutral within a fixed timespan. As storage becomes a more prevalent regulation provider vs.

conventional generation, this will become more important, and more reliable. If so, then maintaining energy neutrality depends on bidding the optimal power value, and having either high energy efficiency or a high charge offset. Given that a high charge offset directly restricts the revenue available from FR service provision, a high energy efficiency is the preferable solution.

By this chain of reasoning, the most important predictive factor is the energy efficiency of the battery when operating with high alternating power calls for a sustained period, followed by the overall thermal response and management.

If so, using a real-world timeseries may be less significant, and a sinusoidal signal could be used instead- the advantage being that the frequency of the sinusoid can be swept from high to low frequencies, and energy efficiency can be tracked. The sinusoidal signal mainly allows for comparison of batteries, and a quick estimate of energy efficiency by cycling for an hour at a given frequency, and calculating.

Appendix E Uncertainty Analysis

- Shunts, voltage measurement have uncertainty in current, voltage
- Taking the maximum of current and voltage in charge, discharge for two examples:
- Maximum error of 0.5% and 1.3%
- plot of error over time, taking the measured value as true and maximum value as approximate

From Section 0, the current shunt and voltage measurements have a degree of uncertainty:

Table 25- Selected Measurement Errors

Load Bank Main Voltage	80 mV
DAQ Channels 1-14	37.5 mV
100 A/100 mV	0.25% ± 0.1 A
300 A/100 mV	0.25% ± 0.3 A
500 A/50 mV	0.25% ± 1 A

A worst-case estimate of the measurement error may be obtained by comparing the measured current and voltage with a signal which deviates from them by the greatest amount. Integrating the measured and maximum-error signals, an estimate of the greatest error in the energy calculations may be found:

From a Tesla 200 A CCCV test, in the charge step, the measured energy accumulation is compared to the maximum energy accumulation based on the product of the maximum currents and voltages. The difference of these values is named Error. A plot of the measured and deviated energy throughput in charge is shown in Figure 68.

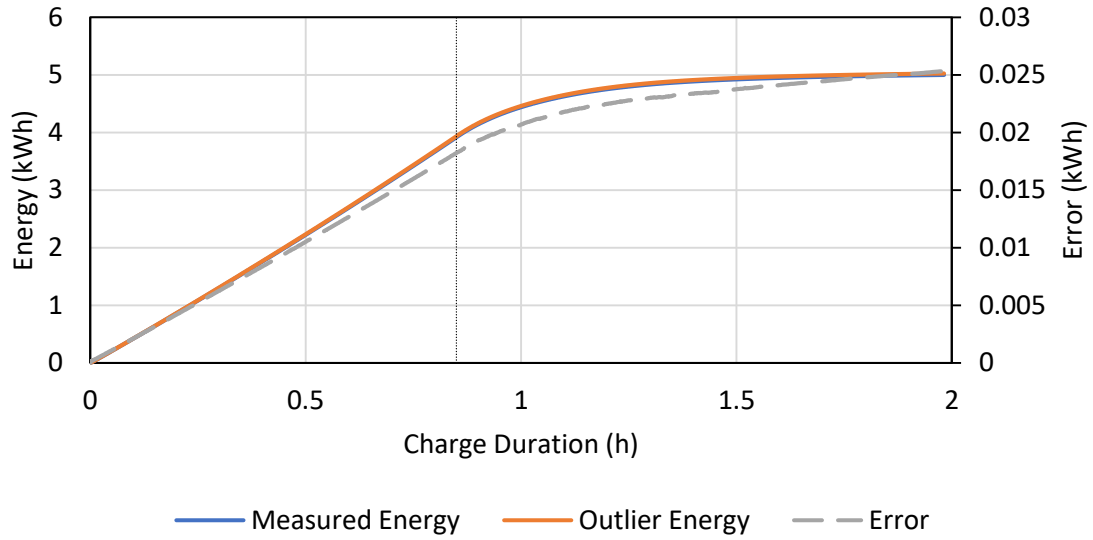


Figure 68- Measured and Greatest-Error Estimate of Charge Energy and Their Error. The dotted vertical line indicates the transition from CC to CV charging. Drawn from a 200 A CCCV Charge with a Panasonic Tesla

The absolute rate of error accumulation slows down once CV charge is entered, but Figure 69 shows the relative error begin to accumulate more in CV mode.

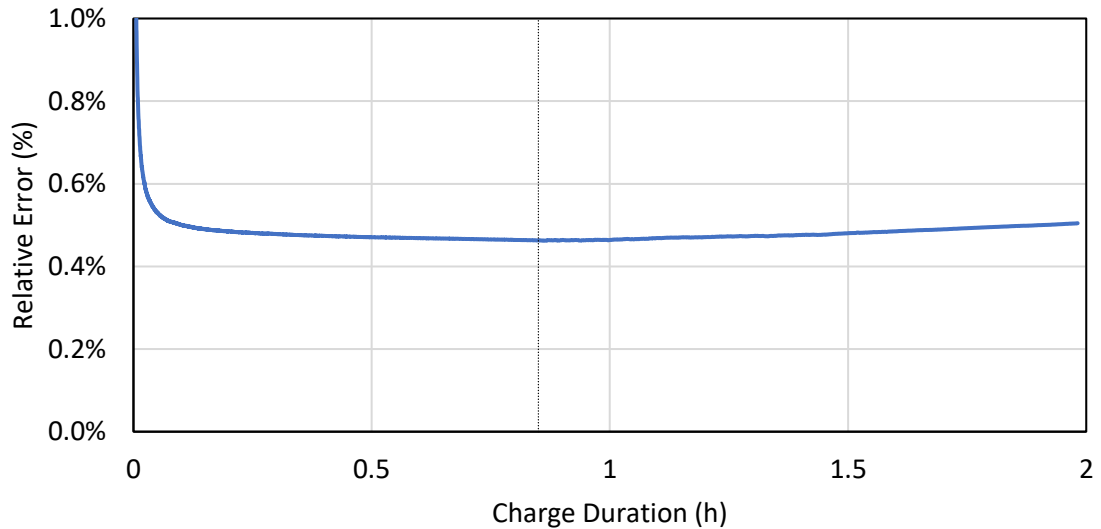


Figure 69- The Relative Error of a 200 A CCCV charge in a Panasonic Tesla

At the termination of charge, the relative error accumulated on charge energy is approximately ½%. For discharge in the same test, the relative error is 0.37%. The energy efficiency becomes 88.2%, from 89.0%.

From a 400 A Tesla CCCV cycle, in the charge step, Figure 70 shows the measured and deviated energy throughput in charge.

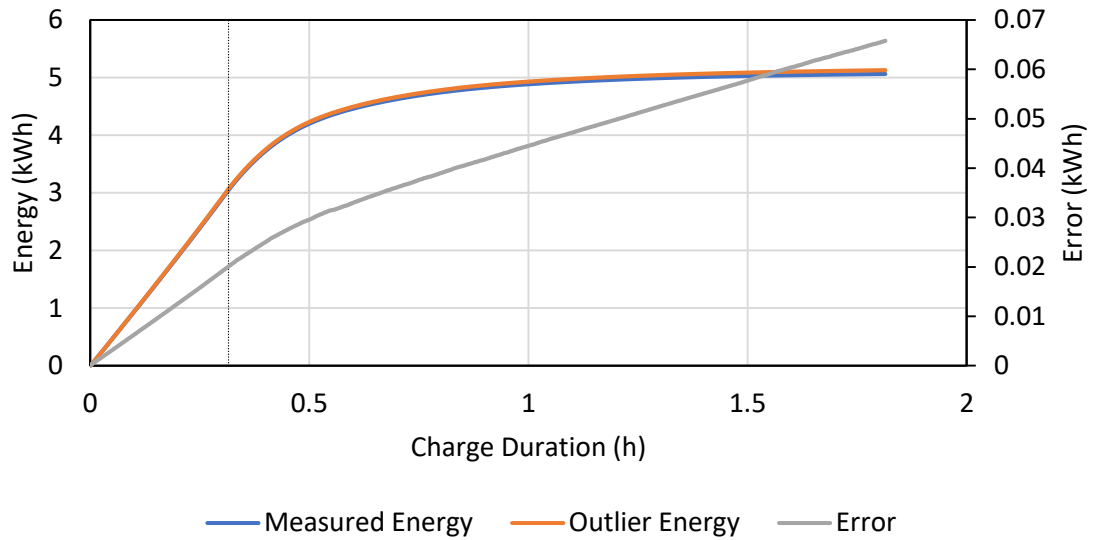


Figure 70- Measured and Maximum-Error Estimates of Energy and Their Error. Drawn from a 400 A CCCV Panasonic Tesla charge step. The dotted line indicates transition from CC to CV charge.

Figure 71 shows the results converted to relative error measurement.

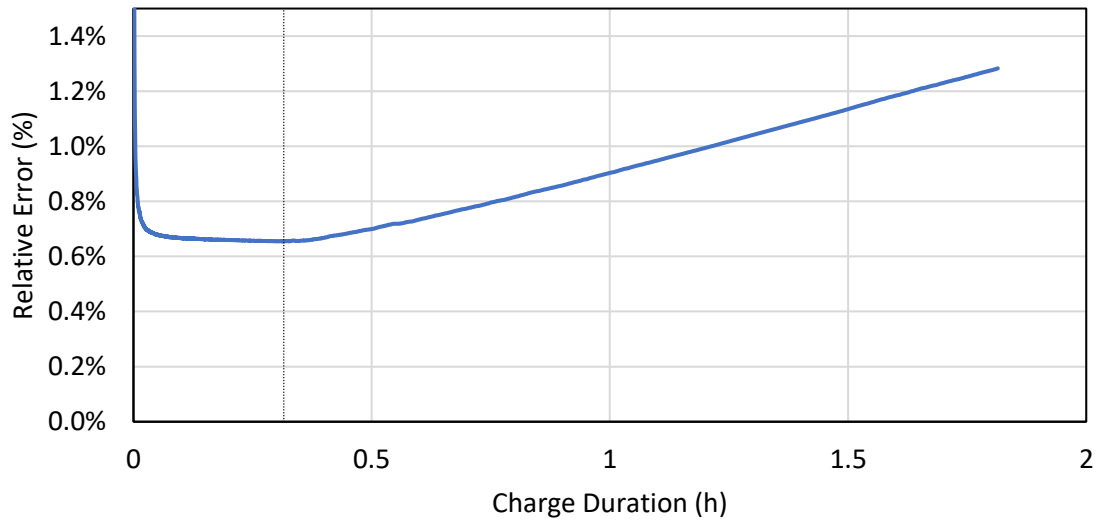


Figure 71- Relative Error in 400 A CCCV Charge with a Panasonic Tesla

The same trend appears with absolute error accumulating more slowly in CV charge, and in relative error increasing in CV charge, except with a more pronounced increase during CV charge. The energy efficiency measurement is found to be 78.6% at worst, compared to the

original 79.9%. Figure 72 shows the rapid rise in error growth as current values decrease, implying that the offset bias in measurement could be a greater source of uncertainty in worst-case scenarios.

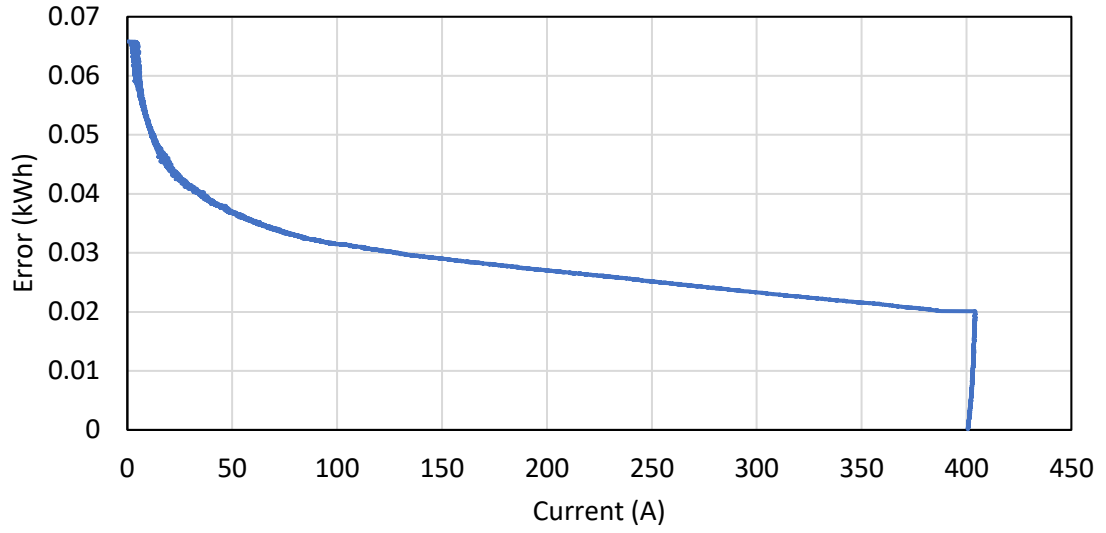


Figure 72- Growth of Error with Change in Current